Spring 2011

An Extensible Mathematical Model of Glucose Metabolism

Caleb L. Adams
Old Dominion University

AN EXTENSIBLE MATHEMATICAL MODEL OF GLUCOSE METABOLISM

by

Caleb L. Adams
M.S. 2004, Old Dominion University
B.S. Mathematics 1997, North Carolina State University
B.S. Math Education 1997, North Carolina State University

A Dissertation Submitted to the Faculty of
Old Dominion University in Partial Fulfillment of the
Requirements for the Degree of

DOCTOR OF PHILOSOPHY

COMPUTATIONAL AND APPLIED MATHEMATICS

OLD DOMINION UNIVERSITY
May 2011

Approved by:

John A. Adam (Director)

D. Glenn Lasseigne

Hideaki Kaneko

Gordon Melrose

Holly Gaff

ABSTRACT

AN EXTENSIBLE MATHEMATICAL MODEL OF GLUCOSE METABOLISM

Caleb L. Adams
Old Dominion University, 2011
Director: Dr. John A. Adam

The American Diabetes Association reports that diabetes is the fifth leading cause of death by disease in the United States. An estimated 23.6 million individuals, or seven percent of the population, have diabetes. Nearly one-third are unaware that they have the disease. The total of the direct and indirect medical costs associated with diabetes in 2007 was projected to be $174 billion, or approximately one out of every ten health care dollars.

One must understand the glucose regulatory system of the healthy body to understand diabetes. blood glucose concentration returns to a constant level after eating and is maintained during exercise. With thousands of chemical reactions involved in the process, a complete mathematical model is not yet realistic. Proposed here is the evolution of a model beginning with a three-variable model of glucose, insulin, and glucagon and ending with its extension to the four-variable model incorporating the additional interdependent mechanics of hepatic glycogen. The three-variable model mimics the return of blood glucose levels to a constant, or basal, state; however, this model is consistent only with short-term dynamics since it excludes consideration of finite energy stores. Thus, the extension includes the effects of a finite store of hepatic glycogen. The solution of the four-variable model demonstrates the short-term return of glucose concentration to near basal levels despite the constant energy usage which draws upon the glycogen stores. Long-term glucose homeostasis is explained by investigating the storage of a glucose load in the postprandial period and dispersion of stored glucose during the extended postprandial period.

Increased hepatic glucose production in people with diabetes is thought to be the driving mechanism for increased basal glucose levels. Analysis of this model indicates the genesis of this phenomenon. Elevated prandial glucose and insulin levels associated with insulin resistance increase the glycogen-storage levels above normal which then increase hepatic glucose production in the postprandial period. Increased energy input exasperates this problem, but only in insulin resistant individuals. This simple model suggests that Type II diabetes results from insulin resistance more than from overeating.

ACKNOWLEDGMENTS

Many thanks, deep gratitude, and appreciation go out to all of my committee members for being part of this project. Special thanks to Dr. Lasseigne and Dr. Adam, my guides in the dissertation process.

I dedicate this dissertation to my family. To my wife, Karen, for all you have done to help me accomplish the seemingly never-ending task I express my love and gratitude. Your understanding, patience, and sturdy shoulder kept me on track. Thank you.

To my children, Trinity, Mattox, and Raelin, let it be known that you can accomplish anything if you put your mind to it and willingness to see it to the end.

TABLE OF CONTENTS

LIST OF TABLES

LIST OF FIGURES

CHAPTER I

INTRODUCTION

The impact of diabetes in the United States is immense. In 2007 the American Diabetes Association reports there are 23.6 million children and adults in the United States, or seven percent of the population, who have diabetes. Nearly one-third of the 23.6 million are unaware that they have the disease (CDC, 2007). The total of the direct and indirect medical costs associated with diabetes in 2007 was estimated to be $174 billion. It is estimated that the average medical expenditures among people diagnosed with diabetes is 2.3 times higher than what expenditures would be in the absence of the disease. Direct medical costs have risen from a 2002 estimate of $92 billion (CDC, 2005) to an estimate of $116 billion in 2007. Even more staggering, at least one out of every ten dollars spent on health care services is attributable to diabetes.

Diabetes is a metabolic disease in which the body does not produce and/or does not properly use *insulin* – a primary regulatory hormone necessary for the body's control of glucose. Insulin enables the absorption of glucose by the body's cells, the conversion of glucose to other needed molecules, and the storage of glucose as glycogen. Type 1 diabetes, also known as insulin-dependent diabetes mellitus (IDDM) or juvenile-onset diabetes, accounts for five to ten percent of all diagnosed cases of diabetes. In people with Type 1 diabetes, the body's immune system destroys pancreatic beta cells, the only cells of the body which produce insulin. The remaining 90%-95% of diagnosed cases of diabetes are Type 2 diabetes, also known as non-insulin-dependent diabetes mellitus (NIDDM). In general, Type 2 diabetes begins with a process called *insulin resistance* where cells in the body do not properly use insulin to regulate changes in blood glucose. As the resistance strengthens, a greater quantity of insulin is required to maintain control. The problem is exasperated by the pancreas' gradual loss of the ability to produce insulin.

On par with insulin's importance in controlling the body's blood glucose level is *glucagon* – a regulatory hormone whose actions counter those of insulin and is required to achieve homeostasis in the glucose regulatory system. Glucagon is secreted at a greater rate in response to low blood glucose levels (hypoglycemia) and triggers glycogenolysis and gluconeogenesis within the system. Between meals, glycogenolysis, or the degradation of stored glycogen into glucose, occurs in the liver in order to counter the body's continual use of glucose and helps maintain the blood glucose concentration. Gluconeogenesis is the biosynthesis of new glucose from non-carbohydrate

This dissertation follows the style of *The Journal of Theoretical Biology*

precursors. This process occurs during periods of fasting, starvation, or intense exercise. As these periods progress, glucose is high in demand by the body, but hepatic glycogen stores are quantifiably low. Thus, the the body synthesizes new glucose from pyruvate, lactate, glycerol, and glucogenic amino acids in order to supply the central nervous system's requirement of approximately 150 grams per day of glucose. If hepatic glycogen stores are depleted, gluconeogenesis becomes the sole source of blood glucose (Smith et al., 2005).

The counter-regulatory hormones, insulin and glucagon, return the blood glucose concentration to a constant level after large inputs associated with eating, and they also maintain the concentration despite large usage rates associated with exercise. The term *basal state* refers to the near-constant levels of blood glucose, insulin, and glucagon the resting body demonstrates for an extended period after absorption of a meal. As food intake increases the readily available glucose supply in the blood stream, the beta cells of the pancreas increase the secretion of insulin while the alpha cells decrease the secretion of glucagon. With an increase in the insulin concentration above basal, the body uses and stores the excess glucose. As the glucose concentration returns to basal, the production of insulin returns to its basal rate. Similarly, in the event glucose concentration dips below basal (as occurs during exercise), the alpha cells of the pancreas increase the secretion of glucagon while the beta cells decrease the secretion of insulin. The increased glucagon concentration draws upon the stores of glucose to accommodate the body's increased requirement of glucose. As with insulin, the body decreases the production rate of glucagon as glucose returns to basal.

Non-zero basal levels of insulin and glucagon in the presence of non-zero disappearance rates of the hormones clearly indicate that these hormones are continuously secreted. Thus, hormone secretion and removal rates determine the basal blood glucose concentration which, in turn, determines the basal secretion rates of the hormones in a continuous feedback process. Many mathematical models use the basal state as a given quantity and suppose that the body only responds when a difference from this basal state exists. Such analysis is appropriate if the resulting model is linear and represents the correction of small excursions from the basal state. However, most of the models are nonlinear, tuned about the basal state for each individual, and applied to large deviations from the basal state. Comparing parameter values derived by fitting the nonlinear model to data gathered from individuals with different basal states leads to misinterpretations of the processes occurring in each individual.

The basal levels of blood glucose, insulin, and glucagon should represent *derivable* quantities in an appropriate nonlinear model and should not appear as explicit parameters. Furthermore, the dependencies of basal values on other parameters (for example, the insulin sensitivity and the glucose threshold for glucagon secretion) provide important clues regarding the health of the individual. This has been done in Lasseigne and Adams (2011). In this thesis, the next step is taken which shows that these basal levels can be nearly maintained even though the system may not be in a steady state. This is achieved by considering the storage and release of glucose as liver glycogen.

CHAPTER II

BACKGROUND

II.1 PURPOSES OF MATHEMATICAL MODELING

A mathematical model is a set of equations expressing a relationship between certain physical quantities and a process or a system. Many mathematical models are derived in order to mimic and understand nature. For a biological/medical system such as glucose metabolism, some experiments have undesirable side effects and are not ethically viable. Instead, creating a mathematical model that simulates the experiment and then analyzing the solutions of the model leads to similar conclusions as would completion of the experiment. From another standpoint, most biological systems are complex and each experiment uses many assumptions and approximations. Investigating the solution of a basic mathematical model may help guide the interpretation of the experimental results.

A number of mathematical models have been developed to illustrate the interactions inherent in the glucose regulatory system. Four such models are described below, each having its strengths, but each also having limitations to the extent of their modeling of glucose metabolism.

II.1.1 Data Fitting – Minimal Model

In the Minimal Model (Bergman et al., 1979), the differential equations governing plasma-glucose concentration, G, and the concentration of insulin in a compartment "remote" from the plasma, X, are

$$\begin{aligned} \frac{dG}{dt} &= (p_1 - X)G + p_4, \\ \frac{dX}{dt} &= p_2 X + p_3 I(t). \end{aligned}$$

Each p_i (for $i = 1-4$) is a chosen independent constant parameter and $I(t)$ represents the measured plasma insulin concentration at a given time t. The Minimal Model was created to compare with clinical results, and the determination of parameter values for an individual indicates the health of that individual. The Minimal Model assumes the following: a) the net hepatic glucose production rate is a linear (decreasing) function of the blood glucose concentration, b) glucose disappears from the blood at a rate proportional to the blood glucose concentration, c) the proportionality factor includes both an insulin-independent term and a term proportional to the insulin in a compartment remote from the plasma (i.e., insulin in the interstitial

fluids), d) the insulin in the interstitial fluids disappears at a rate proportional to itself, and e) insulin enters the remote compartment at a rate proportional to the insulin concentration in the plasma, $I(t)$. As used in a clinical setting, the measured plasma insulin concentration $I(t)$ is treated as an input to the system, and the four independent constants of the model are chosen to fit the measured blood glucose concentration. The fit of the model's solution to experimentally observed glucose profiles in the intravenous glucose tolerance test (IVGTT) is quite good; however, the ability of the model's solution to fit experimental data only proves the solution's generality but does not prove the validity of the model's assumptions. In fact, the results are subject to alternative interpretations.

II.1.2 Simulation – Comprehensive Model

Cobelli and Mari (1983) expand a comprehensive model proposed by Cobelli et al. (1982) which describes human *short-term* glucose metabolism regulation. A validation study using the oral glucose tolerance test (OGTT) data base is included. The comprehensive model consists of seven differential equations, fourteen hyperbolic-tangent functions, and forty-nine parameters. One equation describes the glucose utilization in the plasma and extracellular fluids, two equations account for the storage and release of insulin, three equations model the movement of insulin through three compartments, and one equation details the quantity of glucagon in the plasma and interstitial fluids. Even at this moderate level of complexity, the validation of the model suffers from inherent difficulties such as determining values for the forty-nine parameters corresponding to normal healthy individuals and then determining the values corresponding to individuals in a diseased state.

II.1.3 Explanatory – Illustrative Model

Saunders et al. (1998) proposed a principle of blood glucose control called *integral rein control* where regulation of blood glucose is under the direct effects of both insulin and glucagon. The model proposed is

$$\frac{dG}{dt} = I + \alpha(A,G) - \beta(B,G) - \gamma(R,G), \tag{II.1}$$

$$\frac{dA}{dt} = A(\phi(G)h_1(A,B) - D_{(A)}), \tag{II.2}$$

$$\frac{dB}{dt} = B(\psi(G)h_2(A,B) - D_{(B)}), \tag{II.3}$$

where the concentrations of glucose, glucagon, and insulin are denoted as G, A, and B, respectively. The effects of glucagon and insulin on the blood glucose concentration are represented by $\alpha(A, G)$ and $\beta(B, G)$, respectively. The function $\gamma(R, G)$ represents the uptake of glucose by muscles and other tissues. This uptake is primarily determined by the activity of the organism, represented by the externally determined quantity R. The function $\phi(G)$ represents the dependence of the insulin secretion rate on the blood glucose concentration and is a decreasing function of G. The function $\psi(G)$ represents the dependence of the glucagon secretion rate on the blood glucose concentration and is an increasing function of G. The functions $h_i(A, B)$ (for $i = 1, 2$) represent the mutual and self inhibitions of the secretion rates on the insulin and glucagon levels. The model is of a general nature and is best used for illustrative purposes – not for simulation. This illustrative model is the first model proposed where the basal concentrations are treated as derivable quantities rather than explicitly included as fundamental parameters.

II.1.4 Explanatory to Simulation – Extensible Model

The introductory extensible model proposed in Lasseigne and Adams (2011) begins with an update of the model of Saunders et al. (1998) to mimic the basic glucose-insulin-glucagon counter-regulatory system. The initial three-by-three dynamical system is

$$\begin{aligned}
\frac{dB}{dt} &= -\dot{M}(B) + \dot{H}_P(g, B, I) - \dot{H}_U(I, B, g) - \dot{P}_U(I, B) - \dot{E}(t) \\
&\quad + \dot{F}(t) + \dot{B}_{ex}(t), && \text{(II.4)} \\
\frac{dI}{dt} &= -\delta_I I + \dot{Q}_I(B, I, g) + \dot{I}_{ex}(t), && \text{(II.5)} \\
\frac{dg}{dt} &= -\delta_g g + \dot{Q}_g(B, I, g) + \dot{g}_{ex}(t), && \text{(II.6)}
\end{aligned}$$

where B (the blood glucose concentration), I (the insulin concentration), and g (the glucagon concentration) are the unknowns of the model. The overdot represents that the quantity is a rate of change with respect to time. A single pool of extracellular fluid (volume V_F) is assumed, and the concentrations are the total quantity divided by this volume. The exogenous input rates per volume – $\dot{B}_{ex}(t)$, $\dot{I}_{ex}(t)$, and $\dot{g}_{ex}(t)$ – are prescribed during an experiment. The rates per volume that glucose leaves or enters the blood owing to exercise or food, $\dot{E}(t)$ and $\dot{F}(t)$, are also prescribed functions in the model. The rate per volume that glucose enters the blood owing to hepatic glucose production is defined as $\dot{H}_P$; whereas, $\dot{H}_U$ is the rate per volume that glucose

leaves the blood owing to hepatic glucose uptake. The function $\dot{P}_U$ is the rate per volume of insulin-dependent periphery glucose uptake, and $\dot{M}$ is rate per volume of insulin-independent glucose uptake. The secretion rates per volume of insulin and glucagon, $\dot{Q}_I$ and $\dot{Q}_g$, are predominantly functions of the blood glucose concentration, but depend on the insulin concentration and glucagon concentration if self and mutual inhibitions of secretion exist. The ordering of the arguments of each function implies the major dependencies of each term; for example, $\dot{Q}_g(B, I, g)$ implies that the glucagon secretion rate is mostly determined by the blood glucose concentration with some dependency on the insulin concentration and even less dependency on the glucagon concentration.

II.2 FUTURE OF THE EXTENSIBLE MODEL

The importance of insulin as a regulatory hormone was established in early models of glucose dynamics. More recent models recognize the importance of glucagon as a powerful counter-regulatory hormone of glucose homeostasis with small doses inducing significant glucose elevations. For example, the illustrative model of Saunders et al. (1998), the comprehensive model of Cobelli et al. (1983), and the introductory explanatory model of Lasseigne and Adams (2011) include the effects of glucagon, but at the same time, the models imply that the liver is an *infinite* source of energy. Extension of these models to account for a *finite* amount of energy stored within the body is necessary. At a minimum, a model should eventually include the stores of glycogen in the liver, the stores of glycogen in the muscle, the stores of substrates required for gluconeogenesis, and the stores of fat. Of the four storage compartments mentioned, liver glycogen is the fastest acting, has the greatest effect on the blood glucose concentration during the post-absorptive period, and is the first storage compartment to be depleted of energy. Thus, it seems appropriate that the first extension of the model should account for these effects. In particular, the storage of a glucose load in the postprandial period and dispersion of stored glucose during the extended postprandial period must be explained in order to understand how long-term glucose homeostasis is achieved in the presence of continual glucose usage, especially the usage by the central nervous system.

CHAPTER III

THE MATHEMATICAL MODEL

III.1 STATEMENT OF THE PROBLEM

The many models of glucose metabolism are mostly data centric and focus on the fitting of data resulting from the fasting glucose tolerance test or other similar tests. The tests are limited to the short-term dynamics of the hormonal control of the blood glucose level. The tests start with measuring the basal level of blood glucose and the basal level of insulin after the subject has fasted for a significant amount of time. A bolus of glucose is introduced either intravenously or orally. Then, the blood glucose and insulin levels are measured at discrete times for up to two hours. The mathematical model's parameter values are chosen such that the model's solution fits the observed data. If the parameter values for an individual lie outside of a normal range, the individual is deemed to be in ill health and in need of medical intervention. The previously mentioned Minimal Model and its variants are the most widely used models in the clinical setting. The glucagon level is not measured during these clinical tests, and the Minimal Model does not include an explicit dependence on this important regulatory hormone.

The comprehensive model of Cobelli et al. (1982) and the illustrative model of Saunders et al. (1998) include glucagon as a primary regulatory hormone. Cobelli et al. (1982) employ their comprehensive model to simulate experiments; therefore, the focus remains on fitting the data through determining values for the forty-nine explicit parameters of the system which include the basal concentration values. Conversely, Saunders et al. (1998) attempt to explain how the basal concentration values are determined and maintained by the body. Both models imply that the liver is an *infinite* source of energy through the assumption that a steady state exists in the absence of external energy input but in the presence of a constant utilization rate. Clearly, extending these models to account for the finite energy stores within the body is necessary to more accurately model long-term glucose metabolism.

The primary goal of the research proposed in this thesis is to initiate the creation and validation of a mathematical model for glucose metabolism which is explanatory, but can eventually be used for simulation and data fitting. The pancreas, the liver, muscle tissue, fat tissue, the thyroid, and the kidneys are all major players within the body. However, with the interaction of many different compounds and thousands of chemical reactions, a complete mathematical model is not yet realistic. Therefore an extensible model is proposed which details the interactions of glucose, insulin,

glucagon, and glycogen by updating the illustrative model of Saunders et al. (1998) to more accurately follow the regulatory process. The first step is presented in Lasseigne and Adams (2011), and is summarized in the next section. The second step adds the dynamics of the storage and usage of hepatic glycogen.

III.2 GLUCOSE-INSULIN-GLUCAGON MODEL

III.2.1 3 x 3 Model Construction

The control of blood glucose in the body is dominated by the effects of two hormones: insulin and glucagon. Therefore, the most basic model must account for the presence and disappearance of these hormones in the body and their effect on the blood glucose level. Although inappropriate for a model of a complex organism, a one-compartment model for insulin is assumed. It is assumed that the pancreas has a fixed capacity; therefore, the model assumes the existence of a maximum rate of insulin secretion regardless of the blood glucose level. The build up of insulin in the system is prevented by assuming a half-life for insulin, i.e., insulin levels decay at a rate proportional to the amount of insulin present. The insulin-dependent rate of glucose utilization is assumed to be directly proportional to the insulin concentration.

The assumptions made for the inclusion of glucagon in the model are similar to the assumptions made in the insulin model. A maximum rate of glucagon is assumed to exist, the build up of glucagon in the system is prevented by assuming that the level of glucagon decays at a rate proportional to the amount of glucagon present, and liver glucose production is assumed to be directly proportional to the glucagon concentration.

III.2.2 Basic System

To avoid controversy and to prevent the tendency to prematurely apply the model to fit experimental data, the following pedagogical device is invented:

> The model is an exact representation of glucose metabolism in a fictitious animal species. The first species considered has evolved to a simple state such that exactly two hormones control glucose metabolism: insulin and glucagon. Glucose uptake is expedited by the presence of insulin, but the insulin itself is not consumed by the cells. The release of glucose into the blood stream is catalyzed by the presence of glucagon, but glucagon is not consumed by the cells. Both insulin and glucagon have a natural decay rate independent of how the hormone is used in the glucose regulatory process providing for the disappearance of these hormones. Having created a fictional species, freedom

exists to choose specific mathematical forms for the unit processes and any parameter values. Different parameter values represent different individuals of the species or different states of health in a single individual. By changing the functional dependence of the rates of insulin and glucagon secretion or the functional dependence of the rates of glucose uptake and production, one describes a different fictional species. By extension – such as adding a variable to model liver glycogen stores or accounting for both the fast and slow release of insulin – the model "evolves" to mimic glucose metabolism in a complex animal species.

Since uptake and release of glucose occur at the cellular level, the rates of increase and decrease of glucose are proportional to concentration levels rather than absolute levels. For this particular fictitious animal species, the blood glucose increases at a rate directly proportional to the concentration level of the glucagon in the blood. Likewise, the blood glucose decreases at a rate directly proportional to the concentration level of the insulin in the blood. Release of glucagon and insulin into the blood stream is dependent on the blood glucose concentration. One should also note that a maximum release rate exists for each hormone as it is plausible that the pancreas has a fixed capacity. The maximum release rate for glucagon exists when blood glucose concentration is zero; and, the maximum release rate for insulin exists for very large blood glucose concentration. The initial model investigated is a special case of the system defined in section II.1.4. The above assumptions lead to specifying $\dot{H}_P = \alpha g$ and $\dot{H}_U + \dot{P}_U = \beta BI$ in the generalized system defined by equations (II.4)-(II.6). For simplicity of the first model, the secretion rates are assumed to depend only on the blood glucose concentration and are modeled using hyperbolic tangents. Hyperbolic tangents are often used to model phenomena that transition from one state to another. If a different functional representation is used to model the transition, the results do not change significantly. The resultant model for the first species is:

$$\frac{dB}{dt} = \dot{F}(t) - \dot{E}(t) - \dot{M}_0 + \alpha g - \beta BI, \tag{III.1}$$

$$\frac{dI}{dt} = -\delta_I I + \dot{Q}_I \left\{ \frac{1}{2} + \frac{1}{2} \tanh\left(\frac{B - B_I}{r_I} \right) \right\}, \tag{III.2}$$

$$\frac{dg}{dt} = -\delta_g g + \dot{Q}_g \left\{ \frac{1}{2} + \frac{1}{2} \tanh\left(\frac{B_g - B}{r_g} \right) \right\}. \tag{III.3}$$

Initially, diet and exercise are included as first-order effects. The effects of eating, modeled by prescribing $\dot{F}(t)$, are assumed to be a direct source of blood glucose, and the effects of exercise, modeled by $\dot{E}(t)$, are assumed to be a direct utilization of blood glucose. Eleven parameters relate to the internal workings of an individual. $\dot{M}_0$

is the (constant) insulin-independent rate per volume of glucose uptake. This uptake is primarily due to the central nervous system's constant usage of glucose. Variations of the value of $\dot{M}_0$ may exist over an extended time period due to changes in the body such as increasing muscle mass or through a changes in an individual's weight. Two parameters, δ_I and δ_g, relate to the half-lives of the hormones and account for the disappearance of insulin and glucagon from the blood. β is the constant insulin sensitivity, and α is the glucagon's effectiveness at releasing the glycogen stores and converting proteins to glucose. The development of insulin resistance is reflected in a lowering of the value of β. The size of the glycogen stores and availability of substrates for gluconeogenesis affect the value of α. The constants $\dot{Q}_I$, B_I, and r_I relate to the secretion of insulin, and their values also reflect the health of the individual. Damage to the pancreatic cells that secrete insulin lowers the value of $\dot{Q}_I$ (the maximum rate of insulin release) or increases the values of B_I and r_I, i.e., changes the pancreatic response to the blood glucose concentration. The constants $\dot{Q}_g$, B_g, and r_g relate to the secretion of glucagon. Although not obviously as affected by the health of the individual, variations in this latter set of parameters might be responsible for the pre-diabetes condition of hyperinsulinemia in response to a slightly elevated basal glucose level. The parameters B_I and B_g are often referred to as "threshold values" for insulin and glucagon secretion. With this terminology comes the assumption that the secretion of these hormones is insignificant until the blood glucose concentration reaches these threshold values; however, the basal level depends on the continuous balance between the non-zero secretion of the hormones and their disappearance rate. In the healthy individual, the blood glucose concentration only passes the threshold values during severe hypoglycemia or after significant glucose input such as provided by a carbohydrate meal.

Having created fictional species, freedom exists to choose the values of parameters and then investigate the effects of the various choices. For some choices, the model's solution mimics the time history of the blood glucose concentration in a functioning individual, whereas for other choices, the model's solution might predict impossibly low blood glucose concentrations or other improbable situations. An attempt is made to choose parameter values keeping the model's solution within the context of a human-like species. Thus, the following (rounded) constant values are used throughout the rest of this thesis:

- $\delta_I = 0.14$ min^{-1} sets the half-life of insulin as a little less than five minutes,
- $\delta g = 0.08$ min^{-1} sets the half-life of glucagon as a little less than eight minutes,
- $V_F = 130$ deciliter, which is approximately the volume of the extra-cellular

fluid in a 70 kg individual,

- $V_F \dot{M}_0 = 100$ mg/min representing approximately 6 g/hour,

Initially, the remaining parameters are chosen such that the derived basal values will be

- $B^* = 90$ mg/dl is the basal blood glucose concentration in a healthy individual,
- $I^* = 8$ μU/ml is the basal insulin concentration in a healthy individual,
- $g^* = 120$ pg/ml is the basal glucagon concentration in a healthy individual.

Thus, changing parameter values (e.g., decreasing insulin sensitivity) would then produce a quantifiable change in the basal state.

The model defined in section II.1.4 contains two components of insulin-dependent glucose consumption $\dot{H}_U$ and $\dot{P}_U$. Hence, the term from equation (III.1) associated with insulin, βBI, is partitioned into two new terms: the conversion rate of glucose to glycogen in the liver, $\beta_L BI$, and the usage rate of glucose by the muscles (and other tissues) of the body, $\beta_M BI$. Choosing an accurate relationship between β_L and β_M is impossible since the allocation of glucose between the compartments changes continuously dependent on the state of glycogen storage in the liver and muscles. For simplicity, the relationship $\beta_M = 2\beta_L$ is chosen. With the addition of another parameter the following baseline values have been included:

- $V_F\,(\alpha g^* - \beta_L B^* I^*) = 170$ mg min^{-1} approximately equal to 10 g hour^{-1} is the net rate of hepatic output during basal conditions in a healthy individual,
- $V_F\,(\beta_M B^* I^*) = 70$ mg min^{-1} approximately equal to 4 g hour^{-1} is the *insulin-dependent* rate of consumption of glucose external to the liver during basal conditions.

III.2.3 3 x 3 System Results

With no external source of glucose, the system defined in equations (III.1)-(III.3) maintains homeostasis at the basal levels $B^* = 90$, $I^* = 8$, and $g^* = 120$. The parameter values r_I and B_I for four baseline individuals are in Table 1. Though there exists a variety of values for these two parameters, integration of the differential equations using basal conditions as initial values show that each individual holds the basal state when there is no external glucose source, see Fig. 1. When insulin effectiveness is reduced by a factor of two (i.e., $\beta = 0.5\beta$) a new homeostatic state is achieved. This new state exhibits a greater concentration of insulin in the system due

Table 1
Baseline values of r_I and B_I for four individuals.

Individual, k	r_I	B_I
1	15	105
2	15	115
3	15	125
4	25	125

to its ineffectiveness. However, this elevated insulin concentration is not able to hold the system at the original "starred,"or basal state, and the system exhibits both an elevated glucose concentration and a decreased glucagon concentration. These changes in the basal state are greater when the insulin effectiveness is reduced by a factor of ten (i.e., $\beta = 0.1\beta$).

Upon introducing an exogenous glucose source of finite duration, the secretion rates of insulin and glucagon adjust in order to return the blood glucose level to its basal state. Analysis in Lasseigne and Adams (2011) leads to considering baseline individual #2 as the "normal" healthy individual. Fig. 2 illustrates the system's response to a meal-like external energy input and the return to the basal state during the postprandial period. Here, the meal-like input is the release of glucose into the system defined by the normalized input rate

$$\dot{F}(t) = F_0 \cdot 0.5 d^{-3} t^2 e^{-t/d}, \tag{III.4}$$

where $d = 15$ and $F_0 = 150$. The parameter d is a measure of the time it takes for the glucose in the meal to enter in the blood stream. The constant $F_0 = \int_0^\infty \dot{F}(t)\, dt$ represents the milligrams per deciliter of glucose carbohydrate consumed in a meal. As $d \to 0$, $\dot{F}(t)$ becomes the unit delta function multiplied by F_o.

If a constant glucose input rate in excess of or equal to the resting energy usage rate is prescribed, then a sustainable steady-state solution in the resting individual exists.

Limitations of the 3 x 3 System

Without an external source of glucose, the steady-state solutions corresponding to basal conditions are unsustainable since the body constantly uses energy. For this system, steady states under basal conditions exist since the model contains the implicit assumption that an infinite internal source of energy exists, say from the liver.

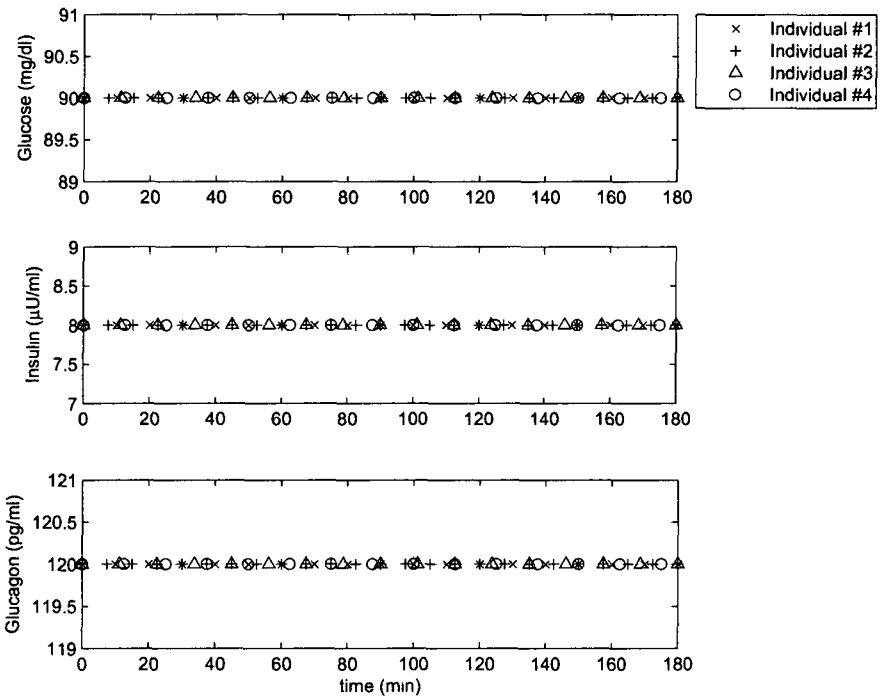

Fig. 1 Basal state for four baseline individuals with no external glucose source.

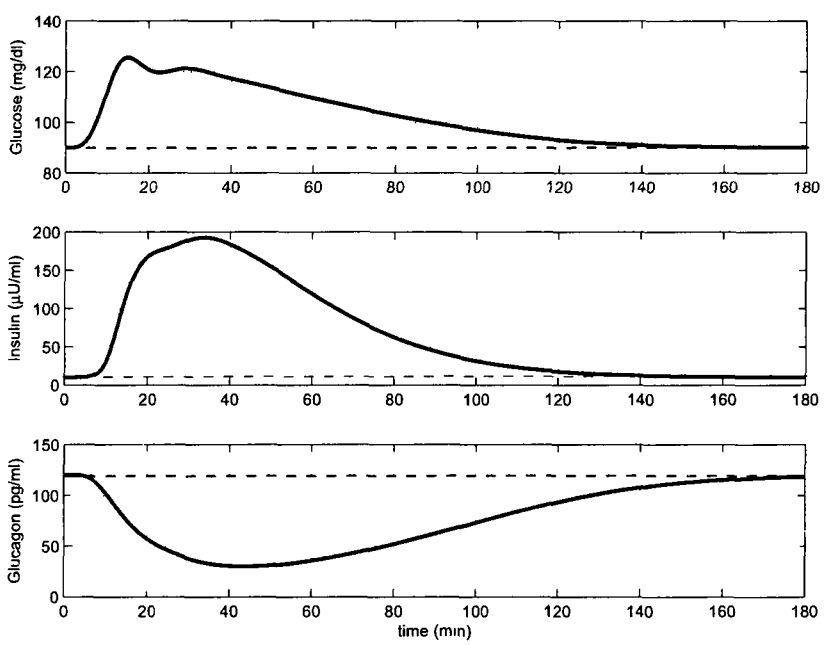

Fig. 2 System's response to a meal-like input of 150 grams of glucose dispersed over 15 minutes starting at time $t = 0$. Dashed line indicates basal levels.

Although the assumption is false for extended time solutions without external energy inputs, the model reasonably predicts the variation of the blood glucose concentration during short-term fasts and meals and predicts the corresponding changes in the insulin and glucagon concentrations. In this model, the term βBI represents the removal of glucose from the blood for storage as fat or as glycogen in the liver and muscle as well as representing the immediate use of glucose in the muscle. The model does not account for the saturation or depletion of the storage sites, but the model should reasonably predict the variation of blood glucose concentration for time periods when saturation or depletion does not occur. Also to be noted, this model contains no feed-forward mechanism that affects the hormone concentrations immediately after the ingestion of a meal. Thus, the hormonal response to a meal-like external energy input (hereafter referred to as a meal) is only determined through the increased blood glucose engendered by the input.

The goal of this thesis is an extension of the original three-by-three model to determine the role of hepatic glycogen storage in maintaining homeostasis. This modification eliminates the assumption of an infinite internal energy source.

III.3 GLUCOSE-INSULIN-GLUCAGON-GLYCOGEN MODEL

Glucose is stored in the liver and muscle as glycogen. Liver glycogen acts as a reserve of glucose to maintain blood glucose between meals or during extreme need (e.g., exercise). The glucose broken down from muscle glycogen is reserved for and burned by muscle tissue and does not enter the blood stream to be used by other tissue.

In response to the increase in blood glucose engendered by the ingestion of dietary carbohydrates, insulin secretion is increased by the pancreas, and the additional insulin promotes glucose uptake. The excess glucose provided by the meal is immediately used or stored as glycogen in both liver and muscle through the process of glycogenesis. Until all excessive glucose is used by the body, glycogenesis continues at a rate faster than the basal rate. When dietary glucose is unavailable, the secretion of the counter-regulatory hormone glucagon increases, and the glucagon passes into the liver promoting conversion of glycogen to glucose via the process of glycogenolysis. Glycogenolysis is necessary for the body to maintain the basal blood glucose concentration in the short term. Though beyond the scope of this thesis, another important mechanism of the regulation of the blood glucose concentration is glucagon stimulated gluconeogenesis. If adequate hepatic glycogen stores are unavailable, the body relies on the creation of glucose from non-carbohydrate substrates to maintain the basal blood glucose concentration.

III.3.1 Glycogenesis – First Modification

The first modification of the basic system introduces dependency of glycogenesis on the quantity of glycogen stored in the liver (say L measured in milligrams) into the original three-by-three model. A fourth equation extends the previous system as

$$\frac{dB}{dt} = \dot{F}(t) - \dot{M}_0 - \beta_M BI - \frac{1}{V_F}\frac{dL}{dt}, \tag{III.5}$$

$$\frac{dI}{dt} = -\delta_I I + \dot{Q}_I \left\{\frac{1}{2} + \frac{1}{2}\tanh\left(\frac{B - B_I}{r_I}\right)\right\}, \tag{III.6}$$

$$\frac{dg}{dt} = -\delta_g g + \dot{Q}_g \left\{\frac{1}{2} + \frac{1}{2}\tanh\left(\frac{B_g - B}{r_g}\right)\right\}, \tag{III.7}$$

$$\frac{dL}{dt} = V_F\left(\beta_L BI\,\frac{\mathrm{erfc}(\gamma_I L)}{\mathrm{erfc}(\gamma_I L^*)} - \alpha g\right), \tag{III.8}$$

where V_F is the volume of interstitial fluids. When the argument of $\mathrm{erfc}(\gamma_I L)$ becomes large, i.e., $\gamma_I L \to \infty$, the value of the complimentary error function tends towards zero and models the suppression of further storage owing to the finite size of the liver. When the argument of $\mathrm{erfc}(\gamma_I L)$ becomes small, i.e., $\gamma_I L \to 0$, the value of the complimentary error function tends towards it's maximum value of unity and models the body's need to replenish its life preserving store of glycogen at the greatest possible rate. The parameter γ_I is a scaling factor to be chosen during the following analysis. The choice of the complimentary error function is not unique. Specifying a different functional relationship which similarly models the above asymptotic behavior would yield comparable results.

Assume the body starts with a baseline liver glycogen level of $L(0) = L^* = 130,000$ mg (130 g) and experiences three meal-like inputs of glucose. A graphical representation of the dependent variables over a 24-hour period, where $t = 0$ represents 7:59 a.m. with multiple values of γ_I, is shown in Fig. 3 and Fig. 4. The three incorporated meals occur at 8:00 a.m., 12:00 p.m., and 6:00 p.m. The appropriate parameter range for γ_I in the healthy individual arises from two restrictions which keep the blood glucose in the physiological range: a) the maximum blood glucose in response to a meal should remain in the range $\sim 120 - 200$ mg dl^{-1}, and b) the blood glucose concentration should not dip below hypoglycemic levels of less than 60 mg dl^{-1} between meals or overnight.

The effect of the choice of γ_I is discovered by examining the blood glucose concentration (Fig. 5 – top), absolute liver glycogen quantity (Fig. 5 – bottom), insulin concentration (Fig. 6 – top), and glucagon concentration (Fig. 6 – bottom) during the consumption, usage, and storage of the first meal. During the time period of the first meal, the glucose and insulin concentrations are high; whereas, the glucagon

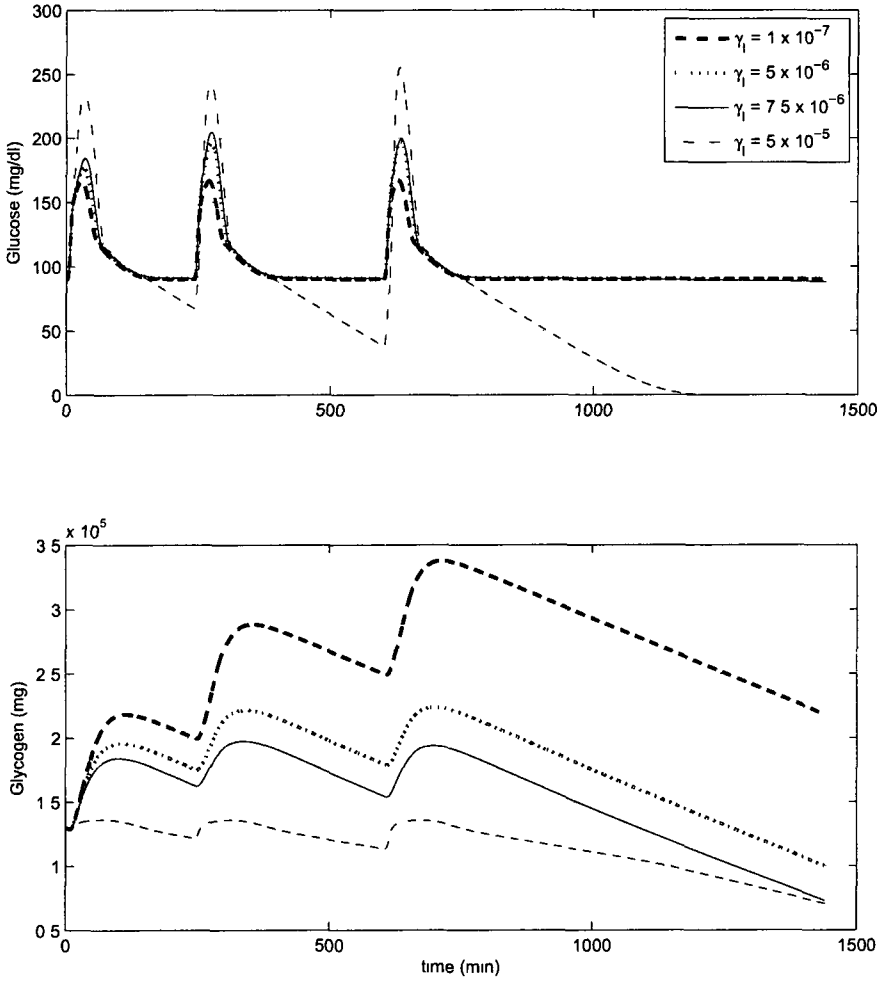

Fig. 3 Glucose concentration (top) and liver glycogen quantity (bottom) for four values of γ_I over a 24-hr period.

concentration is low. As a result, postprandial blood glucose is stored in the liver through the term proportional to β_L, stored and used in the muscle through the term proportional to β_M, and used by the central nervous system through the term $\dot{M}_0$. In the original three-by-three system, a balance between these mechanisms for glucose usage existed and was independent of the state of glycogen storage in the liver. As seen through Fig. 7, very small values of γ_I lead to little dependence on the current liver glycogen level, and the balance established by the original three-by-three system is retained irrespective of the growing glycogen levels. The maximum glycogen level in the liver after the first meal under the original system is $L_{\max} \approx 220,000$ mg. As the value of γ_I increases, more dependence on the current liver glycogen level

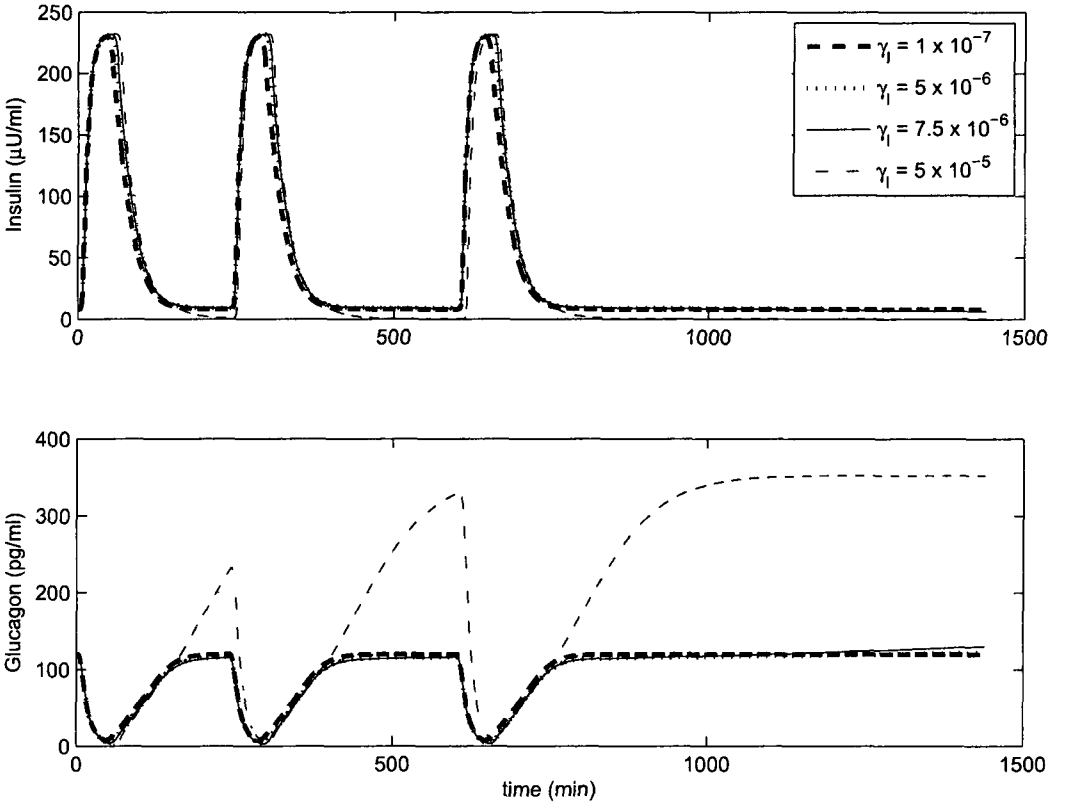

Fig. 4 Insulin (top) and glucagon (bottom) concentration for four values of γ_I.

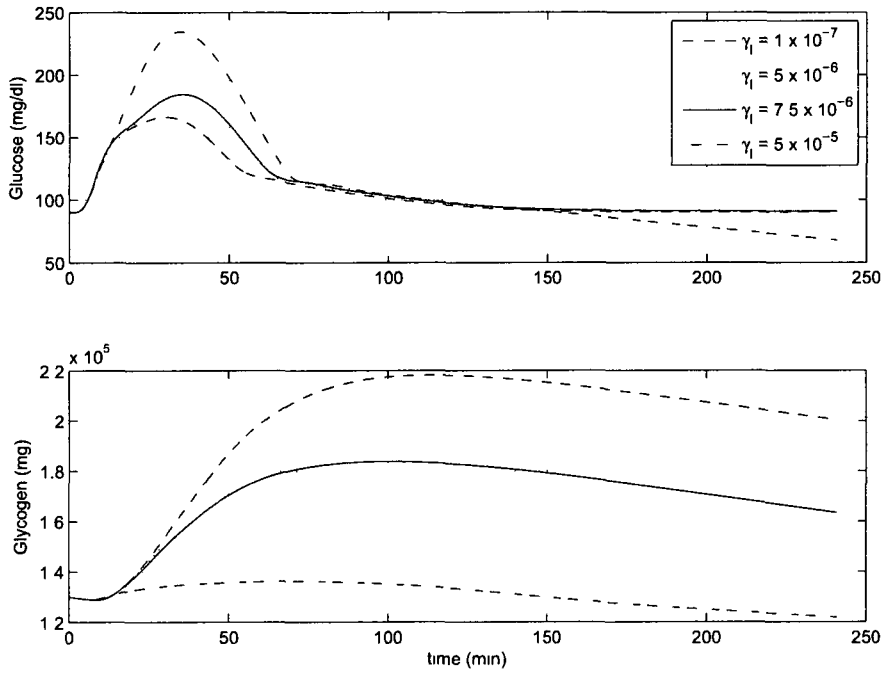

Fig. 5 Glucose concentration (top) and liver glycogen quantity (bottom) for four values of γ_I during the first meal.

is introduced. Since $L > L^*$ immediately following the meal, the glycogen storage rate is significantly decreased for large γ_I values (see Fig. 7), and prandial glucose usage tends toward storage in the muscles and direct usage by the body rather than storage in the liver. Since storage in the liver is limited and since other avenues of usage remain as previously prescribed, the glucose remains in the blood for a longer time period leading to increased postprandial blood glucose concentrations.

Presently, the model does not limit the quantity of glucose which can be stored by the muscle nor does it adjust the rate of storage as a function of muscle glycogen content, thus the balance between storage as hepatic glycogen and storage in the muscle is solely determined by the value of γ_I and the instantaneous liver glycogen content L. As just noted, large values of γ_I lead to almost no storage of glucose in the liver when $L > L^*$ which increases the postprandial glucose in the blood. The excess glucose is eventually used by the central nervous system or the muscles of the individual. On the contrary, small values of γ_I lead to the maximum disposition of an external source of glucose through storage as liver glycogen rather than through the insulin-dependent usage in the rest of the body.

The first post-absorptive period provides further information to determine the

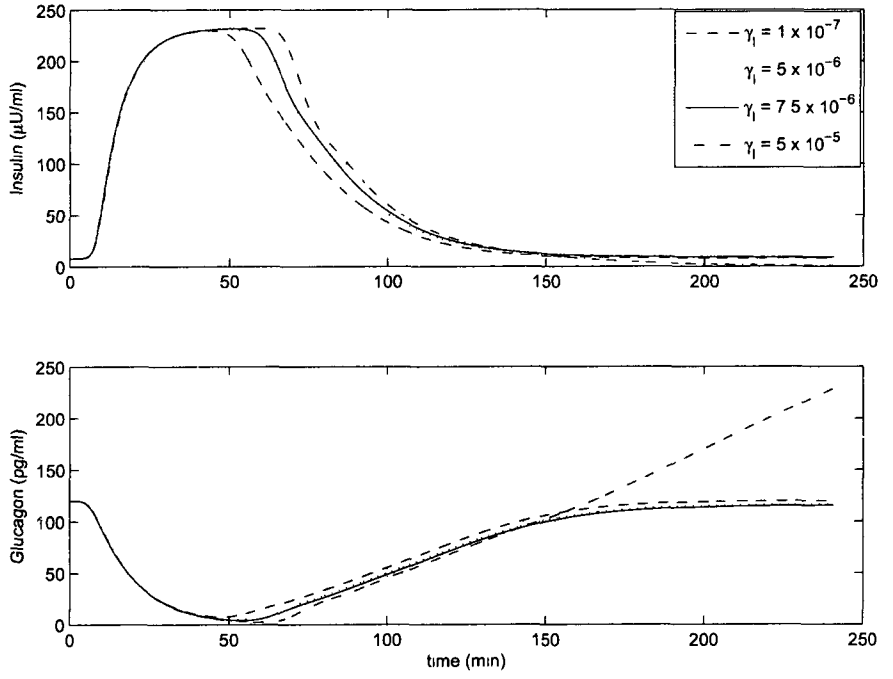

Fig. 6 Insulin (top) and Glucagon (bottom) concentrations for four values of γ_I during the first meal.

effect of the parameter γ_I. In this first extension of the model, the glycogenolysis rate remains independent of the glycogen level and provides the glucose necessary to maintain basal levels between meals. For the three cases when there is sufficient storage of hepatic glycogen, the blood glucose level, the insulin level, and the glucagon level return to the basal values established by the original three-by-three system. The hepatic glycogen depletes at a constant rate between meals, but the glycogen level remains above the original level of L^* except possibly during the extended overnight post-absorptive period.

On the contrary, the largest value investigated $\gamma_I = 5 \times 10^{-5}$ – represented by the *dash-dot* line in Fig. 5 (bottom)– leads to the lowest after-meal storage of glycogen, and in the immediate post-absorptive period the liver glycogen level dips below the initial level of L^*. With this large value of γ_I, the rate of glycogenesis is significantly *increased*; thus, glucose is removed from the blood at a very large rate in an attempt to return the glycogen level to $L = L^*$. This is an indication of hepatic cycling, i.e., the processes of glycogenesis and glycogenolysis occur simultaneously, albeit at differing rates. Without considering a second source of glucose (such as gluconeogenesis) which would supply enough glucose for both usage in the central nervous system and

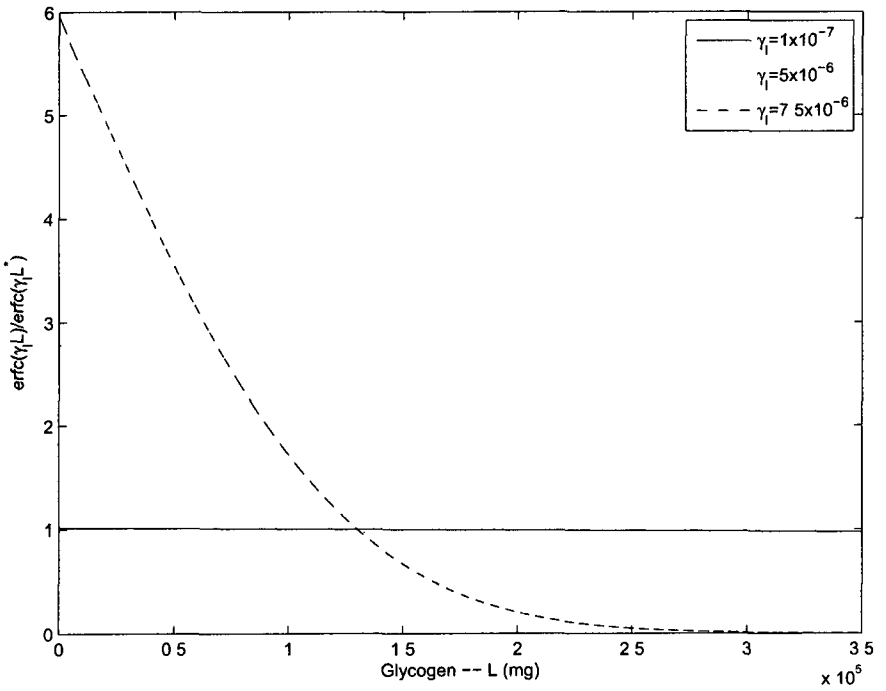

Fig. 7 $\frac{\text{erfc}(\gamma_I L)}{\text{erfc}(\gamma_I L^*)}$ vs. hepatic glycogen for three values of γ_I.

through glycogenesis, a short-term balance cannot be maintained and homeostasis is not achieved. During this period, the glucose concentration drops rapidly, and the body responds by increasing the glucagon level and decreasing the insulin level. Since the solution demonstrates severe bouts of hypoglycemia when $\gamma_I = 5 \times 10^{-5}$, the desired value of γ_I must be less than this value. This extreme case demonstrates that the first modification corrects the deficiency of the original three-by-three model which considered the liver as an infinite source of glucose.

By examining the quantity of liver glycogen over the 24-hour period and including three meals, it is discovered that there is sufficient glycogen stored to maintain $L > L^*$ and basal conditions even during the extended overnight post-absorptive period when using the smallest proposed value, $\gamma_I = 1 \times 10^{-7}$ – displayed in Fig. 3 (bottom) as the *dashed* line. Using the other values of γ_I investigated, $\gamma_I = 5 \times 10^{-6}$ and $\gamma_I = 7.5 \times 10^{-6}$ – *dotted* and *solid* lines, respectively – results in less hepatic glycogen storage, and the level dips below L^* during the extended post-absorptive period which follows the final meal of the day. During this period, the blood glucose concentration decreases slightly but remains near basal as the increased rate of glycogenesis is not as significant as when $\gamma_I = 5 \times 10^{-5}$.

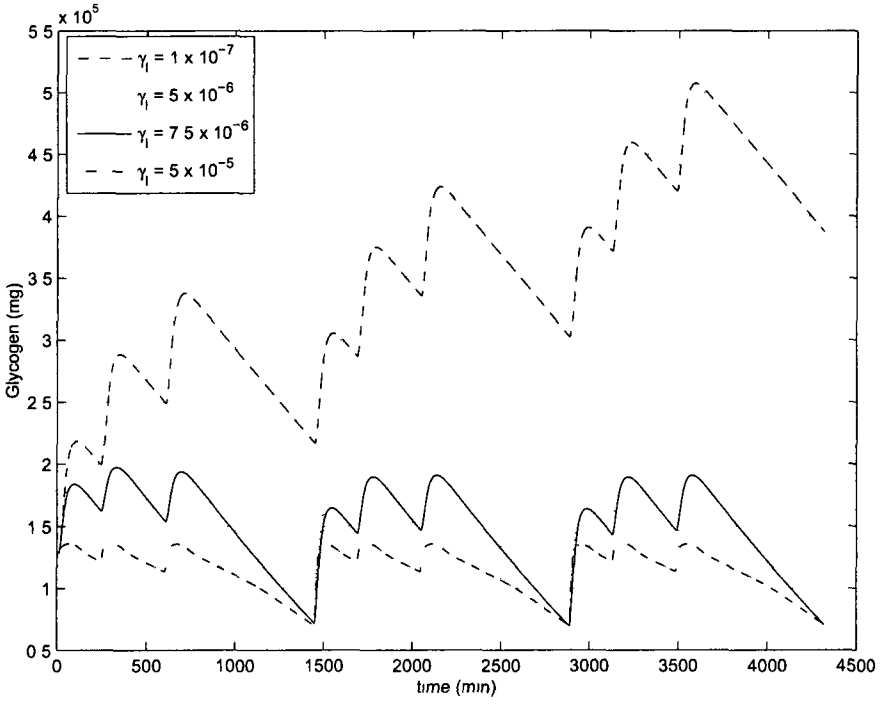

Fig. 8 Liver glycogen quantities over 72 hours for four values of γ_I.

By continuing the calculation through 72 hours with three meals daily (see Fig. 8 for illustration), it is shown that hepatic stores would gradually increase beyond storage capacity for the lowest value of γ_I. For the two intermediate values investigated ($\gamma_I = 5 \times 10^{-6}$ and $\gamma_I = 7.5 \times 10^{-6}$), the blood glucose, insulin, and glucagon concentrations remain well controlled without excessive storage or depletion of glycogen. When $\gamma_I = 5 \times 10^{-5}$, the model predicts repeated unphysical hypoglycemic events occurring between each meal. Thus, the appropriate range of γ_I values for the healthy individual has been determined.

III.3.2 Glycogenolysis – Second Modification

The second modification of the basic system introduces the dependency of glycogenolysis on the concentrations of glucagon and the quantity of glycogen stored in the liver into the original three-by-three model. The first three equations of the model remain the same as in section III.3.1, and the fourth equation is replaced with

$$\frac{dL}{dt} = V_F \left(\beta_L BI - \alpha g \frac{\mathrm{erf}(\gamma_g L)}{\mathrm{erf}(\gamma_g L^*)} \right). \tag{III.9}$$

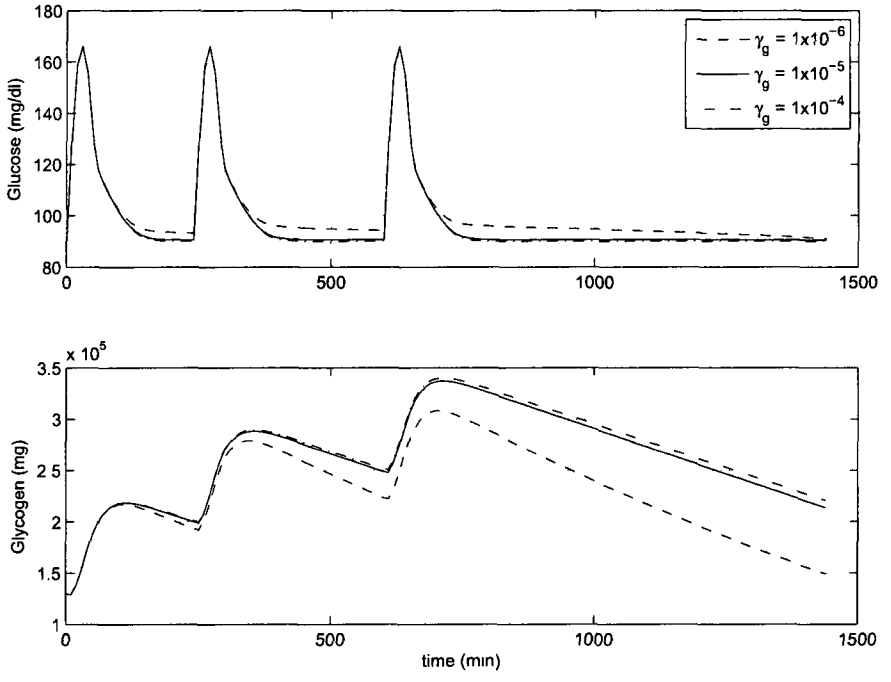

Fig. 9 Glucose concentration (top) and liver glycogen quantity (bottom) for three values of γ_g.

When the argument of $\text{erf}(\gamma_g L)$ becomes large, i.e., $\gamma_g L \to \infty$, the value of the error function tends towards unity and models the tendency of the liver to output glucose at the maximum rate when the liver is saturated with glycogen. When the argument of $\text{erf}(\gamma_g L)$ becomes small, i.e., $\gamma_g L \to 0$, the value of the error function tends towards zero and models the body's attempt to preserve its store of glycogen by greatly decreasing the rate of glycogenolysis. The parameter γ_g is a scaling factor to be chosen during the following analysis. The choice of the error function is not unique. Specifying a different functional relationship which similarly models the above asymptotic behavior would yield comparable results.

Assume the body starts with a baseline liver glycogen level of $L(0) = L^* = 130,000$ mg (130 g) and experiences three meal-like inputs of glucose. A graphical representation of the dependent variables over a 24-hour period, where $t = 0$ represents 7:59 a.m. with multiple values of γ_g, is shown in Fig. 9 and Fig. 10. The three incorporated meals occur at 8:00 a.m., 12:00 p.m., and 6:00 p.m.

As discovered in the previous section, the original three-by-three system represented the conditions leading to the greatest hepatic glycogen storage of a meal. These conditions persist throughout this section. The effect of the choice of γ_g is discovered by examining the blood glucose concentration, absolute liver glycogen quantity, insulin concentration, and glucagon concentration after the consumption,

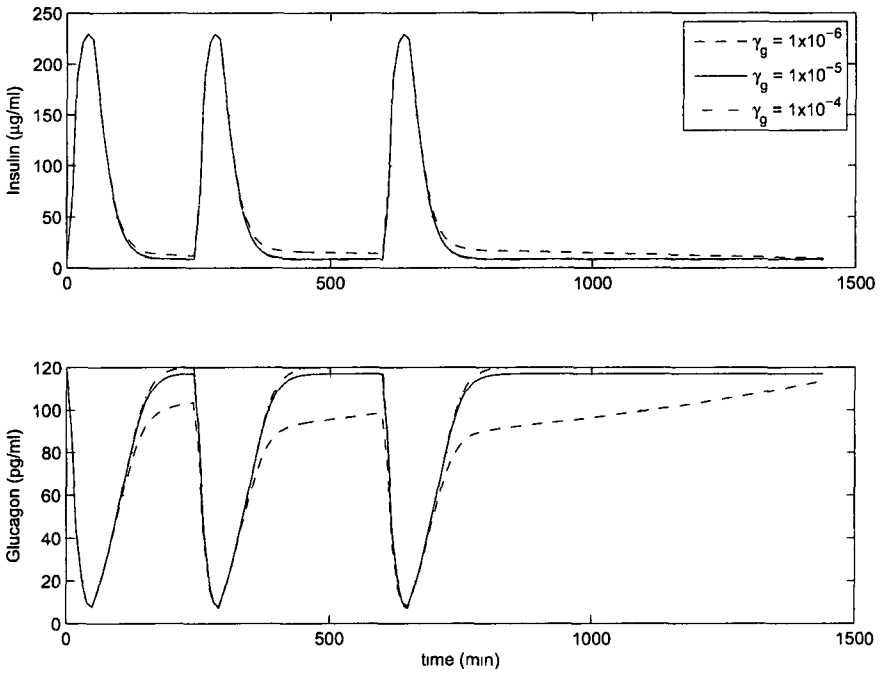

Fig. 10 Insulin (top) and glucagon (bottom) concentration for three values of γ_g.

usage, and storage of the first meal. Fig. 9 shows the solution over a 24-hr period for three values of γ_g: $\gamma_g = 1 \times 10^{-6}$, $\gamma_g = 1 \times 10^{-5}$, and $\gamma_g = 1 \times 10^{-4}$. Since glucagon levels drop immediately upon consumption of a meal, the second modification has no effect on the increase in liver glycogen content occurring as a result of the meal. However, in the immediate postprandial period, the values of γ_g affect the rate of glycogenolysis. As seen through Fig. 11, very large values of γ_g lead to little dependence of the glycogenolysis rate on the current liver glycogen level, and the rate established by the original three-by-three system is retained irrespective of the growing glycogen levels. The maximum glycogen level in the liver after the first meal under all values of γ_g is $L_{\max} \approx 220,000$ mg. Since $L > L^*$ immediately following the meal, the glycogen unloading rate is significantly increased for small γ_g values (see Fig. 11), and this results in blood glucose levels in excess of the basal levels of the original three-by-three system. In none of the cases does the glycogen level fall below L^* before the next meal is consumed. Without the limiting behavior on glycogenesis present owing to saturation-induced insulin insensitivity, the liver "overloads" after each meal, and thus, glycogen levels increase over time. The increase in glycogenolysis rates for small γ_g when $L > L^*$ slows the overloading of glycogen levels as evidenced by examining the solution over 72 hours (see Fig. 12).

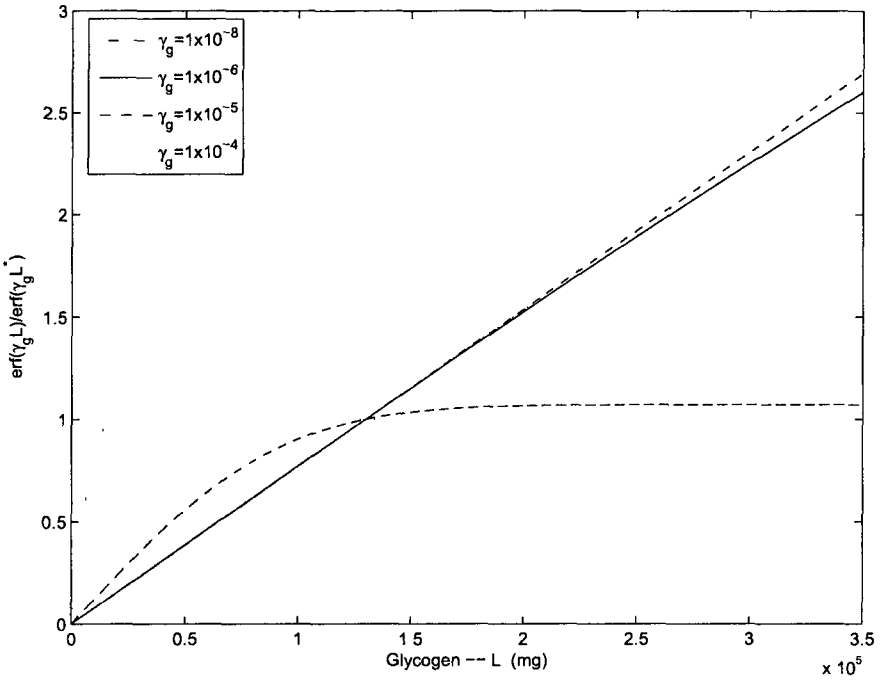

Fig. 11 Unloading factor $\frac{\mathrm{erf}(\gamma_g L)}{\mathrm{erf}(\gamma_g L^*)}$ vs. liver glycogen content for three values of γ_g.

The increased post-absorptive unloading rates for small γ_g with increasing L keeps the post-absorptive blood glucose levels significantly above the basal levels of the original three-by-three system.

To examine the second modification's ability to preserve glycogen stores at appropriate times, the level of glycogen was allowed to drop below L^* by eliminating meals for an extended period of time (thus continuing the overnight fast observed in Fig. 9). For small γ_g, the second modification slowed the rate of glycogenolysis and maintained glycogen levels at the expense of blood glucose levels, which fell below the basal levels of the original three-by-three system. Without the second modification (or for large γ_g), basal blood glucose levels were maintained at the expense of depleting the glycogen store. If an additional internal source of glucose, such as gluconeogenesis, is included in the model, then the smaller value of γ_g would allow for the preservation of glycogen while maintaining basal blood glucose levels as is demonstrated later (see section III.3.5).

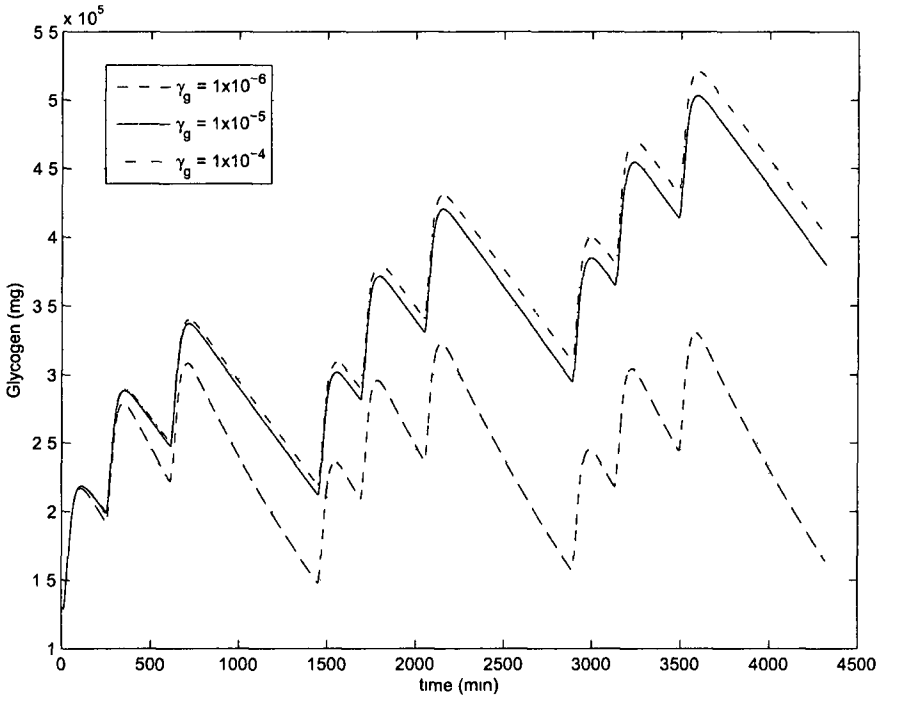

Fig. 12 Liver glycogen over 72 hours for three values of γ_g.

III.3.3 Combination of Modifications

In the previous two sections, the basic three-by-three system was modified to account for the individual effects of hepatic glycogen storage and hepatic glycogen depletion. Now that the effects of the individual modifications are better understood, a model combining the two phenomena is examined. The initial goal of this section is to determine symbiotic values of the parameters γ_I and γ_g which lead to homeostasis at or near the basal state without excessive saturation or depletion of glycogen stores.

Combining the modification into one model yields the following system:

$$\frac{dB}{dt} = \dot{F}(t) - \dot{M}_0 - \beta_M BI - \frac{1}{V_F}\frac{dL}{dt}, \tag{III.10}$$

$$\frac{dI}{dt} = -\delta_I I + \dot{Q}_I \left\{ \frac{1}{2} + \frac{1}{2}\tanh\left(\frac{B - B_I}{r_I}\right) \right\}, \tag{III.11}$$

$$\frac{dg}{dt} = -\delta_g g + \dot{Q}_g \left\{ \frac{1}{2} + \frac{1}{2}\tanh\left(\frac{B_g - B}{r_g}\right) \right\}, \tag{III.12}$$

$$\frac{dL}{dt} = V_F \left(\beta_L BI \frac{\mathrm{erfc}(\gamma_I L)}{\mathrm{erfc}(\gamma_I L^*)} - \alpha g \frac{\mathrm{erf}(\gamma_g L)}{\mathrm{erf}(\gamma_g L^*)} \right). \tag{III.13}$$

If $L \gg L^*$, equation (III.13) reduces to

$$\frac{dL}{dt} = -V_F \frac{\alpha g}{\mathrm{erf}(\gamma_g L^*)}$$

and the system no longer stores glucose as hepatic glycogen due to saturation of the storage site. Increased values of g lead to an increased rate of glycogenolysis; whereas, decreased values of g lead to a decreased rate of glycogenolysis. On the contrary, if $L \ll L^*$, equation (III.13) reduces to

$$\frac{dL}{dt} = V_F \frac{\beta_L B I}{\mathrm{erfc}(\gamma_I L^*)}.$$

Here, the system's hepatic store of energy is nearly depleted. As a response, the system attempts to recover its lacking stores. Increased insulin and glucose concentrations raise the rate of glycogenesis; whereas, decreased insulin and glucose concentrations diminish the rate of glycogenesis.

As done in sections III.3.1 and III.3.2, a series of meal-like inputs are introduced over 24 or 72 hours. As a reminder, the meal-like inputs affect the hormonal response only through the increased blood glucose. Note again, this model contains no feed-forward mechanism that affects the hormone concentrations immediately after the ingestion of a meal. The meal-like inputs are defined by the normalized input-rate function

$$\dot{F}(t) = 0.5 F_0 d^{-3} t^2 e^{-t/d},$$

where d is a measure of the time it takes for the glucose in the meal to enter in the blood stream and F_0 represent the milligrams of glucose carbohydrate consumed in a meal. For this section, let $d = 15$ minutes, $F_0 = 300$ grams of glucose, and $L_0 = L^* = 130,000$ milligrams of glycogen.

Initially, let $\gamma_I = 1 \times 10^{-7}$ and $\gamma_g = 1 \times 10^{-4}$. Fig. 13 illustrates the dynamics of the system over a 24-hour time period. As expected, the small value of γ_I coupled with a large value of γ_g leads to increased hepatic storage of a meal. Over the 24-hour time period, the hepatic glycogen stores increase by approximately 88,000 mg or 67.7%. This trend of increasing hepatic glycogen stores continue through the course of 72 hours. As seen in Fig. 14, glucose, insulin, and glucagon return to their respective basal levels between meals owing to an abundant supply and measured release of available glycogen; however, the glycogen store nearly doubles (2.5726×10^5 mg) the initial store at the end of 72 hours. The solution with these parameter values differs little from the original three-by-three solutions until glycogen stores increase dramatically over long periods of time or until glycogen stores are depleted

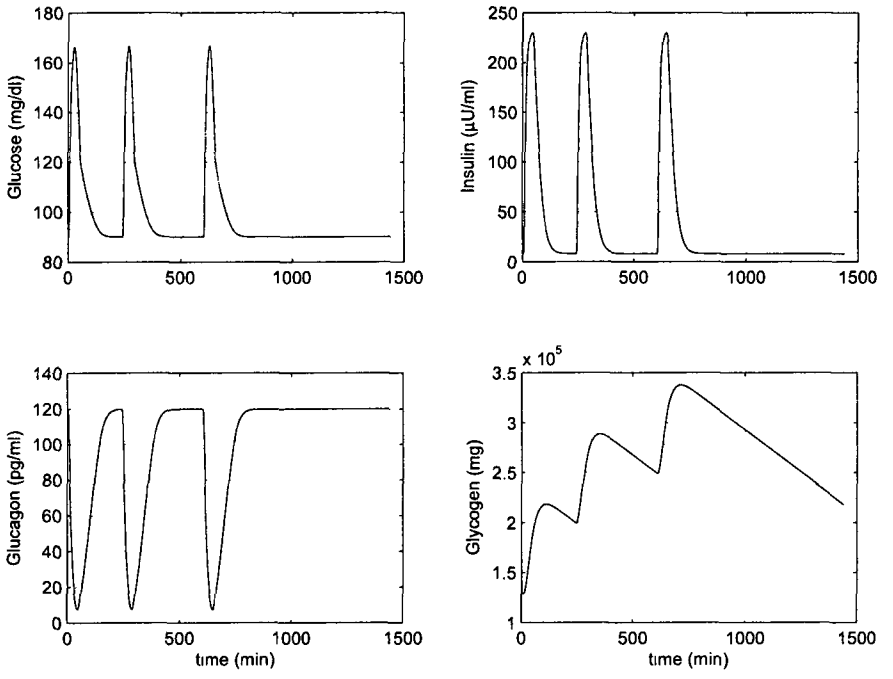

Fig. 13 Combined modified system with $\gamma_I = 1 \times 10^{-7}$ and $\gamma_g = 1 \times 10^{-4}$ over a 24-hour time period.

by cessation of regular meals.

The investigation continues with holding γ_I at $\gamma_I = 1 \times 10^{-7}$ and decreasing γ_g to $\gamma_g = 1 \times 10^{-6}$ (see Fig. 15). In section III.3.2, decreasing γ_g led to a higher blood glucose concentration following the initial meal of the day, and more importantly, the inability of the system to return to it's basal state - even during the overnight period. For these values, the systemic response is almost identical to having only the second modification. As previously demonstrated, control of the system's glycogen is improved but is not fully achieved. In the first 24 hours, hepatic glycogen stores reach a maximum of approximately 306,000 mg and decline during the overnight period to 147,420 mg. Extending the time analysis to 72 hours produces a continuation of the loading-unloading cycle. The nadir in the quantity of glycogen in the liver during the third day is approximately 160,500 mg, representing an increase of 23.5% over the first day nadir. The increasing glycogenolysis rate with elevated glycogen levels leads to the system's inability to maintain homeostasis under the original basal parameters. At the end of the 72-hour time period and just before a meal-like input, the nadir in blood glucose concentration is 91.6937 mg dl^{-1}, representing an increase by nearly 2% in the span of three days. This trend of slowly increasing basal levels

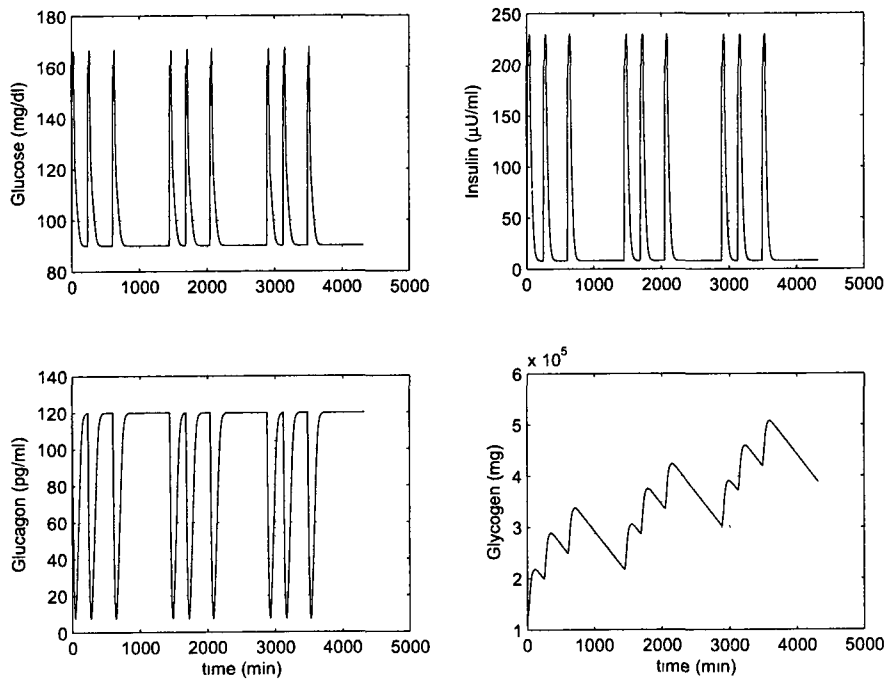

Fig. 14 Combined modified system with $\gamma_I = 1 \times 10^{-7}$ and $\gamma_g = 1 \times 10^{-4}$ over a 72-hour time period.

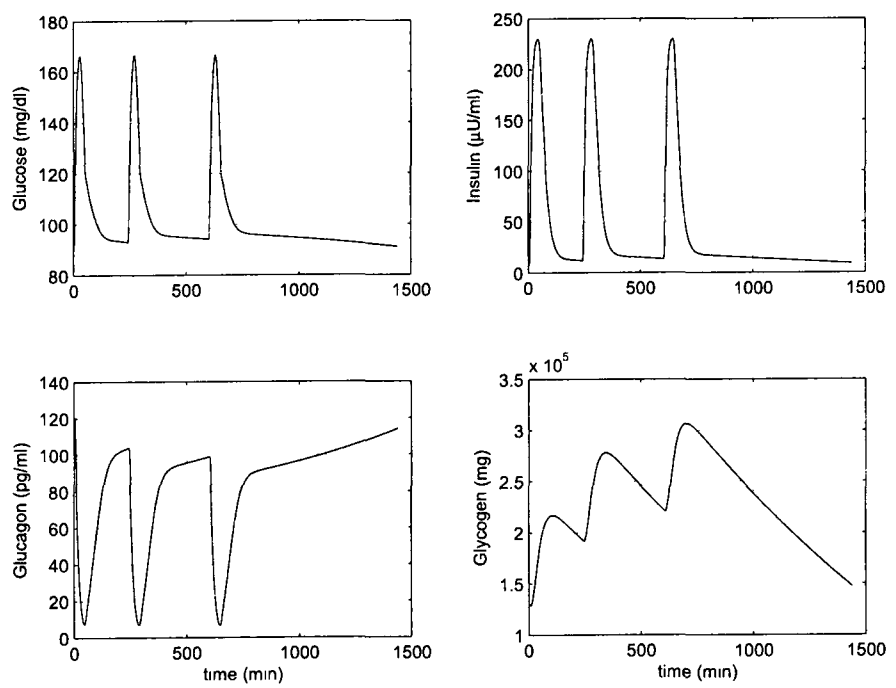

Fig. 15 Combined modified system with $\gamma_I = 1 \times 10^{-7}$ and $\gamma_g = 1 \times 10^{-6}$ over a 24-hour time period.

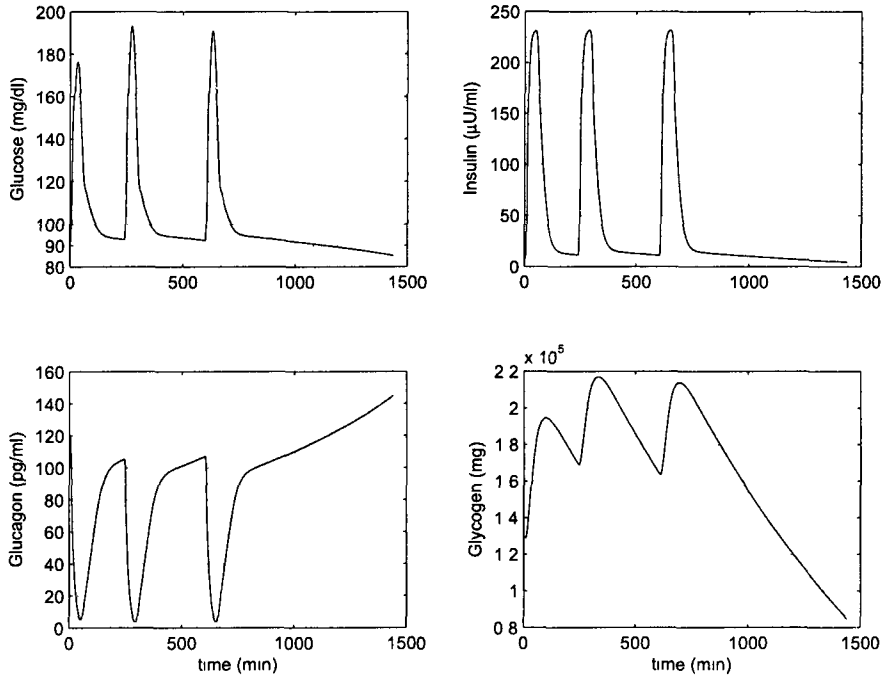

Fig. 16 Combined modified system with $\gamma_I = 5 \times 10^{-6}$ and $\gamma_g = 1 \times 10^{-6}$ over a 24-hour time period.

would continue as time passes.

In this next investigation, assume γ_g remains at 1×10^{-6} while increasing γ_I by a factor of 50 (i.e., decrease glycogen storage when $L > L^*$). Comparing Fig. 16 to Fig. 13, the maximum blood glucose concentration following meals is seen to increase as the storage of hepatic glycogen lessens. In the period between the first two meals, the blood glucose concentration remains slightly elevated owing to the increased glycogenolysis rate when $L > L^*$. During the extended post-absorptive period following the last meal, the steady use of glucose by the central nervous system causes the glycogen store to fall below the value L^*. At this point, the model predicts that the blood glucose begins a steady decrease as the glycogenolysis rate falls and as the glycogenesis rate increases. Both of these rate changes represent an attempt to preserve the hepatic glycogen store. At the end of the 24 hours, the blood glucose concentration is approximately 85 mg dl^{-1}. Extending the analysis to 72 hours (see Fig. 17) reveals that hepatic glycogen remains balanced – neither excessive synthesis nor uptake of glycogen exists. The daily nadir of hepatic glycogen stores is slowly decreasing after each 24-hour period – after the first 24 hours, approximately 84,000 mg is stored in the liver; after 48 hours approximately 82,000 mg is stored in the

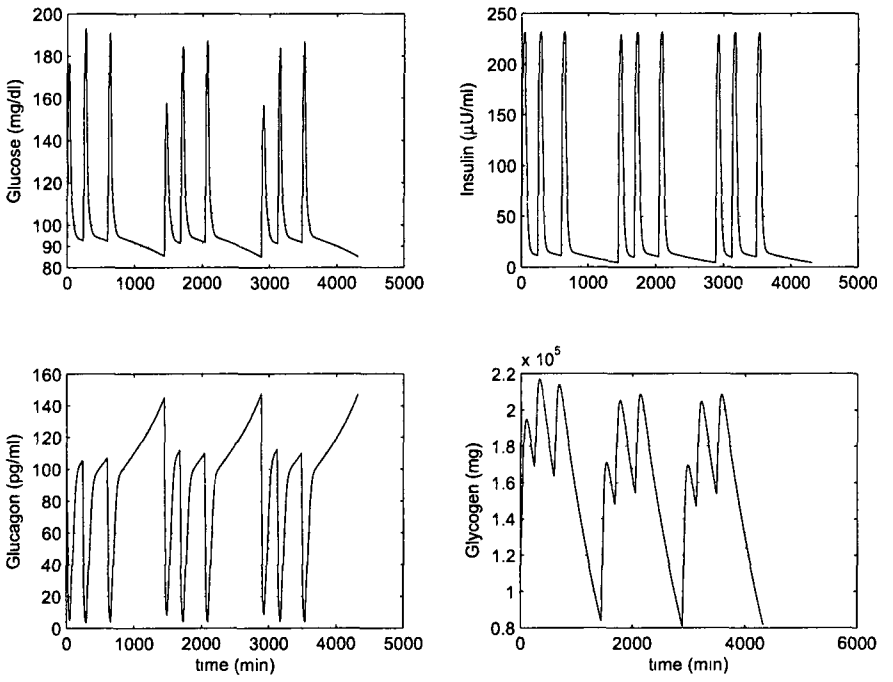

Fig. 17 Combined modified system with $\gamma_I = 5 \times 10^{-6}$ and $\gamma_g = 1 \times 10^{-6}$ over a 72-hour time period.

liver; and, after 72 hours approximately 81,800 mg is stored in the liver. The decline is slow, but needs to be held in check, possibly by a slight increase in feeding.

III.3.4 Adjustment of Combined Modifications

Initially, this investigation started with a three-by-three system that demonstrated short-term control of the blood glucose concentration using glucagon and insulin; however, the model is ill suited as a long-term model of glucose control since it predicts that blood glucose is maintained at a constant basal rate forever in the absence of external energy input. The first two modifications and the combined model account for the loading and depletion of liver glycogen in an attempt to create a new model that demonstrates proper long-term behavior – i.e., regular meals are needed to maintain a non-zero blood glucose level. With $\gamma_I < 1 \times 10^{-6}$ and $\gamma_g \geq 1 \times 10^{-4}$, the new combined modified system shows the same blood glucose control as the original system under regular feeding; however, the glycogen stores increase to unphysical levels over long periods of time. Upon using the values of $\gamma_I = 5 \times 10^{-6}$ and $\gamma_g = 1 \times 10^{-6}$, the model solutions demonstrate systemic control of both the blood glucose concentration and the hepatic glycogen stores during regular feedings along

with demonstrating that the insulin and glucagon concentrations act appropriately. When feedings are stopped, the blood glucose is no longer inappropriately maintained at a non-zero level forever as in the original three-by-three system.

When put into the context of the construction of a fictional species, the model has passed the tests that were laid out in advance:

- to demonstrate a between meal "basal" level of blood glucose, insulin, and glucagon,
- to demonstrate appropriate maximum blood glucose levels after each meal,
- to demonstrate proper loading and unloading of liver glycogen.

Although the model is a success as a fictional species under the prescribed conditions, the model represents just one possibility. In particular, this model was tuned using $L^* = 130,000$ mg and the rates of glycogenolysis and glycogenesis responded as glycogen differed from this level. Perhaps most at odds with the conventional view of the basal levels of blood glucose, glucagon, and insulin being near constant is that the increased glycogenolysis when $L > L^*$ created a slight rise in after meal blood glucose levels. This section explores the effects of using a separate tuning of the glycogenolysis and glycogenesis rates. One may consider this adjustment of the modified system as creating a slightly more advanced fictional species.

Let us now consider an adaptation to equation (III.13) given by

$$\frac{dL}{dt} = V_F \left(\beta_L B I \frac{\operatorname{erfc}(\gamma_I L)}{\operatorname{erfc}(\gamma_I L_I^*)} - \alpha g \frac{\operatorname{erf}(\gamma_g L)}{\operatorname{erf}(\gamma_g L_g^*)} \right). \tag{III.14}$$

The system introduced in section III.3.3 held $L_I^* = L_g^* = 130,000$ mg. An investigation follows examining the effects that changes in the values of L_I^* and L_g^* have on the system. As done previously, three meal-like inputs are prescribed over the course of 24 hours, where $t = 0$ represents 7:59 a.m. Displayed in Fig. 18 are the blood glucose and hepatic-glycogen solutions of the adjusted system with $L_I^* = 90,000$ mg and $L_g^* \in \{90{,}000,\ 130{,}000,\ 170{,}000,\ 210{,}000\}$ while holding $\gamma_I = 5 \times 10^{-6}$ and $\gamma_g = 1 \times 10^{-6}$. From Fig. 11 and Fig. 7,

$$\frac{\operatorname{erf}(\gamma_g L)}{\operatorname{erf}(\gamma_g L_g^*)} > 1 \quad \text{when} \quad L > L_g^*$$

demonstrating an increase in hepatic glycogen stores leads to a rise in the rate of glycogenolysis. Thus, if initial stores are set as $L^* = 130,000$ mg, glycogenolysis occurs sooner and to a greater extent for smaller values of L_g^* and slower for larger L_g^* – see Fig. 18 (bottom) *dashed-dot* and *dotted* lines, respectively. Table 2 details

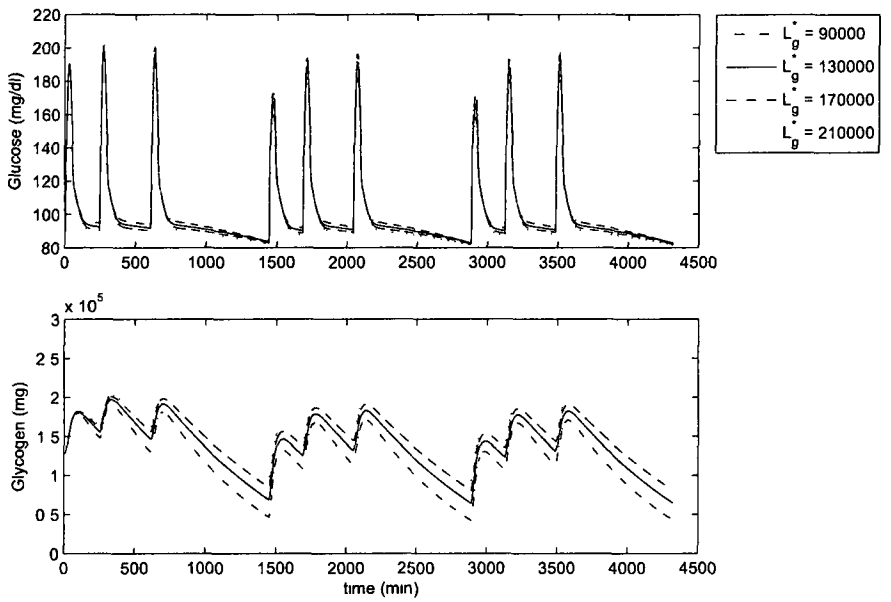

Fig. 18 Blood glucose concentration (top) and liver glycogen quantity (bottom) in the adjusted system system with $L_I^* = 90,000$ mg and $L_g^* \in \{90{,}000,\ 130{,}000,\ 170{,}000,\ 210{,}000\}$ mg over a 72-hour time period.

Table 2
Glycogenolysis factor for varied L_g^*

L_g^*	$1/\operatorname{erf}(\gamma_g L_g^*)$
90,000	9.8736
130,000	6.8556
170,000	5.2634
210,000	4.2823

the numerical impact of this factor. Hepatic loading of the initial meal is nearly independent of the parameter L_g^*, and the maximum blood glucose following the initial meal is nearly identical ($\approx$ 190 mg/dl) for all cases. This independence is due to the small values of g during this time interval. During the post-absorptive phase occurring after the first meal, the differences in the glycogenolysis rates start to become evident. As seen in Table 2, the glycogenolysis rate decreases greatly for increased L_g^*, and by the end of the first post-absorptive phase, the glycogen levels are higher for the large L_g^* cases. The increased glycogenolysis rate for smaller L_g^* leads to an elevated postprandial glucose concentration, and by the end of the first post-absorptive phase, the glycogen levels are lower for the small L_g^* cases. This

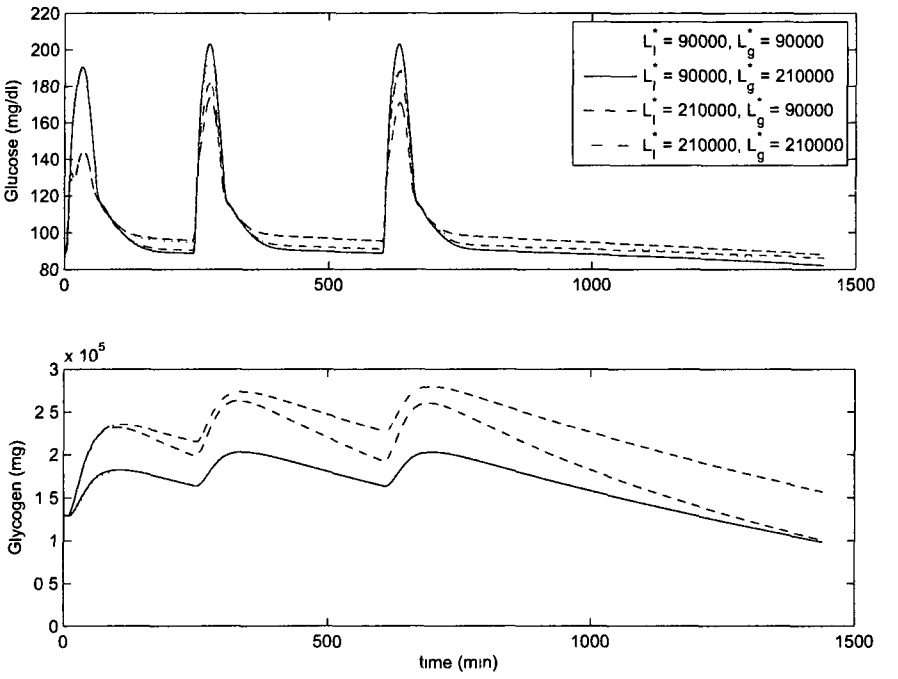

Fig. 19 blood glucose concentration (top) and liver glycogen (bottom) in the adjusted system system mixing values of L_I^* and L_g^* over a 24-hour time period.

difference in glycogen levels leads to a differing response to the consumption of the second meal of the day. The storage through glycogenesis is suppressed by the higher glycogen levels at the time of the second meal consumption, and the maximum blood glucose level is higher for these cases since the glucose supplied by the meal is left in the blood to be used by the central nervous system and the muscles. Thus, a situation develops where the maximum blood glucose is lower when L_g^* is small, but the post-absorptive blood glucose level is higher when L_g^* is small. The nonlinearity of the system is the cause of this unpredictability.

As time progresses, a pattern develops where the blood glucose maximum after the first meal of the day is lower than the blood glucose maximums after the second and third meals. This is a result of the faster loading of the glycogen in the liver. In fact, the dominant trait during the feeding process is the loading of liver. When glycogen stores are significantly above the prescribed value of L_I^*, the glycogenesis rate is suppressed. Once glycogen falls below L_I^*, the glycogenesis rate quickly increases. The effects on the glucose levels has been noted. These traits are illustrated in Fig. 19 upon considering a different level for L_I^*. When comparing the case of $L_I^* = 210,000$ mg to $L_I^* = 90,000$ mg, one finds that loading of the liver during the meal is

Table 3
Glycogenolysis rates during a prolonged fast

Length of fast (hours)	Glycogen Content ($\mu Mol/g$ liver)	Rate of Glycogenolysis ($\mu Mol/kg \cdot min$)
0	300	–
2	260	4.3
4	216	4.3
24	42	1.7
64	16	0.3

significantly increased leading to lower blood glucose maximums. Unloading of the liver is higher when $L_g^* = 90,000$ mg compared to $L_g^* = 210,000$ mg which mostly affects the post-absorptive blood glucose levels.

III.3.5 Gluconeogenesis – A First Look

With the absence of continual feedings, the body relies on its liver glycogen stores to fuel essential functions such as the central nervous system. These stores are limited; therefore, as currently modeled, the individual is doomed within 24 hours if no additional external glucose sources are provided. Missing from the current model is the process of gluconeogenesis which stretches the dwindling stores of hepatic glycogen during a prolonged fast. During the prolonged fast, the rate of glycogenolysis decreases significantly. Table 3 (Smith et al., 2005) shows glycogen content declines to 14% of its original content over the span of a 24-hour fast while the rate of glycogenolysis falls to nearly 40% of the postprandial rate. Extension of the fast to 64 hours continues this decline, and the glycogen content falls to 5.33% of its original content. At this point the glycogenolysis rate slows to 7% of the postprandial rate. Considering that the central nervous system usage remains constant, glucose must be supplied to the body by an increasing rate of gluconeogenesis or other processes such as lipogenolysis.

The model presented in this thesis is now lightly adapted in an attempt to mirror these results. Inclusion of gluconeogenesis as a endogenous source of glucose requires a dependency on the glucagon concentration. Gluconeogenesis is primarily generated from non- carbohydrate carbon substrates (e.g., pyruvate, lactate, glycerol, and amino acids); however, the dependence of the gluconeogenesis rate on the concentration of these quantities is not modeled. Rather, a simplistic form of gluconeogenesis is included in the glucose and liver equations. Here equations (III.10) and (III.13)

are replaced by

$$\frac{dB}{dt} = \dot{F}(t) - \dot{M}_0 - \beta_M BI + G_n \alpha g - \frac{1}{V_F}\frac{dL}{dt}, \tag{III.15}$$

$$\frac{dL}{dt} = V_F\left(\beta_L BI \frac{\mathrm{erfc}(\gamma_I L)}{\mathrm{erfc}(\gamma_I L_I^*)} - (1-G_n)\alpha g \frac{\mathrm{erf}(\gamma_g L)}{\mathrm{erf}(\gamma_g L_g^*)}\right), \tag{III.16}$$

where the constant G_n represents the fraction of glucose provided through gluconeogenesis when $L = L_g^*$. In the absence of the modifications introduced to account for the hepatic glycogen stores (i.e., the original three-by-three system), the results are independent of the value of G_n. The addition of this new term allows for glucose to temporarily remain at basal for an extended postprandial time period in spite of declining hepatic stores. The blood glucose and hepatic-glycogen solutions of the new system over the course of 36 hours are displayed in Fig. 20 with $G_n \in \{0, 0.30\}$. Meals are introduced at 8 a.m., 12 p.m., and 6 p.m. then cease for the remaining 26 hours. With the additional internal glucose source present, the between meal blood glucose concentrations are steadier than when no gluconeogenesis is present.

In both cases where gluconeogenesis is present, the elevated blood glucose concentration causes a slight decline in glycogenolysis, regardless of the amount of glycogen present in the liver – see *solid* and *dotted* lines. In the case where $L_I^* = L_g^* = 210,000$ mg, about 25% of glycogen remains at the end of the 24-hr fast when $G_n = 0$, and about 50% of glycogen remains when $G_n = 0.30$. Similar numbers apply for the other case.

When $G_n = 0$, the maximum blood glucose concentration following the third meal is approximately 188 mg/dl at $t \approx 660$ min. Over the span of the next 25.5 hours, the glucose concentration drops to an end concentration of approximately 74 mg/dl. Hepatic glycogen content is 250,000 mg at $t = 660$ min and is approximately 70,000 mg at the end of the simulation, or a decline of 72% over the span the fast. By increasing G_n to $G_n = 0.30$, the maximum blood glucose concentration following the third meal rises to approximately 192 mg/dl at $t \approx 660$ min. Over the span of the next 25.5 hours, the glucose concentration drops to an end concentration of approximately 86 mg/dl. Hepatic glycogen content is 282,000 mg at $t = 660$ min and is approximately 113,000 mg at the end of the simulation, or a drop of 60% over the span the fast. Most importantly, the blood glucose level remains within normal ranges when $G_n = 0.30$.

Fig. 21 displays the per-minute change in glycogen, dL, with $L_I^* = L_g^* = 210,000$ over an extended non-fed time period starting at the time of peak glucose concentration following the third meal. Net glycogenolysis occurs when $dL < 0$ and net glycogenesis occurs when $dL > 0$. Storage in the liver appears to be unaffected

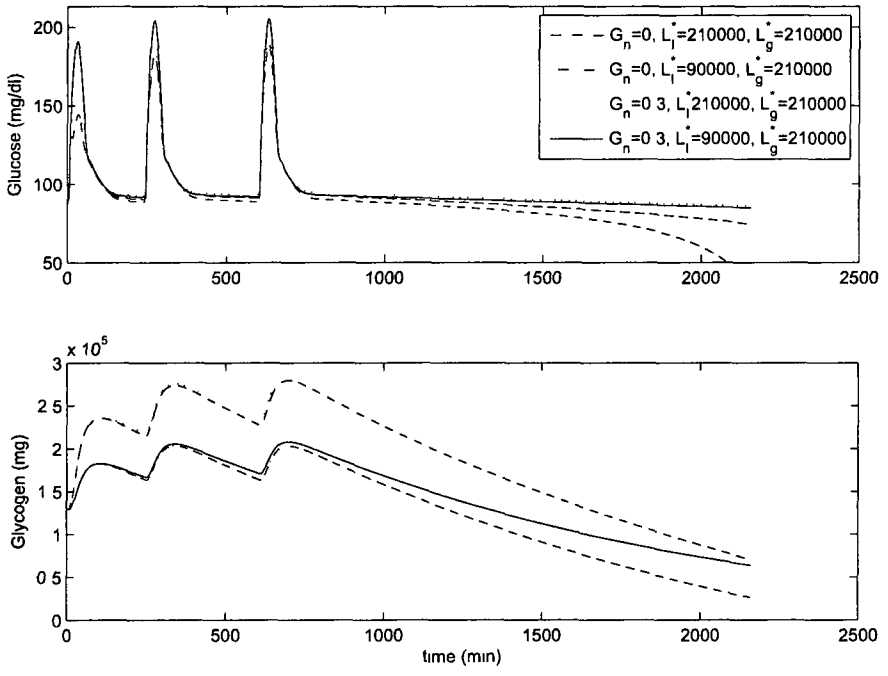

Fig. 20 Blood glucose concentration (top) and liver glycogen quantity (bottom) under gluconeogenesis with $L_l^* \in \{90{,}000,\ 210{,}000\}$ mg, $L_g^* = 210{,}000$ mg, and $G_n \in \{0\ 0.30\}$ over a 36-hour time period.

by the presence of the gluconeogenesis term. After approximately one hour from time of peak glucose, the system shifts from storage into the liver to the usage of glycogen. With gluconeogenesis present, the glycogenolysis rate is slightly decreased; however, this decrease is maintained throughout the fast which leads to significant conservation of glycogen stores.

III.4 FURTHER ANALYSIS

The parameter studies performed in the previous sections provide a start to the validation process. If the model is to approximate the glucose metabolism of a human, the chosen parameter values should provide a reasonable time history of the blood glucose level after a meal. Such time histories were demonstrated in Fig. 19. In addition to approximating the time history, the model is validated by examining the steady state solutions and the response of the body to small perturbations from this steady state.

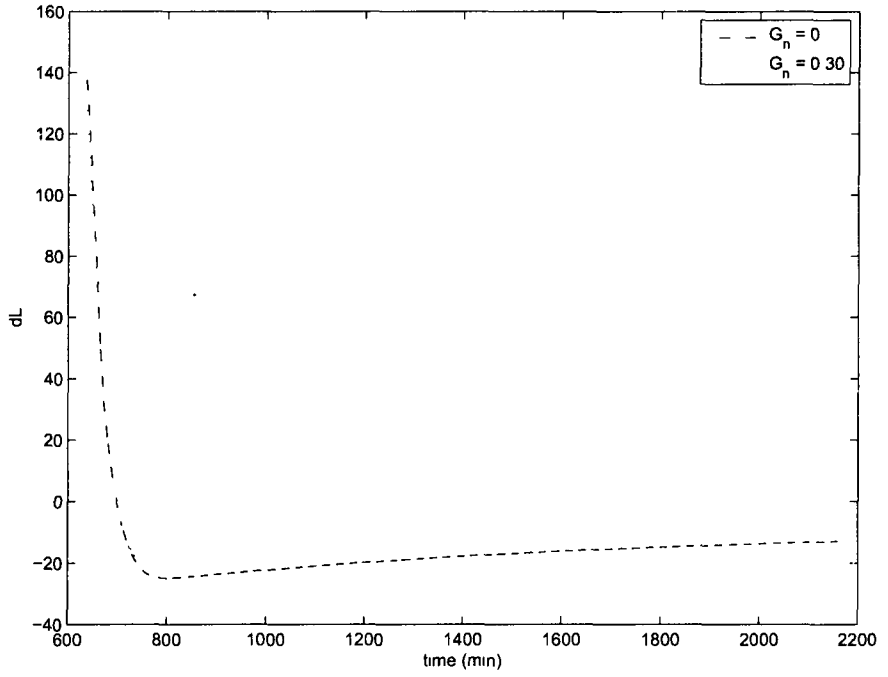

Fig. 21 Rate of change in liver glycogen content during a extended non-feeding period.

III.4.1 Steady States versus Basal States

The basic three-by-three system (equations (III.1)-(III.3)) admits a steady-state solution even when glucose input is zero. It is common to refer to this steady state as the basal state. Since the body is constantly consuming energy in the form of glucose, achieving a steady state under zero-input conditions is a physical impossibility. Thus, the existence of a steady state exposes a fundamental flaw in the basic three-by-three model, i.e., an infinite source of endogenous glucose exists within the model. The first and second modifications address this fundamental flaw. Examining the system, equations (III.10)-(III.12) and (III.14), reveals that a steady state only exists if the glucose input $\dot{F}(t)$ is a constant that exactly meets the body's energy requirements. If the glucose input $\dot{F}(t)$ is less than this energy-balanced value, the body shows continued depletion of the glycogen stores in the liver. If the glucose input $\dot{F}(t)$ is more than this energy-balanced value, the body shows continued growth of the glycogen stores in the liver. Thus, the basal state of the four-by-four system is not a steady-state for all four dependent variables, but does represent a temporary state in which three of the dependent variables (B, I, and g) are near constant and the rate of change of the fourth dependent variable ($\dot{L}$) is also a near constant.

Mathematically, steady-state solutions describe physical conditions that, once established, continue to exist forever; however, the exact conditions required by a

steady-state solution are rarely realized. Examining the stability of a steady-state solution, i.e., examining the response of the system to small deviations from the steady state, is often used to develop criteria delineating the controlled states (exponential decay of disturbances) from the uncontrolled states (exponential growth of disturbances). The structure of the glucose-insulin-glucagon system guarantees that the steady-state solutions are always stable in the classical sense, so a stability analysis does not provide a clear explanation of healthy *vs.* unhealthy states. An alternate view of the linear dynamics of the glucose system is that positive deviations represent responses to necessary energy additions, and these deviations must decay *sufficiently fast* so that the additional glucose is processed before the next meal. Thus, proper control requires more stringent criteria than determining when the system is stable in the sense of exponential decay of disturbances. This aspect of control was studied in Lasseigne and Adams (2011) by using a series of forced initial value problems. Below, a series of forced initial value problems are analyzed to determine the effects of glycogen stores under a variety of conditions. Thus, a more complete understanding of the parameter space for this model is developed.

III.4.2 Linearization

The model is further investigated by examining the solution of the linear system produced by introducing small perturbations to a base state. Two base state cases are considered: the zero-food case $\dot{F}(t) = 0$ and the energy-balanced case $\dot{F}(t) = F^{\#}$. In the latter case, the input rate $F^{\#}$ is chosen such that the net hepatic glucose production rate starts at zero, and the base state remains constant in time. In the former case, the net hepatic glucose production rate is near constant, and the base state is a function of time. The perturbations are modeled to represent the addition of glucose to the system in the form of a very small distributed meal. In the original three-by-three system, the blood glucose concentration in the zero-food case and the energy-balanced case was shown to be maintained by two different mechanisms (see Lasseigne and Adams, 2011). This analysis determines if the level of glycogen affects the results.

The linearization starts from the four-by-four model which is repeated here for

convenience:

$$\frac{dB}{dt} = \dot{F}(t) - \dot{M}_0 - \beta_M BI - \left(\beta_L BI \frac{\mathrm{erfc}(\gamma_I L)}{\mathrm{erfc}(\gamma_I L_I^*)} - \alpha g \frac{\mathrm{erf}(\gamma_g L)}{\mathrm{erf}(\gamma_g L_g^*)}\right), \quad \text{(III.17)}$$

$$\frac{dI}{dt} = -\delta_I I + \dot{Q}_I \left\{\frac{1}{2} + \frac{1}{2}\tanh\left(\frac{B - B_I}{r_I}\right)\right\}, \quad \text{(III.18)}$$

$$\frac{dg}{dt} = -\delta_g g + \dot{Q}_g \left\{\frac{1}{2} + \frac{1}{2}\tanh\left(\frac{B_g - B}{r_g}\right)\right\}, \quad \text{(III.19)}$$

$$\frac{dL}{dt} = V_F \left(\beta_L BI \frac{\mathrm{erfc}(\gamma_I L)}{\mathrm{erfc}(\gamma_I L_I^*)} - \alpha g \frac{\mathrm{erf}(\gamma_g L)}{\mathrm{erf}(\gamma_g L_g^*)}\right). \quad \text{(III.20)}$$

The general form of the above system may be written as

$$\frac{dB}{dt} = F_1(B, I, g, L) + \dot{F}(t), \quad \text{(III.21)}$$

$$\frac{dI}{dt} = F_2(B, I, g, L), \quad \text{(III.22)}$$

$$\frac{dg}{dt} = F_3(B, I, g, L), \quad \text{(III.23)}$$

$$\frac{dL}{dt} = F_4(B, I, g, L). \quad \text{(III.24)}$$

The base state for the zero-food case is defined to satisfy

$$\frac{dB^0}{dt} = F_1(B^0, I^0, g^0, L^0), \quad \text{(III.25)}$$

$$\frac{dI^0}{dt} = F_2(B^0, I^0, g^0, L^0), \quad \text{(III.26)}$$

$$\frac{dg^0}{dt} = F_3(B^0, I^0, g^0, L^0), \quad \text{(III.27)}$$

$$\frac{dL^0}{dt} = F_4(B^0, I^0, g^0, L^0), \quad \text{(III.28)}$$

and the (constant) energy balanced state is defined through:

$$F_1(B^\#, I^\#, g^\#, L^\#) = -\dot{F}^\#, \quad \text{(III.29)}$$

$$F_2(B^\#, I^\#, g^\#, L^\#) = 0, \quad \text{(III.30)}$$

$$F_3(B^\#, I^\#, g^\#, L^\#) = 0, \quad \text{(III.31)}$$

$$F_4(B^\#, I^\#, g^\#, L^\#) = 0. \quad \text{(III.32)}$$

The development of the linear system to be studied is demonstrated for the zero-food

case by introducing the perturbed variables

$$
\begin{aligned}
B &= B^0 + \epsilon \hat{B}, && \text{(III.33)}\\
I &= I^0 + \epsilon \hat{I}, && \text{(III.34)}\\
g &= g^0 + \epsilon \hat{g}, && \text{(III.35)}\\
L &= L^0 + \epsilon \hat{L}, && \text{(III.36)}\\
\dot{F} &= \epsilon \hat{\dot{F}}, && \text{(III.37)}
\end{aligned}
$$

into the governing equations (III.17)-(III.20) and keeping only terms proportional to epsilon. Upon executing this linearization, one obtains

$$
\begin{aligned}
\frac{d\hat{B}}{dt} &= F^0_{1_B}\hat{B} + F^0_{1_I}\hat{I} + F^0_{1_g}\hat{g} + F^0_{1_L}\hat{L} + \hat{\dot{F}}, && \text{(III.38)}\\
\frac{d\hat{I}}{dt} &= F^0_{2_B}\hat{B} + F^0_{2_I}\hat{I} + F^0_{2_g}\hat{g} + F^0_{2_L}\hat{L}, && \text{(III.39)}\\
\frac{d\hat{g}}{dt} &= F^0_{3_B}\hat{B} + F^0_{3_I}\hat{I} + F^0_{3_g}\hat{g} + F^0_{3_L}\hat{L}, && \text{(III.40)}\\
\frac{d\hat{L}}{dt} &= F^0_{4_B}\hat{B} + F^0_{4_I}\hat{I} + F^0_{4_g}\hat{g} + F^0_{4_L}\hat{L}, && \text{(III.41)}
\end{aligned}
$$

where $F^0_{1_B}(t) \equiv \frac{\partial F_1}{\partial B}|_{(B^0(t),\ I^0(t),\ g^0(t),\ L^0(t))}$. The general linear system has 12 non-zero coefficients, either constant or time dependent. The assumptions of constant insulin sensitivity, no mutual- or self-inhibitions of hormonal secretion, and disappearance rates proportional to the hormone concentration lead to the values

$$
\begin{aligned}
F^0_{2_g} &= F^0_{3_I} = F^0_{2_L} = F^0_{3_L} = 0, && \text{(III.42)}\\
F^0_{1_B} &= -\beta_M I^0 - \beta_L I^0 \frac{\operatorname{erfc}(\gamma_I L^0)}{\operatorname{erfc}(\gamma_I L^*_I)}, && \text{(III.43)}\\
F^0_{1_I} &= -\beta_M B^0 - \beta_L B^0 \frac{\operatorname{erfc}(\gamma_I L^0)}{\operatorname{erfc}(\gamma_I L^*_I)}, && \text{(III.44)}\\
F^0_{1_g} &= \alpha \frac{\operatorname{erf}(\gamma_g L^0)}{\operatorname{erf}(\gamma_g L^*_g)}, && \text{(III.45)}\\
F^0_{1_L} &= \frac{2\gamma_I \beta_L B^0 I^0}{\sqrt{\pi}\operatorname{erfc}(\gamma_I L^*_I)} e^{-(\gamma_I L^0)^2} + \frac{2\gamma_g \alpha g^0}{\sqrt{\pi}\operatorname{erf}(\gamma_g L^*_g)} e^{-(\gamma_g L^0)^2}, && \text{(III.46)}\\
F^0_{2_B} &= \frac{\dot{Q}_I}{2r_I}\operatorname{sech}^2\left(\frac{B^0 - B_I}{r_I}\right), && \text{(III.47)}\\
F^0_{2_I} &= -\delta_I, && \text{(III.48)}\\
F^0_{3_B} &= -\frac{\dot{Q}_g}{2r_g}\operatorname{sech}^2\left(\frac{B_g - B^0}{r_g}\right), && \text{(III.49)}\\
F^0_{3_g} &= -\delta_g, && \text{(III.50)}
\end{aligned}
$$

$$F^0_{4_B} = V_F \beta_L I^0 \frac{\mathrm{erfc}(\gamma_I L^0)}{\mathrm{erfc}(\gamma_I L^*_I)}, \tag{III.51}$$

$$F^0_{4_I} = V_F \beta_L B^0 \frac{\mathrm{erfc}(\gamma_I L^0)}{\mathrm{erfc}(\gamma_I L^*_I)}, \tag{III.52}$$

$$F^0_{4_g} = -V_F \alpha \frac{\mathrm{erfc}(\gamma_g L^0)}{\mathrm{erf}(\gamma_g L^*_g)}, \tag{III.53}$$

$$F^0_{4_L} = -\frac{2V_F \gamma_I \beta_L B^0 I^0}{\sqrt{\pi}\,\mathrm{erfc}(\gamma_I L^*_I)} e^{-(\gamma_I L^0)^2} - \frac{2V_F \gamma_g \alpha g^0}{\sqrt{\pi}\,\mathrm{erf}(\gamma_g L^*_g)} e^{-(\gamma_g L^0)^2}. \tag{III.54}$$

Upon defining $F^0_{2_B} \equiv \dot{q}^0_I$, $F^0_{3_B} \equiv -\dot{q}^0_g$, $F^0_{1_L} \equiv \nu^0_1$, $F^0_{4_L} \equiv -V_F \nu^0_1$, $\bar{\beta}_L \equiv \beta_L \frac{\mathrm{erfc}(\gamma_I L^0)}{\mathrm{erfc}(\gamma_I L^*_I)}$, and $\bar{\alpha} \equiv \alpha \frac{\mathrm{erf}(\gamma_g L^0)}{\mathrm{erf}(\gamma_g L^*_g)}$, the system reduces to

$$\frac{d}{dt}\hat{\mathbf{x}} = \mathbf{A}^0(t)\hat{\mathbf{x}} + \hat{\dot{\mathbf{F}}}(t), \tag{III.55}$$

where

$$\hat{\mathbf{x}} = \begin{bmatrix} \hat{B} \\ \hat{I} \\ \hat{g} \\ \hat{L} \end{bmatrix}, \tag{III.56}$$

$$\mathbf{A}^0(t) = \begin{bmatrix} -\left(\beta_M + \bar{\beta}_L\right) I^0 & -\left(\beta_M + \bar{\beta}_L\right) B^0 & \bar{\alpha} & \nu^0_1 \\ \dot{q}^0_I & -\delta_I & 0 & 0 \\ -\dot{q}^0_g & 0 & -\delta_g & 0 \\ V_F \bar{\beta}_L I^0 & V_F \bar{\beta}_L B^0 & -V_F \bar{\alpha} & -V_F \nu^0_1 \end{bmatrix}, \tag{III.57}$$

and

$$\hat{\dot{\mathbf{F}}}(t) = \begin{bmatrix} \hat{\dot{F}}(t) \\ 0 \\ 0 \\ 0 \end{bmatrix}. \tag{III.58}$$

The above system is written in terms of the base-state delineated by using the naught superscript. A similar system governing the disturbance variables exists for the energy-balanced case using the pound superscript to represent the base quantities. It should be noted that for the energy-balanced case, the glucose input term is written as $\dot{F} = \dot{F}^{\#} + \epsilon \hat{\dot{F}}$ instead of $\dot{F} = \epsilon \hat{\dot{F}}$.

Under standard stability analysis, control is achieved if all eigenvalues of the coefficient matrix $\mathbf{A}^0$ have negative real parts and the solution demonstrates exponential return to the steady-state. The eigenvalues under basal-state conditions and energy-balanced conditions are examined; however, as shown for the three-by-three case (see Lasseigne and Adams, 2011), the stability analysis focused on the existence of exponentially decaying solutions is insufficient in determining the control to meal-like inputs. Therefore, in addition to determining the eigenvalues, the responses of glucose, insulin, glucagon, and glycogen to the normalized input $\hat{\dot{F}}(t) = 0.5d^{-3}t^2e^{-t/d}$ are also examined.

Zero-Food Input Case

With no external source of energy, the system is reliant on its internal stores of hepatic glycogen to fuel the system. This being so, it is not possible to achieve steady glucose, insulin, and glucagon levels unless it is that which describes a system that is over saturated with glycogen. Further analysis is found in section IV.2.1 for this "well-fed state." The system *sans* external energy sources can also enter a "near-starved state" where hepatic glycogen stores are near depletion. See section IV.2.2 for additional analysis of a system in the near-starved state. Although a steady state is not achievable without an exogenous source of glucose, a linear analysis of the system can be completed under the assumption $\dot{F}(t) = 0$.

It is desired to examine the case where $B^0(0) = B^* = 90$, $I^0(0) = I^* = 8$, $g^0(0) = g^* = 120$, and $L^0(0) = L^* = L_0$. Parameter values in the original three-by-three system were chosen such that these basal values could be maintained for all time. The four-by-four system uses these parameter values which leads to insulin and glucagon starting in homeostasis denoted as

$$\begin{aligned} \left.\frac{dI^0}{dt}\right|_{t=0} &= 0, \\ \left.\frac{dg^0}{dt}\right|_{t=0} &= 0. \end{aligned}$$

Whether or not the blood glucose also starts out in homeostasis, $\frac{dB^0}{dt}(0) = 0$, depends on the initial net glycogenolysis rate defined as $\frac{dL^0}{dt}(0) = -\dot{L}_0$. The value $\dot{L}_0 = 170$ produces a homeostatic start, and the results of the four-by-four system should be compared to the results of the original three-by-three system with the constant basal state. For each choice of L_I^* and L_g^* a homeostatic start only occurs for a specific value of the initial glycogen level, L_0. If the choices $L_I^* = L_g^* = L^*$ are made, then the specific value is $L_0 = L^*$. If values of $L_I^* \neq L_g^* \neq L^*$ are chosen, then the value L_0 needs to be adjusted so that the system starts in homeostasis. The effects of changing

Table 4
Initial net glycogenolysis rates for chosen L_I^*, L_g^*, and L_0

L_I^*	L_g^*	L_0	$\dot{L}_0$
90000	90000	130000	−271.360
90000	130000	130000	−181.134
90000	210000	130000	−104.165
90000	90000	210000	−463.480
90000	130000	210000	−319.001
90000	210000	210000	−195.8207
90000	130000	900000	−107.339
90000	210000	90000	−53.9104
130000	90000	130000	−260.247
130000	90000	210000	−459.217
130000	210000	130000	−93.051
210000	90000	90000	−71.548
210000	90000	130000	−204.169
210000	90000	210000	−437.667
210000	130000	130000	−113.923

the parameters L_I^*, L_g^*, and L_0 on the initial net glycogenolysis rate are summarized in Table 4. For the cases indicating a decrease in this rate ($|\dot{L}_0| < 170$), the system does not have enough glycogen and the base state approaches hypoglycemia. These cases are possible after an overnight fast. For the cases resulting in an increase in this rate, the blood glucose concentration initially elevates; however, the hyperglycemia has a finite duration as hepatic glycogen stores are decreasing and limited. A stability analysis of the linear system is only appropriate for the cases of near homeostasis.

In order to achieve homeostasis in the case of zero food input, a more appropriate value of L_0 is required for each pair of specified values L_I^* and L_g^*. Define

$$\theta_I = \frac{\beta_L B^* I^*}{\operatorname{erfc}(\gamma_I L_I^*)}, \tag{III.59}$$

$$\theta_g = \frac{\alpha g^*}{\operatorname{erf}(\gamma_g L_g^*)}, \tag{III.60}$$

$$\Theta(L) = -\theta_I \operatorname{erfc}(\gamma_I L) + \theta_g \operatorname{erf}(\gamma_g L), \tag{III.61}$$

where the choice of $L_I^* = 90,000$ mg and $L_g^* = 210,000$ mg is made based on the observations from section III.3.4. The value of L_0 producing initial homeostasis satisfies $V_F\Theta(L_0) = 170$. As seen in Fig. 22, the intersection of $V_F\Theta(L)$ and 170 occurs at $L_0 = 186,390$ mg. Upon referring to the results from section III.3.4, the

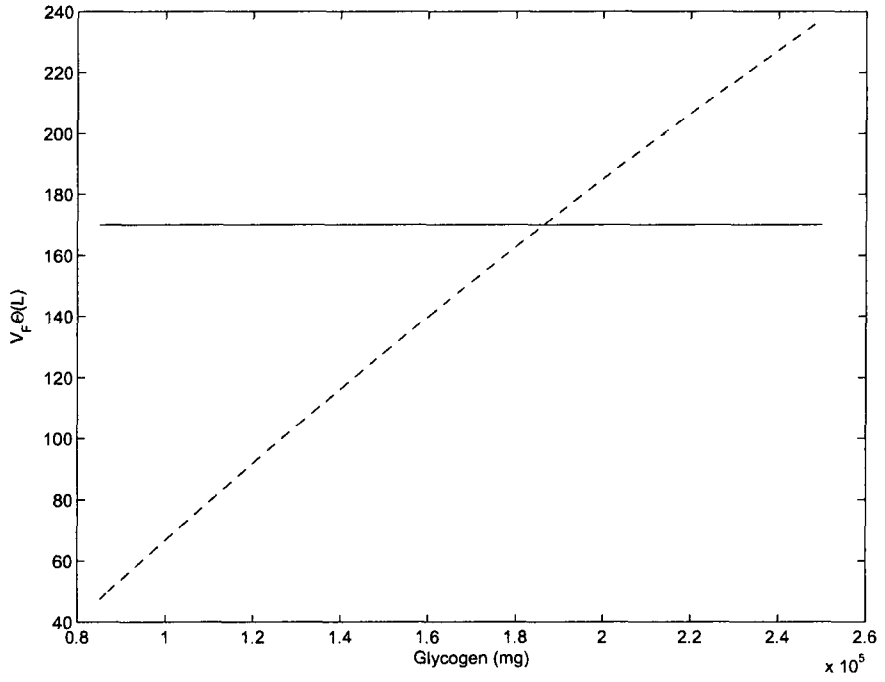

Fig. 22 $V_F\Theta(L)$ versus L intersecting the glycogenolysis rate of 170 mg/min.

value $L_0 = 186,390$ is found to be within the range maintained throughout the day by continuous feeding. Thus, the net rate of glycogenolysis is near the value 170, and the body is near homeostasis during the zero-food post-absorptive period.

The four eigenvalues of the initial coefficient matrix $\mathbf{A}^0(0)$, subject to setting $B^0 = B^*$, $I^0 = I^*$, $g^0 = g^*$, and $L^0 = L_0 = 186,390$, are given in Table 5 and is hereafter referred to as Case I. For comparison, the eigenvalues from the original three-by-three system are also included in Table 5. The real part of each eigenvalue is negative, thus the zero-food case corresponding to basal conditions is considered linearly stable; however, as shown in Lasseigne and Adams (2011), the imaginary part of the complex eigenvalue pair is more important in controlling the blood glucose response to a distributed input. Note that this imaginary part for the four-by-four system is slightly less than the imaginary part for the three-by-three system. As shown below, this slightly lessens the control of the blood glucose response to distributed input.

As might be imagined after an extended overnight fast, the initial glycogen level in the morning could be $L_0 = 90,000$. Using this value in the Jacobi matrix, the eigenvalues of the matrix, $\mathbf{A}^0(0)$, are given in Table 5 and hereafter referred to as Case II. As compared to the Case I, the imaginary part of the complex eigenvalue

Table 5
Eigenvalues of coefficient matrix $\mathbf{A}^0$ under varied conditions.

Case	λ_1	λ_2	$\lambda_{3,4}$
3 x 3	—	-0.1002	$-0.0644 \pm 0.1274i$
I	-0.0005545	-0.1032	$-0.06220 \pm 0.1121i$
II	-0.0006755	-0.09123	$-0.06918 \pm 0.1134i$
III	-0.0004559	-0.1212	$-0.05102 \pm 0.05225i$

pair is nearly the same, but the real parts slightly differ. It is impossible to know the effects of these differences until a specific initial value problem is solved. It should be noted that Case II is somewhat artificial as $|\dot{L}_0| < 170$ and the system does not start near homeostasis. Alternatively, the base state is allowed to progress in time until near homeostatic conditions exist (say $t = 80$), and these values are then chosen as new initial conditions for the depleted glycogen case. The eigenvalues of $\mathbf{A}^0(0)$ using the initial base-state values, $B_0 = 79.32$, $I_0 = 1.99$, $g_0 = 180.48$, $L_0 = 81,625$, are given in Table 5 and hereafter referred to as Case III. The real part of the eigenvalues indicates slightly slower decay of the responses; however, the imaginary part is half the value of the previous cases which leads to considerably slower control in response to distributed input. For reference, the time history of the base state subject to the above initial conditions is given in Fig. 23. Near homeostatic conditions are seen to exist in Case I and Case III, and the transient to near homeostatic conditions is seen in the Case II.

The time history of the linear system subject to non-zero $\hat{\hat{F}}(t)$ explores how the body responds to small inputs when the body is near homeostasis. First, the base state is held constant, and the solution to equation (III.55) with $\mathbf{A}^0(t)$ is replaced by $\mathbf{A}^0(0)$ is examined subject to both an impulsive load $\hat{\hat{F}}(t) = \delta(t)$ and a distributed load $\hat{\hat{F}}(t) = 0.5d^{-3}t^2e^{-t/d}$. Upon examining the response to the impulsive load, the original three-by-three system, Case I and Case II all show "overcorrection" of the disturbance in the blood glucose level occurring about 15 minutes after the impulsive load. On the contrary, Case III shows steady decay in the perturbed blood glucose level. In all cases, the disturbance has essentially vanished within 80 minutes. Mathematically, the difference in the responses is directly traceable to the imaginary part of the eigenvalues which is significantly less in Case III. Biologically, the difference in the responses is directly traceable to the difference in the secretion of insulin. Case III shows significantly less initial secretion leading to the initially slower correction of the blood glucose disturbance. Higher perturbed insulin levels in the other cases promote

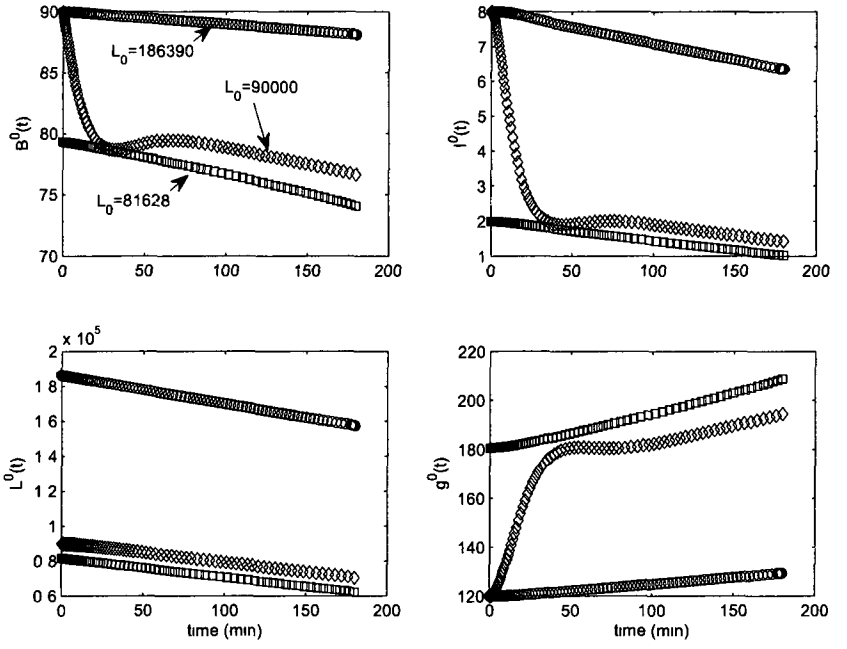

Fig. 23 Time history of base states

faster uptake of perturbed blood glucose, including faster storage as glycogen evidenced by the difference in the $\hat{L}$ variable. The perturbed glucagon also responds to the impulsive load. Negative values of $\hat{g}$ indicate that glucagon has been suppressed. These negative values also lead to a positive response in the $\hat{L}$ variable which is interpreted as a decrease in the rate of glycogenolysis relative to the base state. The initial suppression of the glucagon secretion rate is the same for all cases. In all but Case III, the perturbed blood glucose responds to the increased in perturbed insulin. The perturbed insulin and perturbed glucagon secretion rates subsequently adjust to the blood glucose response. This results in an oscillatory response of these three perturbed variables which decay at a rate highly dependent on the disappearance rates of insulin and glucagon (see Lasseigne and Adams, 2011). The perturbed insulin and glucagon responses are out of phase in relation to the perturbed blood glucose response. As these variables approach zero, the perturbed value $\hat{L}$ nears a constant since there is no further glycogenesis or suppression of glycogenolysis. Thus, a net increase of stored glycogen due to the impulsive load occurs. On a time scale much greater than two hours, the excess stored glycogen is released, and $\hat{L}$ slowly approaches zero. The release rate for $\hat{L}$ is greater when the base state L_0 is lower.

Lasseigne and Adams (2011) showed that the response to the distributed input is

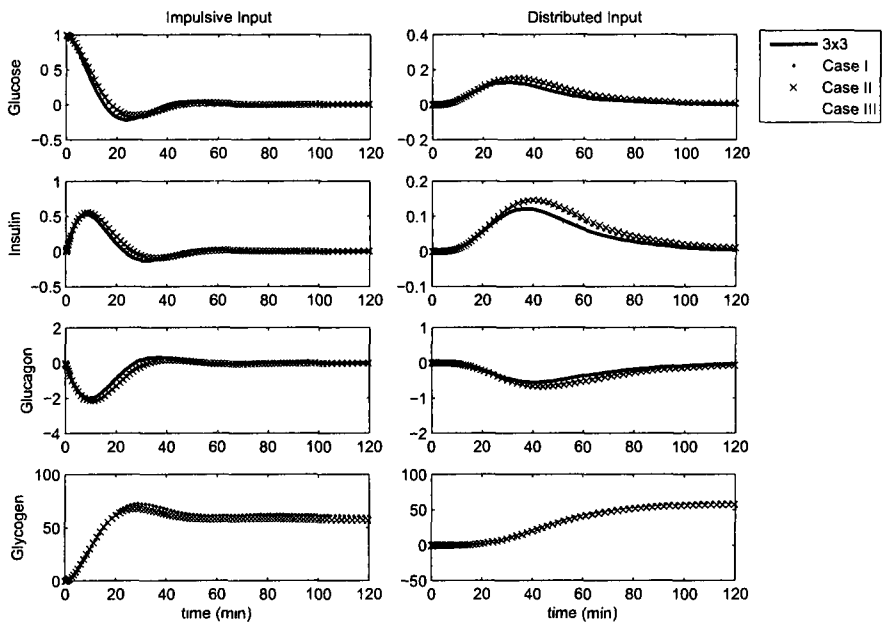

Fig. 24 System response to impulsive and distributed input under constant conditions.

highly dependent on the imaginary part of the complex eigenvalue pair. Thus, Case III with a smaller imaginary part of the eigenvalue is expected to show the least blood glucose control to the distributed input, and Case I and Case II should show slightly less control than the original three-by-three system. These expectations are clearly realized in Fig. 24 using $d = 15$ for the distributed input. As in the impulsive response, the net increase in stored glycogen due to the distributed load is greater in Case III. As previously mentioned, the imaginary part of the eigenvalue in Case I and in Case II is slightly greater than in the original three-by-three system. This leads to slower control of the perturbed blood glucose response to the distributed input for these two cases in spite of a greater perturbed insulin and glucagon response. A close examination shows that the initial perturbed secretion rates of insulin and glucagon are identical for the original three-by-three system, Case I, and Case II. However, the insulin effectiveness $F^0_{1_I}$ is the same or smaller in Case I and Case II, and the glucagon effectiveness $F^0_{1_g}$ is smaller in both Case I and Case II. Thus, the initial blood glucose control is slower, and Case I and Case II need more insulin and less glucagon for long-time control. Overall, these results combined with the results from Lasseigne and Adams (2011) show that the processing of an external input depends mostly on the base blood glucose level at the time of input. Higher base blood glucose levels produce faster control in the linear system, mostly due to

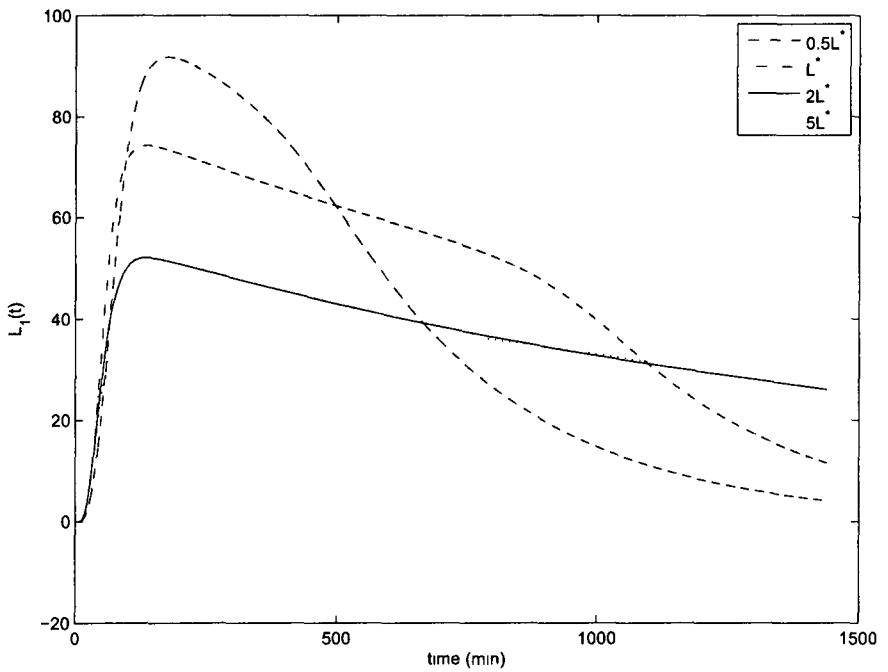

Fig. 25 Glycogen loading and unloading of a meal with four different initial values of $L_0(0)$ under a 24-hr time period.

faster insulin response at the higher base blood glucose levels. As expected, control is mostly determined through a combination of the effects of secretion rate responses and effectiveness of the two counter-regulatory hormones.

To finish the analysis, recall that the system does not provide a steady-state solution under the condition of zero-food input in the base state. Thus, the above analysis should be repeated by solving equation (III.55) subject to $\mathbf{A}^0(t)$ rather than $\mathbf{A}^0(0)$. For Case I and Case III, Fig. 23 shows that the base state is near homeostasis. Upon calculating the solution over a two-hour period, very little difference is found by using $\mathbf{A}^0(t)$ rather than $\mathbf{A}^0(0)$ for these cases (graph not shown). Thus, the response to small external inputs discovered above are applicable to the post-absorptive states which are near homeostasis, and one needs the current blood glucose, insulin, glucagon and glycogen levels to determine the response to small perturbations on the time scale of absorbing a meal.

The final calculation, shown in Fig. 25, demonstrates the differences in the perturbed glycogen response to a meal for the cases with initial glycogen loads $L^0(0) = .5L^*, L^*, 2L^*, 5L^*$ where $L^* = 130,000$ mg. The initial rate of loading is greater for the smaller values of $L^0(0)$ and continues for a longer period of time. After the absorption, the cases with a lower initial glycogen load call upon the perturbed stores much sooner than the cases with a higher initial glycogen load.

Energy-Balanced Input Case

Presently, with the model not including a second endogenous source, such as the inclusion of gluconeogenesis briefly mentioned in section III.3.5, a steady state under the conditions of zero-food input is not possible. With the introduction of a constant-rate exogenous source of glucose, it is possible for the system to achieve a steady-state solution.

In the original three-by-three system, a set point exists for each individual where the input rate exactly matches the resting usage rate, $\dot{F}_0 = \dot{M}_0 + \beta_M B^{\#} I^{\#}$. The external source of energy replaces the system's reliance on the hepatic stores to maintain a constant blood glucose level. Thus, the net hepatic output is zero, i.e., $\alpha g^{\#} - \beta_L B^{\#} I^{\#} = 0$. The generalized three-by-three system in steady state form is

$$0 = \alpha g^{\#} - \beta_L B^{\#} I^{\#}, \tag{III.62}$$

$$0 = -\delta_I I^{\#} + \dot{Q}_I \left\{ \frac{1}{2} + \frac{1}{2} \tanh\left(\frac{B^{\#} - B_I}{r_I} \right) \right\}, \tag{III.63}$$

$$0 = -\delta_g g^{\#} + \dot{Q}_g \left\{ \frac{1}{2} + \frac{1}{2} \tanh\left(\frac{B_g - B^{\#}}{r_g} \right) \right\} \tag{III.64}$$

Solving for $I^{\#}$ and $g^{\#}$ from equations (III.63) and (III.64), respectively, and substituting into equation (III.62) yields

$$\frac{\alpha \dot{Q}_g}{\delta_g} \left[\frac{1}{2} + \frac{1}{2} \tanh\left(\frac{B_g - B^{\#}}{r_g} \right) \right] = \frac{\beta_L B^{\#} \dot{Q}_I}{\delta_I} \left[\frac{1}{2} + \frac{1}{2} \tanh\left(\frac{B^{\#} - B_I}{r_I} \right) \right]. \tag{III.65}$$

Upon defining $\beta^{\#}$ as

$$\beta^{\#} = \frac{\beta_L \dot{Q}_I \delta g}{\alpha \dot{Q}_g \delta_I}, \tag{III.66}$$

equation (III.65) becomes

$$\frac{1}{2} + \frac{1}{2} \tanh\left(\frac{B_g - B^{\#}}{r_g} \right) = \beta^{\#} B^{\#} \left[\frac{1}{2} + \frac{1}{2} \tanh\left(\frac{B^{\#} - B_I}{r_I} \right) \right]. \tag{III.67}$$

All four baseline individuals have the same normalized glucose-synthesis function (left-hand side of equation (III.67)); whereas, the normalized glucose-uptake function (right-hand side of equation (III.67)) depends on the values of B_I and r_I which change with each individual and are previously defined in Table 1. The intersection of the normalized glucose-synthesis function and the normalized glucose-uptake function for each of the four baseline individuals identifies the glucose energy-balanced set point $B^{\#}$ as seen in Fig. 26 and Fig. 27.

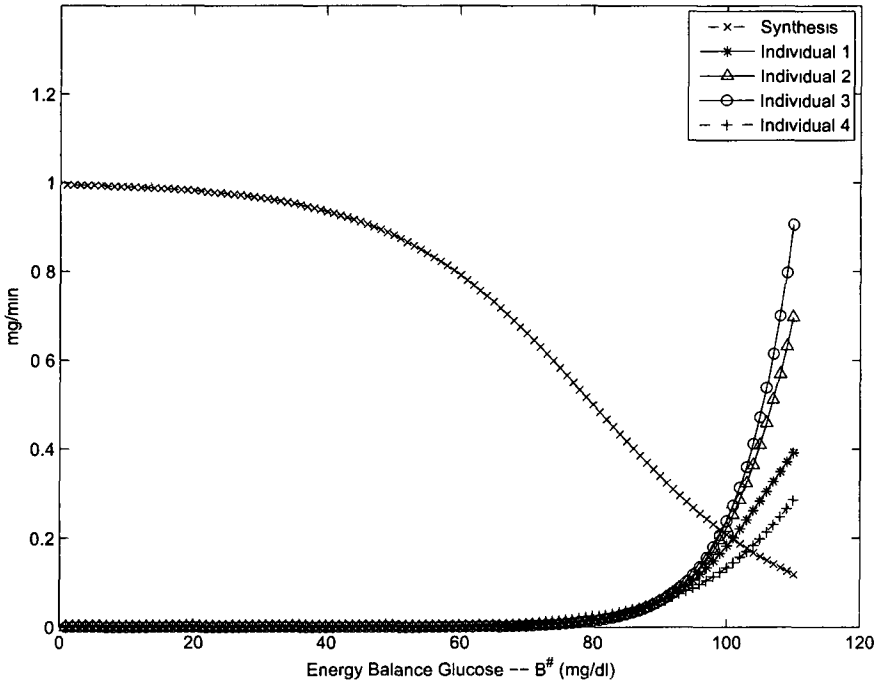

Fig. 26 Energy-balanced set point: Synthesis vs. Uptake for four baseline individuals

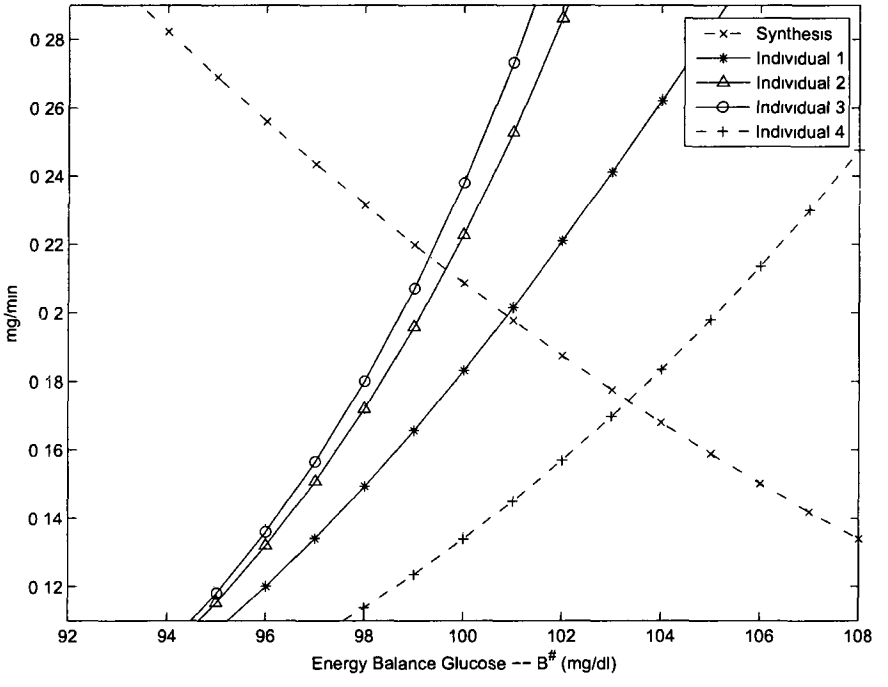

Fig. 27 Energy-balanced set point – zoomed in view of Fig. 26

Table 6
Energy-balanced set points of glucose, insulin, and glucagon in three-by-three system for four base-line individuals

Individual	$B^{\#}$	$I^{\#}$	$g^{\#}$
1	100.8703	30.6804	70.4597
2	99.6249	33.1109	75.2617
3	99.3033	33.7977	76.5398
4	103.3348	26.1978	61.6446

Substituting the glucose energy-balanced set point of each individual into equations (III.63) and (III.64) leads to the energy-balanced set points for insulin and glucagon, respectively. Table 6 lists the energy-balanced set point for glucose $B^{\#}$, insulin $I^{\#}$, and glucagon $g^{\#}$ for the four baseline individuals. Further analysis in this section considers expanding the three-by-three system to cover the mechanics of the hepatic glycogen in individual #2, the base-line individual of choice. The four-equation steady-state system is given by

$$0 = \dot{F}^{\#} - \dot{M}_0 - \beta_M B^{\#} I^{\#}, \tag{III.68}$$

$$0 = -\delta_I I^{\#} + \dot{Q}_I \left\{ \frac{1}{2} + \frac{1}{2} \tanh\left(\frac{B^{\#} - B_I}{r_I} \right) \right\}, \tag{III.69}$$

$$0 = -\delta_g g^{\#} + \dot{Q}_g \left\{ \frac{1}{2} + \frac{1}{2} \tanh\left(\frac{B_g - B^{\#}}{r_g} \right) \right\}, \tag{III.70}$$

$$0 = V_F \left(\beta_L B^{\#} I^{\#} \frac{\operatorname{erfc}(\gamma_I L^{\#})}{\operatorname{erfc}(\gamma_I L_I^*)} - \alpha g^{\#} \frac{\operatorname{erf}(\gamma_g L^{\#})}{\operatorname{erf}(\gamma_g L_g^*)} \right), \tag{III.71}$$

and the system has five unknowns. The original system was a three-equation, steady-state system in four unknowns, and an extra condition of zero net hepatic glucose production provided a fourth equation that led to a unique solution. Here, the fourth equation naturally represents the steady-state as a situation of zero net hepatic glucose production; however a fifth variable, the current glycogen level $L^{\#}$ is present. Thus, a unique solution will not exist. As seen in the case presented in section III.4.2, a steady state is unachievable if $\dot{F}^{\#} = 0$ and glycogen is in flux. A near homeostatic condition was achieved by determining initial conditions such that $\dot{L}^0$ was initially zero; however, in all cases, $\dot{L}^0$ did not remain zero as needed for a steady state. Thus, $\dot{F}^{\#}$ must attain a minimum value for steady state to exist. For each value of $\dot{F}^{\#}$ above this minimum, a unique set of values for the variables $B^{\#}$, $I^{\#}$, $g^{\#}$, and $L^{\#}$ produce a steady state. It is possible that a maximum value of $\dot{F}^{\#}$ may also exist above which no steady state occurs.

Although biologically the metabolic variables follow the input rate, it is mathematically easier to specify the glycogen level and then determine the input rate that leads to steady state. Thus, begin by choosing an $L^{\#}$ which reduces equation (III.68) to

$$\beta_L B^{\#} I^{\#} \frac{\operatorname{erfc}(\gamma_I L^{\#})}{\operatorname{erfc}(\gamma_I L_I^*)} = \alpha g^{\#} \frac{\operatorname{erf}(\gamma_g L^{\#})}{\operatorname{erf}(\gamma_g L_g^*)}. \tag{III.72}$$

Substituting the equivalent expressions of $I^{\#}$ and $g^{\#}$ from equations (III.69) and (III.70) into equation (III.72) and rearranging terms yields

$$\frac{1}{2} + \frac{1}{2}\tanh\left(\frac{B_g - B^{\#}}{r_g}\right) = B^{\#}\beta^{\#}\left(\frac{1}{2} + \frac{1}{2}\tanh\left(\frac{B_g - B^{\#}}{r_g}\right)\right) E^{\#}, \tag{III.73}$$

where

$$E^{\#} = \frac{\operatorname{erfc}(\gamma_I L^{\#})\operatorname{erf}(\gamma_g L_g^*)}{\operatorname{erfc}(\gamma_I L_I^*)\operatorname{erf}(\gamma_g L^{\#})}$$

and $\beta^{\#}$ as previously defined (see equation (III.66)). Equation (III.73) is primarily a function of $B^{\#}$. Plotting the left-hand side versus the right-hand side, the intersection is the value of the glucose set point for the chosen $L^{\#}$. Once the glucose set point is determined, the corresponding insulin and glucagon set points are derived, and then the appropriate energy-balanced input, $\dot{F}^{\#} = \dot{M}_0 + \beta_L B^{\#} I^{\#}$, is calculated. Fig. 28 displays the energy-balanced glucose set point, $B^{\#}$, associated with $L^{\#} = 100,000$, $L^{\#} = 130,000$, $L^{\#} = 170,000$, and $L^{\#} = 200,000$. Table 7 lists the corresponding values of $B^{\#}$, $I^{\#}$, $g^{\#}$, and $F^{\#}$ for each chosen $L^{\#}$. Note that the lowest glycogen energy-balanced set point, $L^{\#} = 10,000$, leads to the lowest glucose energy-balanced set point. In fact, as $\dot{F}^{\#}$ approaches the constant insulin-independent uptake rate $\dot{M}_0 \approx .77$ from above, the quantities $L^{\#}$ and $B^{\#}$ approach zero. Even with the glycogen level as low as $L^{\#} = 10,000$, the energy-balanced glucose set point is still a reasonable $B^{\#} \approx 80$ and the corresponding input rate is $\dot{F}^{\#} \approx 0.8948$. With $L^{\#} = 500,000$, the energy-balanced glucose set point is $B^{\#} \approx 180$ and the corresponding input rate is $\dot{F}^{\#} \approx 32.2286$.

The generalized Jacobi matrix defined in equation (III.57) is updated under energy-balanced conditions and is written as

$$\mathbf{A}(t) = \begin{bmatrix} -\left(\beta_M + \bar{\beta}_L\right) I^{\#} & -\left(\beta_M + \bar{\beta}_L\right) B^{\#} & \bar{\alpha} & \nu_1^{\#} \\ \dot{q}_I^{\#} & -\delta_I & 0 & 0 \\ -\dot{q}_g^{\#} & 0 & -\delta_g & 0 \\ V_F \bar{\beta}_L I^{\#} & V_F \bar{\beta}_L B^{\#} & -V_F \bar{\alpha} & -V_F \nu_1^{\#} \end{bmatrix}. \tag{III.74}$$

The four eigenvalues associated with each energy-balanced glycogen level of the coefficient matrix defined in equation (III.74) are found in Table 8. In all cases, the real

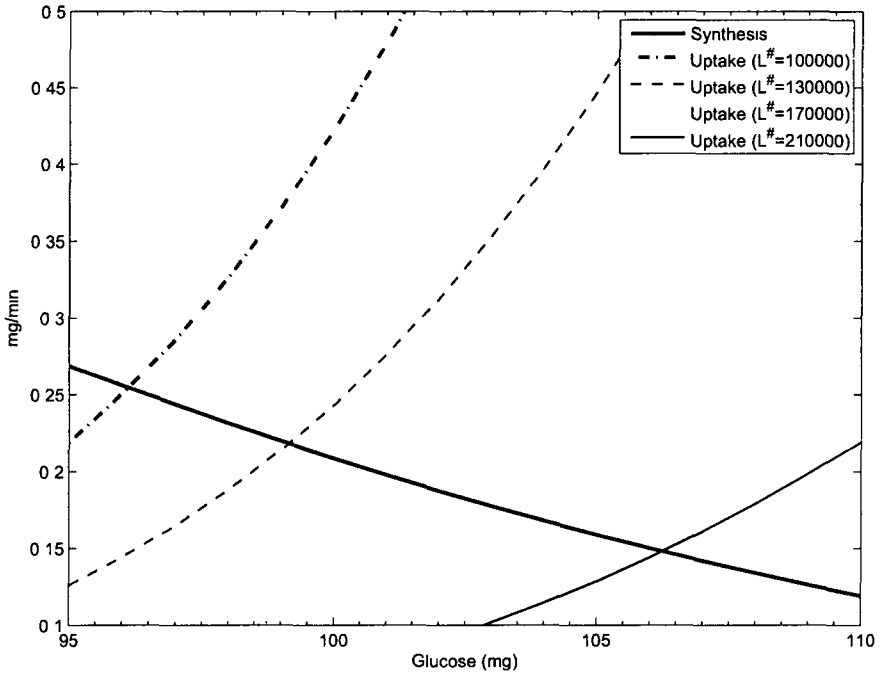

Fig. 28 Energy-balanced glucose set point. The intersection of the right-hand and left-hand sides of equation (III.73) is the value of the energy balance glucose set point for Individual #2.

Table 7
energy-balanced set points for glucose, insulin, glucagon, and food input.

$L^{\#}$	$B^{\#}$	$I^{\#}$	$g^{\#}$	$F^{\#}$
10,000	79.7869	2.1036	178.1203	0.8948
40,000	88.5183	6.6066	127.9522	1.2066
70,000	92.7823	11.4165	105.7581	1.5614
100,000	96.1164	17.3304	90.0458	2.0150
130,000	99.1435	25.0193	77.1807	2.6243
170,000	103.1201	39.5368	62.3766	3.8183
200,000	106.2392	55.0898	52.4006	5.1462
250,000	112.1016	93.9629	37.2332	8.6468
300,000	119.6106	150.7375	23.5456	14.2531
350,000	130.3374	205.6461	11.9224	20.8145
400,000	145.0219	228.0876	4.5755	25.5068
450,000	162.2358	231.8265	1.4652	28.8968
500,000	181.1467	232.2187	0.4165	32.2286

Table 8
Eigenvalues for four $L^{\#}$ scenarios in energy balance.

$L^{\#}$	λ_1	λ_2	$\lambda_{3,4}$
10,000	-0.0007238	-0.1004	$-0.06169 \pm 0.02349i$
40,000	-0.000820	-0.08621	$-0.07153 \pm 0.1035i$
70,000	-0.0007551	-0.08525	$-0.07447 \pm 0.1422i$
100,000	-0.0008670	-0.08458	$-0.07743 \pm 0.1732i$
130,000	-0.009963	-0.08393	$-0.08082 \pm 0.2020i$
170,000	-0.001163	-0.08308	$-0.08666 \pm 0.2404i$
200,000	-0.001255	-0.08250	$-0.09258 \pm 0.2692i$
250,000	-0.001284	-0.08175	$-0.1069 \pm 0.3093i$
300,000	-0.001096	-0.08138	$-0.1275 \pm 0.3052i$
350,000	-0.0007081	-0.08162	$-0.1471 \pm 0.2111i$
400,000	-0.0003368	-0.08250	$-0.1544 \pm 0.09204i$
450,000	-0.0001323	-0.08193	$-0.1558 \pm 0.02732i$
500,000	-0.00004491	-0.08069	$-0.1429,\ -0.1701$

eigenvalue designated as λ_1 remains very small and the real eigenvalue designated as λ_2 remains nearly constant as the value of $L^{\#}$ changes. The differences manifest in the complex eigenvalue pair designated as $\lambda_{3,4}$ where an exponentially-decaying, oscillatory response to an impulsive input is predictable from the non-zero imaginary part of the eigenvalues for all but the $L^{\#} = 500,000$ case. The imaginary part increases from a near-zero value when $L^{\#} = 10,000$ to a maximum when $L^{\#} = 250,000$ and returns to zero between $L^{\#} = 450,000$ and $L^{\#} = 500,000$. The decay rate defined by the negative of the real part of eigenvalues $\lambda_{3,4}$ increases uniformly as $L^{\#}$ increases.

Although generalizations can be made upon examining the eigenvalues, it is important to study specific initial value problems. In Fig. 29, the solution to an impulsive forcing is shown for the original three-by-three system and five of the cases from Table 8. First, the modifications presented in this thesis were designed to mimic the results of the three-by-three system when the glycogen level is approximately 130,000 mg. Clearly, this has been achieved. Second, the new model shows that a portion of the additional external glucose input is stored as extra glycogen as L_1 is non-zero at the end of a one-hour period. The level of L_1 eventually decays to zero on a time scale determined by the eigenvalue λ_1 – the eigenvalue that is missing in the original three-by-three system. Third, Fig. 29 shows that significant storage as glycogen occurs for the cases $L^{\#} = 40,000$ and $L^{\#} = 130,000$ and that these are the only cases to show a significant decrease in glucagon (i.e., negative g_1 resulting in reduced glycogenolysis)

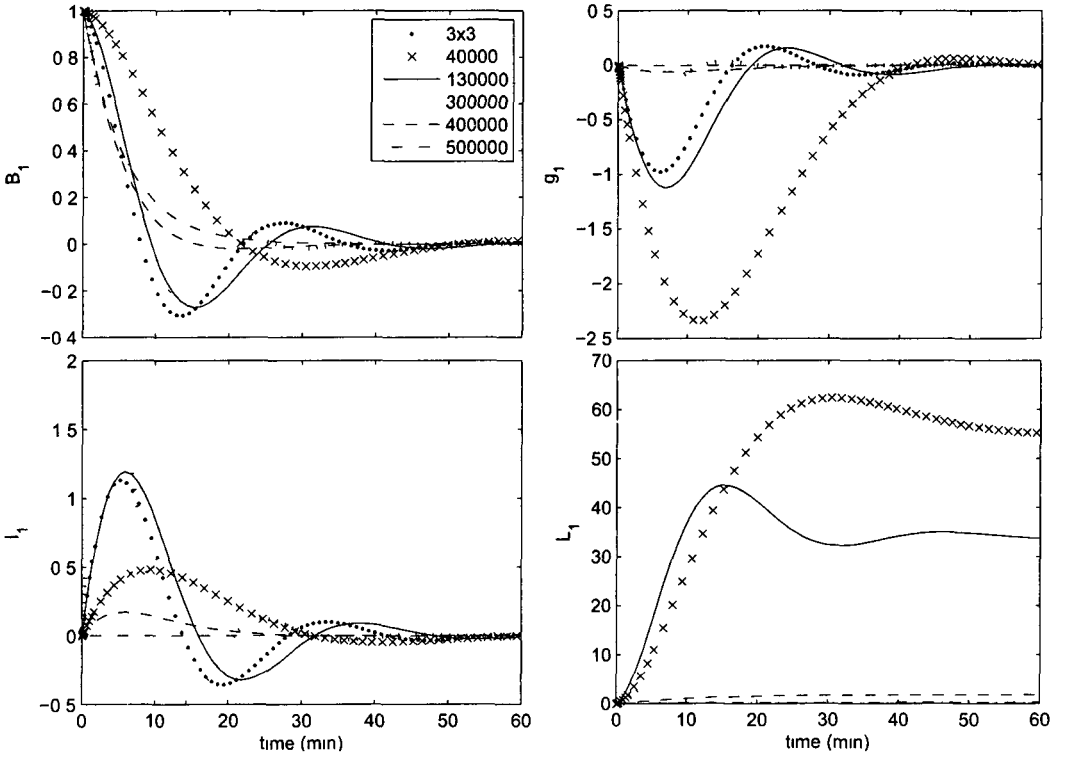

Fig. 29 Systemic response to impulsive load in an energy-balanced state for the original three-by-three (3x3) system and various values of $L^{\#}$

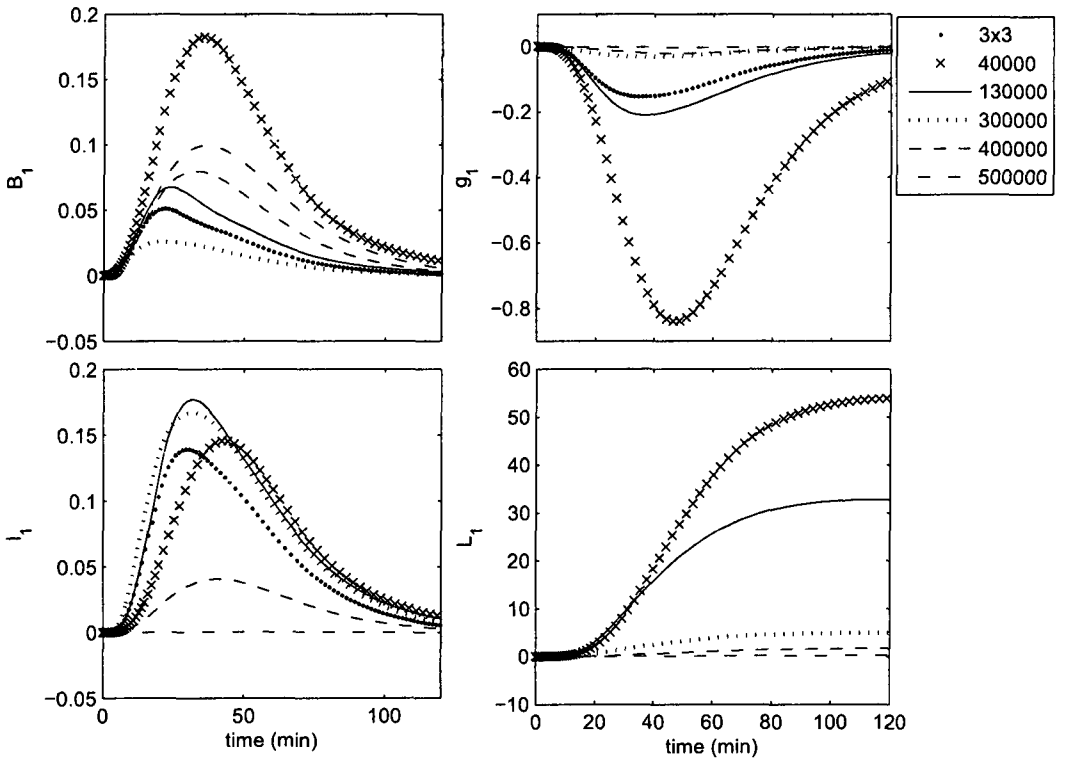

Fig. 30 Systemic response to dynamic load in an energy-balanced state for the original three-by-three (3x3) system and various values of $L^{\#}$.

in response to the increase in blood glucose. Of the cases presented in Fig. 29, the case $L^{\#} = 300,000$ stands out as having the quickest insulin response which leads to overcorrection of the blood glucose level. The rapid decay of the blood glucose level for $L^{\#} = 400,000$ and $L^{\#} = 500,000$ is attributable to the very high base levels of insulin $I^{\#} \approx 230$ which is near the maximum level. In the case $L^{\#} = 400,000$, a very weak response of the disturbance quantities I_1 and g_1 helps control the blood glucose level; whereas, there is almost no response of the disturbance quantities I_1 and g_1 for the case $L^{\#} = 500,000$. The blood glucose response of the latter case approaches zero near $t = 30$ and shows no overcorrection; whereas, the blood glucose response of the former case shows a very slight overcorrection. Note that $L^{\#} = 500,000$ is the only case to show no overcorrection and is the only case to have all real eigenvalues.

The solution to distributed forcing for the original three-by-three system and five of the cases from Table 8 is shown in Fig. 30. The case with the smallest maximum glucose response ($L^{\#} = 300,000$) is the case with the largest imaginary part of the eigenvalues $\lambda_{3,4}$. This shows that to control the response to a smooth distributed

input, it is necessary to have overcorrection of the response to an impulsive input. When two cases have comparable imaginary parts of the eigenvalue, e.g., the cases $L^{\#} = 40,000$ and $L^{\#} = 400,000$,, then the decay rate governed by the real part of the eigenvalue determines the degree of control. There is slightly better control of the case $L^{\#} = 400,000$ over the case $L^{\#} = 500,000$ even though the decay rates are comparable. Again, this is due to the slight overcorrection of the impulsive forcing in the case $L^{\#} = 400,000$ that is absent in the case $L^{\#} = 500,000$. The value of L_1 at the end of a two-hour period in response to the distributed input is comparable to the value of L_1 at the end of a one-hour period in response to the impulsive input since the total additional glucose is the same for both scenarios.

CHAPTER IV

FURTHER DISCUSSION

This chapter will be divided into two parts: IV.1 Variation of Model Parameters and IV.2 Mathematical Analysis of Fed States. In section IV.1, a number of the parameters will be chosen and their respective values modified. An in depth look at how these changes effect the system modeled will follow. Following the change of parameters, various fed states are formally examined. The fed states of interest include the fasting state, an energy-balanced state, an excess-energy state, and the well-fed state.

IV.1 VARIATION OF MODEL PARAMETERS

In chapter III, the responses of glucose, insulin, glucagon and glycogen in individuals subjected to a meal of constant glycemic index was examined. The meal was modeled as a time-dependent input of the form $\dot{F}(t) = 0.5F_0d^{-3}t^2e^{-t/d}$ and the values $d = 15$ and $F_0 = 300$ were chosen to represent a meal of moderate size and moderate glycemic index. Likewise, the investigation of system dynamics in chapter III was completed on individuals with a fixed insulin resistance, β. The following is an investigation into the effects generated by varying the model parameters d, β, and F_0.

IV.1.1 Glycemic Index Effects

The glycemic index of carbohydrate-based foods ranks each food according to its effect on the blood glucose level achieved in normal individuals after consumption of a standard amount. One definition of the glycemic index of a food is based on the area under the two-hour blood glucose response curve following its ingestion. This area is normalized by the area under the curve of the two-hour blood glucose response following the ingestion of a standard food, such as pure glucose or white bread (Jenkins et al., 1981, Foster-Powell et al., 2002). The glycemic index of the standard food is deemed to be 100. Foods with a low glycemic index produce relatively small increases in blood glucose and insulin levels. Foods with a high glycemic index produce relatively large increases in blood glucose and insulin levels. It is surmised that foods with a high glycemic index are rapidly broken down in the digestive tract allowing the glucose to quickly enter the blood. The following analysis shows that the speed in which the glucose enters the system upon ingestion of a meal does indeed effect the glycemic index.

As defined in section III.2.3, a meal-like input is modeled as the measured release

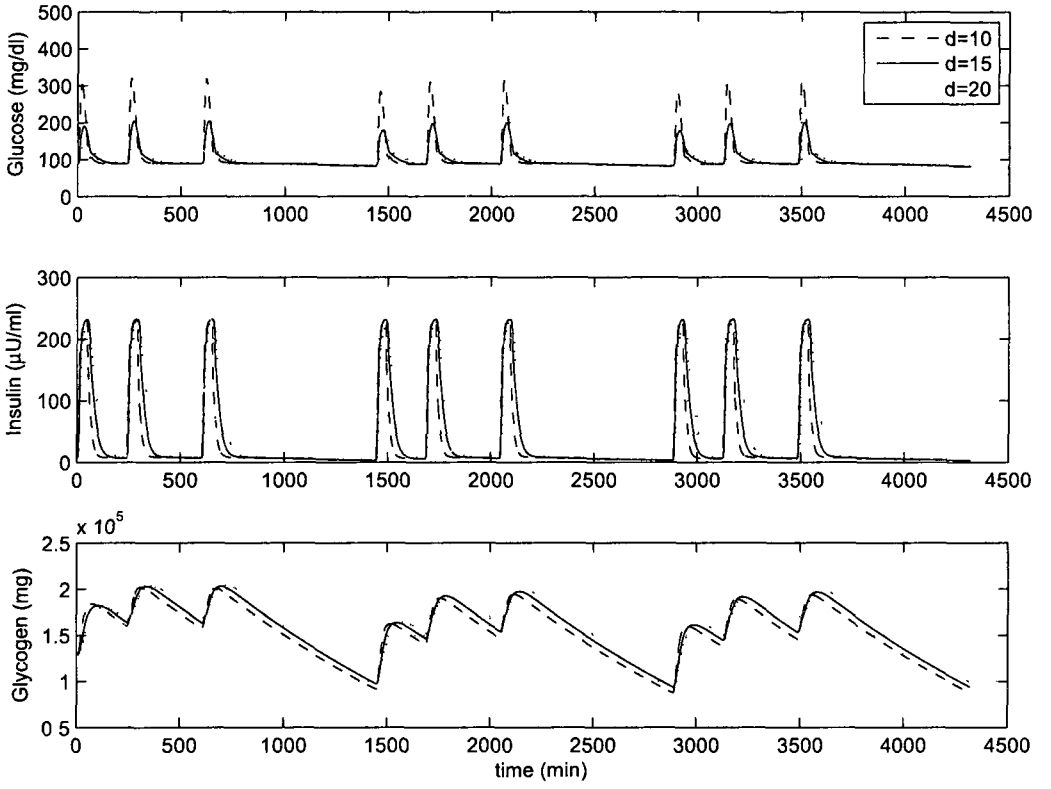

Fig. 31 The base-state response of glucose, insulin, and glycogen over a 72-hr period to three daily meals with varied values of d.

of glucose into the system defined by the normalized input-rate function

$$\dot{F}(t) = 0.5F_o d^{-3}t^2 e^{-t/d},$$

where d is a measure of the time it takes for the glucose in the meal to enter in the blood stream and F_o represents the milligrams of glucose generated by a meal. As $d \to 0$, $\dot{F}(t)$ becomes the unit delta function multiplied by F_o, and this scenario presumes to model a meal with the highest glycemic index. Increasing the value of d presumes to model the glucose input of meals with low glycemic indices. Displayed in Fig. 31 are the resulting differences in the model's response to repeated meals of differing values of d. Fig. 32 is an enlargement of the response to the second meal represented in Fig. 31. As surmised, the meal with the highest glycemic index (as measured by area under the curve) results from the smallest value of d (faster input), and the meal with the lowest glycemic index results from the largest value of d (slower input). This model predicts the return to the basal state is much faster for

high glycemic index foods, and thus, the insulin levels also return to basal state much faster for the high glycemic index foods. The model predicts that the area under the insulin curve is greater for lower glycemic index foods; however, it must be remembered that there is no feed-forward mechanism built into this model. Inclusion of such a feed-forward mechanism would greatly affect this result. The effect of the glycemic index on the overall glycogen level is determined to be negligible, but it is noted that the foods with low glycemic indices lead to slightly greater glycogen storage as the blood glucose remains above basal for a longer time period.

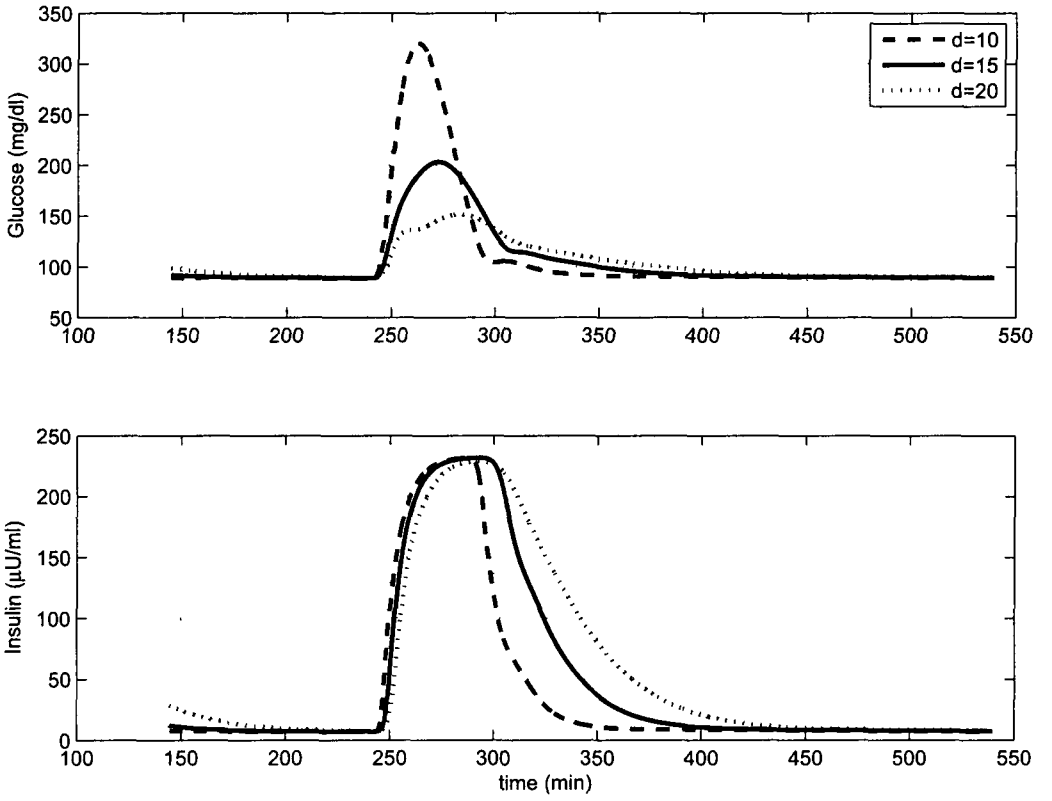

Fig. 32 The base-state response of glucose (top) and insulin (bottom) following the second daily meal with varied values of d.

IV.1.2 Insulin Effectiveness

One aspect of Type II diabetes is the body's inability to regulate the blood glucose concentration due to a decrease in insulin effectiveness through insulin resistance. The normal response of the pancreas to elevated glucose levels is to release insulin to stem the rising tide of glucose level by promoting the uptake and usage of glucose. If the body is insulin resistant, normal amounts of insulin are inadequate to produce a

normal insulin response by the muscle, fat and liver cells; thus, the pancreas produces additional insulin as a result of the continuing high glucose levels. Eventually, the pancreas cannot keep up with the body's requirement for insulin, and excess glucose builds up in the bloodstream resulting in high basal levels. Individuals with insulin resistance simultaneously have both elevated levels of blood glucose and elevated levels of insulin circulating in their blood. The cause of insulin resistance is not fully understood. It is thought to be due partly to genetic factors, including ethnicity, and partly to lifestyle, such as excessive caloric intake and inadequate exercise. This latter cause might be due to saturation of the glycogen storage sites in the liver and muscles. For most individuals, the body is able to keep pace with the need for extra insulin production, and the effects are subtle and complications are years in the making. Thus, individuals with insulin resistance often do not have any significant symptoms and do not realize that this process is taking place in their bodies.

In this thesis, insulin resistance is modeled by decreasing the value of β. The model predicts that insulin resistance in liver cells reduces the rate of storage of glycogen at a fixed glucose, insulin, and glucagon level. However, insulin resistance leads to elevated levels of blood glucose and elevated levels of insulin circulating in the blood, which each increase the rate of storage of glycogen. Thus, the net effect of insulin resistance on the glycogen level is not obvious due to the nonlinear nature of the response.

Three cases are illustrated and analyzed for the course of a 72-hour period where three meals are incorporated every 24 hours. In the first case, the base state is established maintaining the parameter β at its normal value. This case has been thoroughly analyzed throughout the thesis and illustrated in section IV.1.1 (see Fig. 31).

The effects on the system by a decrease in β to one-half its value (0.5β) and one-tenth its value (0.1β) is illustrated in Fig. 33 and Fig. 34, respectively.

With such large decreases in β, the insulin is considerably less effective in controlling the glucose concentration which leads to extremely elevated postprandial glucose concentrations in the most resistant case. The insulin resistant glucose responses to the second meal (see Fig. 35) are to be compared to the normal case (see Fig. 32). Although reasonable control of the postprandial glucose level was achieved in response to all meal types when the insulin response is normal, control is only achieved for meals with a low glycemic index when insulin resistance is present. Even though the maximum glucose concentrations are very high in the insulin resistant cases, a return to basal does occur in all cases. The return to basal level takes a longer time as the insulin resistance increases. Thus, the time duration for which the insulin is released at a maximum rate is extended for the scenarios where β is decreased.

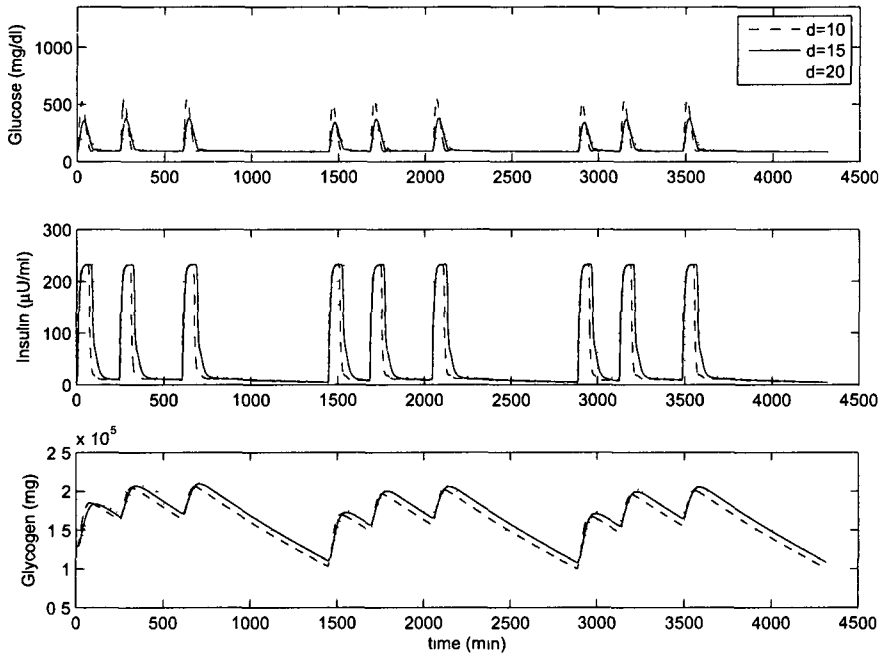

Fig. 33 Response of glucose, insulin, and glycogen over a 72-hr period to three daily meals where $\beta = 0.5\beta$.

To analyze the effect of insulin resistance on glycogen storage, consider that the postprandial glucagon concentration tends towards zero under the conditions

$$\begin{aligned} \beta_{new} &< \beta, \\ I &\to I^{max}, \\ B &\gg B_{basal}. \end{aligned}$$

Thus,

$$\frac{dL}{dt} \to \beta_{new} B I^{max} \frac{\mathrm{erfc}(\gamma_I L)}{\mathrm{erfc}(\gamma_I L_I^*)}. \tag{IV.1}$$

The decrease in β suggests there should be a decrease in the hepatic storage rate; however, due to the excessive glucose and insulin in the system, glucose continues to be stored as hepatic glycogen at a greater rate. It is determined that the maximum postprandial glycogen level is *increased* in comparison to the base-state glycogen level as is seen by comparing Fig. 34 to both Fig. 33 and Fig. 31. The greater the insulin resistance, the higher the average glycogen level will be. A similar analysis

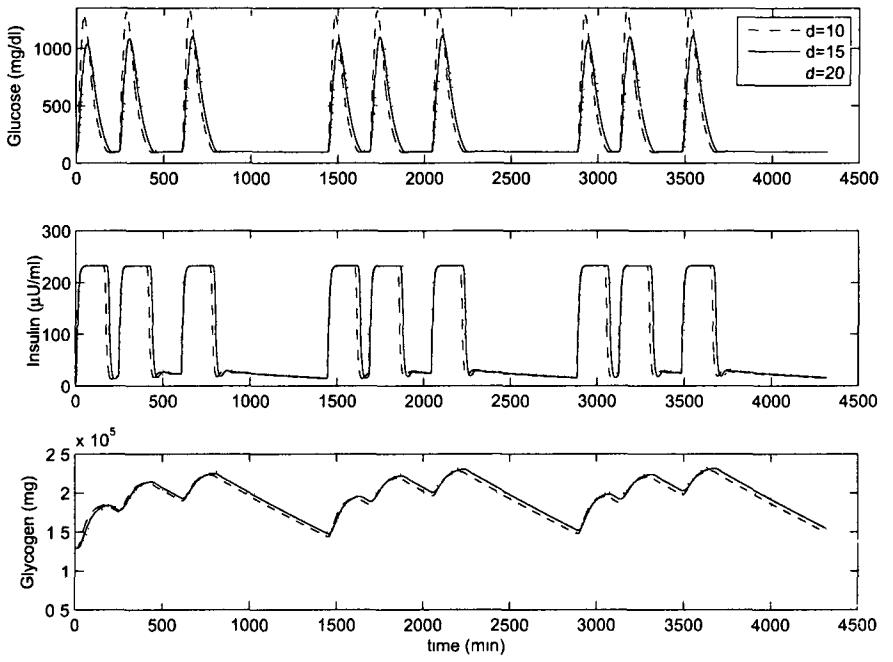

Fig. 34 Response of glucose, insulin, and glycogen over a 72-hr period to three daily meals where $\beta = 0.1\beta$.

will be needed in order to determine the effects of insulin resistance on the storage of glucose as muscle glycogen and as adipose tissue.

IV.1.3 Increased Energy Input

The prior analysis has used a constant magnitude for the meal size. It is natural to wonder how the system reacts to a significant change in the energy input as would occur in nature. To that end, Fig. 36 shows the results of doubling the magnitude of the meal size. The system reacts much as expected. First, the immediate rise in glucose upon ingestion of a meal is much greater in response to a meal of double the size. Second, the basal states, which are the near-constant values of glucose, insulin, and glucagon between meals, show a slight increase in glucose and insulin levels while a more significant decrease in the basal glucagon level is observed. Third, the body responds to the increased energy input by significantly changing the level of stored glycogen.

With the additional energy input, one might expect the glycogen level to continue rising day-after-day. However, the increase in stored glycogen drives a corresponding increase in the net hepatic production rate between meals. This increased production

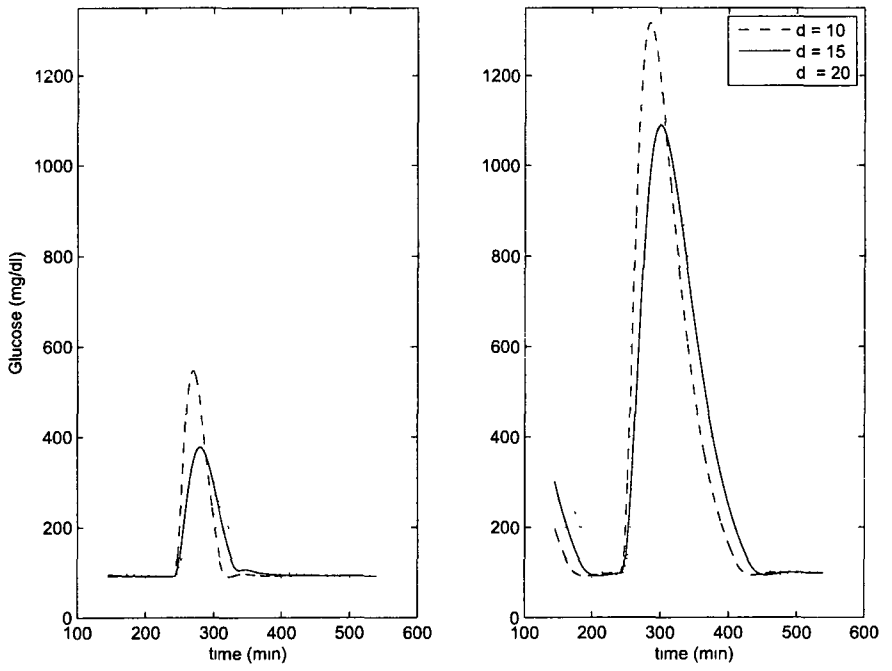

Fig. 35 The response of glucose following the second daily meal with varied values of d and decreased value of β: 0.5β (left) and 0.1β (right).

rate produces the slight adjustments to the basal state seen in Fig. 36. Under the increased-energy input scenario, more glycogen is converted during between-meal periods (especially the overnight period) which establishes a new balance and prevents the glycogen level from continually increasing. This balance is established within the first 72 hours and is maintained indefinitely.

This analysis brings to light new questions as to the nature of hepatic glucose metabolism in Type II diabetics. It is now commonly thought that net hepatic glucose production is significantly increased in people with diabetes, and that this increased production is the *reason* for the increased basal blood glucose levels. This analysis indicates elevated *prandial* blood glucose and insulin levels associated with insulin resistance increase the glycogen-storage levels. The larger glycogen-storage level, in turn, drives an increase in the net *postprandial* hepatic glucose production which leads to increased basal blood glucose levels (especially in insulin resistant individuals). Of course, the glycogen storage level is also effected by the level of energy input; however, in the absence of insulin resistance, the resulting increase in the net hepatic glucose production only causes a small elevation in the basal blood glucose and insulin levels. For the insulin-resistant individual, the increased energy

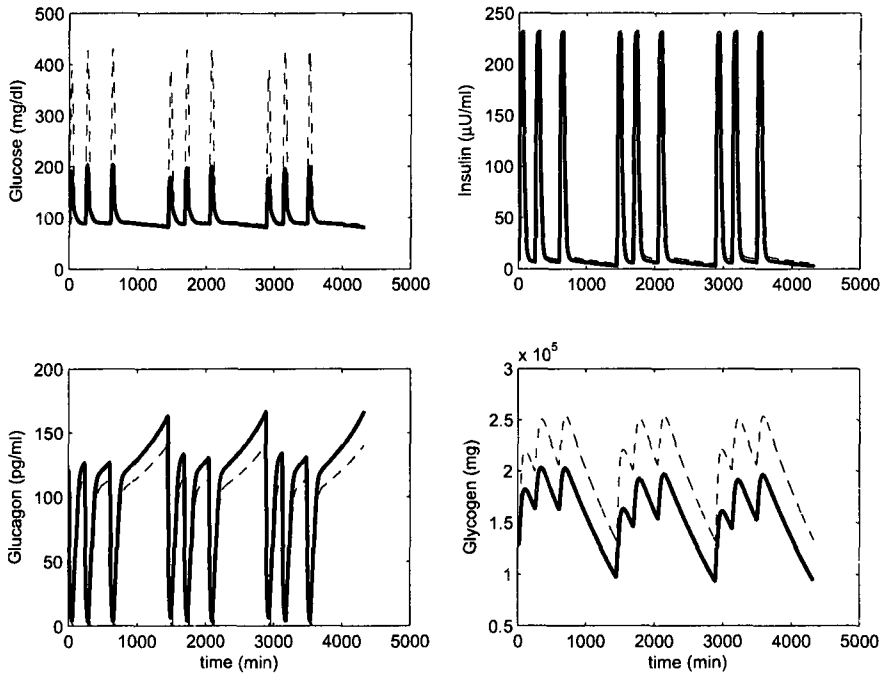

Fig. 36 Comparison of systemic responses between the base state (solid line) and doubled energy input (dashed line)

input would exasperate the problem of elevated basal blood glucose and insulin levels and elevated glycogen storage. This analysis gives some clue to the answer of the classic question –"Which came first, the chicken or the egg?"– as it relates to the development of Type II diabetes. This simple model indicates that Type II diabetes *results* from the development of insulin resistance more than from overeating.

IV.2 MATHEMATICAL ANALYSIS OF FED STATES

IV.2.1 Well-Fed State

The analysis contained in the previous section leads to an interesting question concerning whether the increase net hepatic glucose production seen in diabetics is a cause or effect. By mathematically analyzing the case of a "very" well-fed individual, this model is seen to predict that the increase in hepatic production is mostly an effect and not a cause.

The system of nonlinear ordinary differentiable equations relating concentrations of blood glucose, insulin, glucagon, and the absolute level of liver glycogen is

$$\frac{dB}{dt} = \dot{F}(t) - \dot{M}_0 - \beta_M BI - \frac{1}{V_F}\frac{dL}{dt}, \tag{IV.2}$$

$$\frac{dI}{dt} = -\delta_I I + \dot{Q}_I \left\{\frac{1}{2} + \frac{1}{2}\tanh\left(\frac{B - B_I}{r_I}\right)\right\}, \tag{IV.3}$$

$$\frac{dg}{dt} = -\delta_g g + \dot{Q}_g \left\{\frac{1}{2} + \frac{1}{2}\tanh\left(\frac{B_g - B}{r_g}\right)\right\}, \tag{IV.4}$$

$$\frac{dL}{dt} = V_F\left(\tilde{\beta}_L BI\,\mathrm{erfc}(\gamma_I L) - \tilde{\alpha} g\,\mathrm{erf}(\gamma_g L)\right), \tag{IV.5}$$

where $\tilde{\beta}_L \equiv \frac{\beta_L}{\mathrm{erfc}(\gamma_I L_I^*)}$ and $\tilde{\alpha} \equiv \frac{\alpha}{\mathrm{erf}(\gamma_g L_g^*)}$.

Now, consider the system under the condition of being "very" well fed over an extended period of time such that the glycogen storage level is very large. Thus, the system is studied subject to the initial conditions $B(0) = B_0$, $I(0) = I_0$, $g(0) = g_0$, and $L(0) = L_0$ along with the additional assumption $L_0 \gg 1$. This last condition implies that $\mathrm{erfc}(\gamma_I L_0) \to 0$, $\mathrm{erf}(\gamma_g L_0) \to 1$, and $L \sim L_0 - V_F\tilde{\alpha} g_0 t$. Hence, the glycogenolysis rate is near constant, but the rate remains unknown until the value of g_0 is determined. The value of g_0 is determined by requiring that the body is in homeostasis. The homeostasis assumption requires that B, I, and g remain near the initial values B_0, I_0, and g_0 which must satisfy the three-by-three relationship:

$$0 = -\dot{M}_0 - \beta_M B_0 I_0 + \tilde{\alpha} g_0, \tag{IV.6}$$

$$0 = -\delta_I I_0 + \dot{Q}_I \left\{\frac{1}{2} + \frac{1}{2}\tanh\left(\frac{B_0 - B_I}{r_I}\right)\right\}, \tag{IV.7}$$

$$0 = -\delta_g g_0 + \dot{Q}_g \left\{\frac{1}{2} + \frac{1}{2}\tanh\left(\frac{B_g - B_0}{r_g}\right)\right\}. \tag{IV.8}$$

Substitution of I_0 and g_0 from equations (IV.7) and (IV.8), respectively, into equation (IV.6) results in a single equation in terms of B_0:

$$\dot{M}_0 + \frac{\beta_M B_0 \dot{Q}_I}{\delta_I}\left\{\frac{1}{2} + \frac{1}{2}\tanh\left(\frac{B_0 - B_I}{r_I}\right)\right\} = \frac{\tilde{\alpha}\dot{Q}_g}{\delta_g}\left\{\frac{1}{2} + \frac{1}{2}\tanh\left(\frac{B_g - B_0}{r_g}\right)\right\}.$$

The intersection of the left-hand side (glucose uptake) and right-hand side (glucose synthesis) is the value of B_0 which satisfies the three-by-three system presented in this section. Fig. 37 (top) illustrates this for a "normal" or base case and two different factors of insulin resistance: 0.5β and 0.1β. Table 9 lists the corresponding well-fed values of B_0, I_0, and g_0 for each specification of β. As expected, the well-fed base case has a higher homeostatic glucose point than the original three-by-three system ($B^* = 90$) since there is zero conversion of glucose into liver glycogen. The higher glucose level leads to a higher insulin level and a lower glucagon level. Imposing

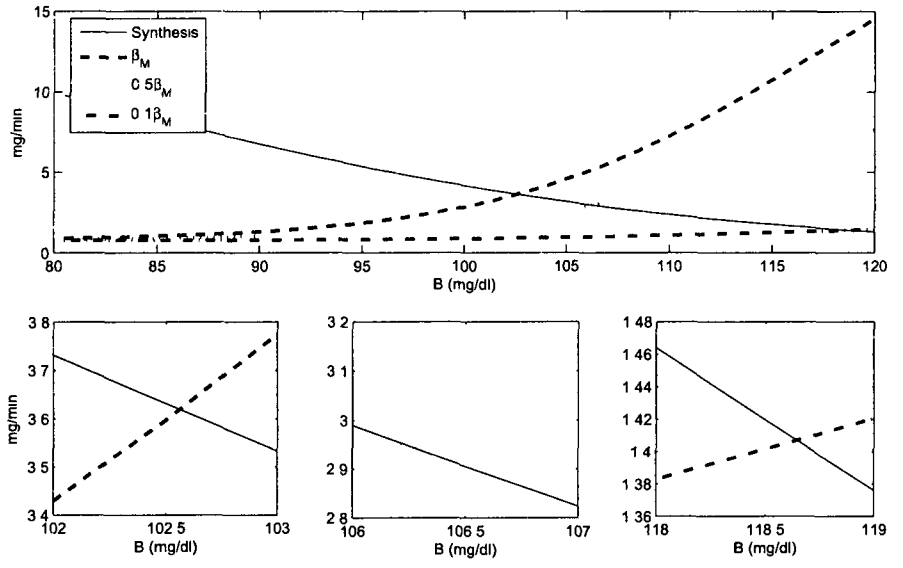

Fig. 37 The intersection of glucose uptake and glucose synthesis (top) in the well-fed three-by-three system for multiple levels of insulin resistance. β_M (bottom left), 0.5β (bottom center), and 0.1β (bottom right).

Table 9
Set points for glucose, insulin, and glucagon for specifications of β in the three-by-three well-fed system.

	B_0	I_0	g_0
β_M	102.5611	37.1514	64.3144
$\frac{1}{2}\beta_M$	106.2164	64.9622	143.7902
$\frac{1}{10}\beta_M$	118.6433	52.4685	25.0031

insulin resistance within the system means that the glucose uptake rate (left side of equation IV.2.1) is greatly reduced which leads to even higher homeostatic glucose points.

If hepatic glycogen remains as the only fuel source for the system, then the maintenance of homeostasis of the system relies on an increased rate of glycogenolysis – here approximately 470 mg/min. Being the basal level of glucagon in the well-fed state is significantly lower than that in a normal state, it may appear surprising that the net hepatic production rate is actually *increased.* Recall that under the assumption $L \gg 1$ the term containing β_L is nonexistent, and the action of glycogen is that of usage versus storage. With no glycogen being stored, there is no delimiting factor on glycogen usage besides that of the current level of glucagon. Therefore

comparing the normal net hepatic production rate versus the well-fed net hepatic production rate one sees

$$\alpha g^* - \beta_L B^* I^* < \alpha g_0.$$

Deviation of the system from homeostasis is found by analyzing the system in the limit $\tau = \gamma_g(L_0 - V_F\tilde{\alpha}g_0 t) \to \infty$. Upon examining the asymptotic expansion of the error function,

$$\operatorname{erf}(\gamma_g L) \sim 1 - \frac{e^{-(\gamma_g L)^2}}{\sqrt{\pi}}\left(\frac{1}{\gamma_g L} - \frac{1}{2(\gamma_g L)^2} + \cdots\right),$$

one finds the appropriate perturbed variables are

$$\begin{aligned} B &= B_0 + e^{-\tau^2} B_1(\tau), && \text{(IV.9)} \\ I &= I_0 + e^{-\tau^2} I_1(\tau), && \text{(IV.10)} \\ g &= g_0 + e^{-\tau^2} g_1(\tau), && \text{(IV.11)} \\ L &= \frac{1}{\gamma_g}\tau + e^{-\tau^2} L_1(\tau). && \text{(IV.12)} \end{aligned}$$

First, the glycogen equation is analyzed. Begin with the substitution $L = \frac{1}{\gamma_g}\tau + e^{-\tau^2} L_1(\tau)$ into the left-hand side of equation (IV.5) which yields

$$\begin{aligned} \frac{dL}{dt} &= \frac{dL}{d\tau}\frac{d\tau}{dt} \\ &= (-\gamma_g V_F \tilde{\alpha} g_0)\frac{dL}{d\tau} \\ &= (-V_F\tilde{\alpha}g_0)\left(1 + \gamma_g \frac{d}{d\tau}\left[e^{-\tau^2} L_1(\tau)\right]\right). \\ &= (-V_F\tilde{\alpha}g_0)\left(1 + \gamma_g\left[-2\tau L_1(\tau) + \frac{dL_1}{d\tau}\right] e^{-\tau^2}\right). \end{aligned}$$

Next, substitute the perturbed variables into the right-hand side of equation (IV.5),

$$\begin{aligned} V_F \Bigg[\tilde{\beta}_L \left(B_0 + e^{-\tau^2} B_1(\tau)\right)\left(I_0 + e^{-\tau^2} I_1(\tau)\right) \operatorname{erfc}\left(\gamma_I\left(\frac{\tau}{\gamma_g} + e^{-\tau^2} L_1(\tau)\right)\right) \\ -\tilde{\alpha}\left(g_0 + e^{-\tau^2} g_1(\tau)\right) \operatorname{erf}\left(\tau + \gamma_g e^{-\tau^2} L_1(\tau)\right)\Bigg], \end{aligned}$$

which is expanded to yield

$$\begin{aligned} -V_F\tilde{\alpha}g_0 + V_F\tilde{\alpha}g_0 \frac{e^{-\tau^2}}{\sqrt{\pi}}\left(\frac{1}{\tau} - \frac{1}{2\tau^3} + \mathcal{O}\left(\frac{1}{\tau^5}\right)\right) - V_F\tilde{\alpha}e^{-\tau^2} g_1(\tau) \\ + \mathcal{O}\left(e^{-2\tau^2}, e^{-\frac{\gamma_I^2}{\gamma_g^2}\tau^2}\right). \end{aligned} \qquad \text{(IV.13)}$$

Matching terms from the left-hand and right-hand sides proportional to $e^{-\tau^2}$ and neglecting terms on the order of $e^{-2\tau^2}$ and $\exp(-\gamma_I^2\tau^2/\gamma_g^2)$ gives

$$-V_F\tilde{\alpha}g_0\gamma_g\left[-2\tau L_1(\tau)+\frac{dL_1}{d\tau}\right] = V_F\tilde{\alpha}g_0\frac{1}{\sqrt{\pi}}\left(\frac{1}{\tau}-\frac{1}{2\tau^3}+\mathcal{O}\left(\frac{1}{\tau^5}\right)\right) -V_F\tilde{\alpha}g_1(\tau). \tag{IV.14}$$

The other equations are analyzed by substituting equations (IV.9)-(IV.11) into the first three governing equations (IV.2)-(IV.4) using the relationships

$$\tanh\left(\frac{B_0+e^{-\tau^2}B_1(\tau)-B_I}{r_I}\right) = \tanh\left(\frac{B_0-B_I}{r_I}\right) +\operatorname{sech}^2\left(\frac{B_0-B_I}{r_I}\right)\frac{B_1(\tau)}{r_I}e^{-\tau^2} +\mathcal{O}\left(e^{-2\tau^2}\right) \tag{IV.15}$$

and

$$\tanh\left(\frac{B_g-B_0-e^{-\tau^2}B_1(\tau)}{r_g}\right) = \tanh\left(\frac{B_g-B_0}{r_g}\right) -\operatorname{sech}^2\left(\frac{B_g-B_0}{r_g}\right)\frac{B_1(\tau)}{r_g}e^{-\tau^2} +\mathcal{O}\left(e^{-2\tau^2}\right). \tag{IV.16}$$

By neglecting terms smaller than $e^{-\tau^2}$ and by using the equations defining B_0, I_0, and g_0, the perturbed system becomes

$$\frac{dB_1(\tau)}{d\tau}-2\tau B_1(\tau) = \frac{1}{\gamma_g V_F\tilde{\alpha}g_0}\left[\beta_M(I_0B_1(\tau)+B_0I_1(\tau)) +\frac{\tilde{\alpha}g_0}{\sqrt{\pi}}\left(\frac{1}{\tau}-\frac{1}{2\tau^3}+\mathcal{O}\left(\frac{1}{\tau^5}\right)\right) -\tilde{\alpha}g_1(\tau)\right], \tag{IV.17}$$

$$\frac{dI_1(\tau)}{d\tau}-2\tau I_1(\tau) = \frac{1}{\gamma_g V_F\tilde{\alpha}g_0}\left[\delta_I I_1(\tau) -\frac{\dot{Q}_I}{2r_I}\operatorname{sech}^2\left(\frac{B_0-B_I}{r_I}\right)B_1(\tau)\right], \tag{IV.18}$$

$$\frac{dg_1(\tau)}{d\tau} - 2\tau g_1(\tau) = \frac{1}{\gamma_g V_F \tilde{\alpha} g_0}\left[\delta_g g_1(\tau) + \frac{\dot{Q}_g}{2r_g}\operatorname{sech}^2\left(\frac{B_g - B_0}{r_g}\right) B_1(\tau)\right], \tag{IV.19}$$

$$\frac{dL_1(\tau)}{d\tau} - 2\tau L_1(\tau) = \frac{1}{\gamma_g V_F \tilde{\alpha} g_0}\left[V_F \tilde{\alpha} g_1(\tau) - \frac{V_F \tilde{\alpha} g_0}{\sqrt{\pi}}\left(\frac{1}{\tau} - \frac{1}{2\tau^3} + \mathcal{O}\left(\frac{1}{\tau^5}\right)\right)\right]. \tag{IV.20}$$

Upon defining

$$\hat{A} = \frac{\dot{Q}_I \operatorname{sech}^2\left(\frac{B_0 - B_I}{r_I}\right)}{2r_I}, \quad \hat{C} = \frac{\dot{Q}_g}{2r_g}\operatorname{sech}^2\left(\frac{B_g - B_0}{r_g}\right), \quad \text{and} \quad \mu = \frac{1}{\gamma_g V_F \tilde{\alpha} g_0},$$

equations (IV.17)-(IV.19) are rewritten in the form of a four-by-four system of ordinary differential equations as

$$\left(\frac{d}{d\tau} - 2\tau\right)\begin{bmatrix} B_1(\tau) \\ I_1(\tau) \\ g_1(\tau) \\ L_1(\tau) \end{bmatrix} = \mu \begin{bmatrix} \beta_M I_0 & \beta_M B_0 & -\tilde{\alpha} & 0 \\ -\hat{A} & \delta_I & 0 & 0 \\ \hat{C} & 0 & \delta_g & 0 \\ 0 & 0 & V_F \tilde{\alpha} & 0 \end{bmatrix} \begin{bmatrix} B_1(\tau) \\ I_1(\tau) \\ g_1(\tau) \\ L_1(\tau) \end{bmatrix} + \mu \begin{bmatrix} \frac{\tilde{\alpha} g_0}{\sqrt{\pi}}\left(\frac{1}{\tau} - \frac{1}{2\tau^3} + \mathcal{O}\left(\frac{1}{\tau^5}\right)\right) \\ 0 \\ 0 \\ -\frac{V_F \tilde{\alpha} g_0}{\sqrt{\pi}}\left(\frac{1}{\tau} - \frac{1}{2\tau^3} + \mathcal{O}\left(\frac{1}{\tau^5}\right)\right) \end{bmatrix}. \tag{IV.21}$$

The system is solved by introducing the infinite power series forms,

$$B_1(\tau) = \sum_{k=1}^{\infty} b_k \tau^{-k-1}, \tag{IV.22}$$

$$I_1(\tau) = \sum_{k=1}^{\infty} a_k \tau^{-k-1}, \tag{IV.23}$$

$$g_1(\tau) = \sum_{k=1}^{\infty} c_k \tau^{-k-1}, \tag{IV.24}$$

$$L_1(\tau) = \sum_{k=1}^{\infty} d_k \tau^{-k-1}, \tag{IV.25}$$

into the equation. The constant values are determined to be:

$$b_1 = -\frac{\mu\tilde{\alpha}g_0}{2\sqrt{\pi}}, \tag{IV.26}$$

$$b_2 = \frac{\mu^2\beta_M I_0\tilde{\alpha}g_0}{4\sqrt{\pi}}, \tag{IV.27}$$

$$b_3 = \frac{\mu\tilde{\alpha}g_0}{2\sqrt{\pi}}\left[-\frac{\mu^2}{4}\left(\beta_M^2 I_0^2 - \hat{A}\beta_M B_0 I_0 - \hat{C}\right) - \frac{3}{2}\right], \tag{IV.28}$$

$$a_1 = 0, \tag{IV.29}$$

$$a_2 = -\frac{\mu^2\hat{A}\tilde{\alpha}g_0}{4\sqrt{\pi}}, \tag{IV.30}$$

$$a_3 = \frac{\mu^2\hat{A}\tilde{\alpha}g_0}{8\sqrt{\pi}}\left(\mu\beta_M I_0 + \delta_I\right), \tag{IV.31}$$

$$c_1 = 0, \tag{IV.32}$$

$$c_2 = \frac{\mu^2\hat{C}\tilde{\alpha}g_0}{4\sqrt{\pi}}, \tag{IV.33}$$

$$c_3 = -\frac{\mu^3\hat{C}\tilde{\alpha}g_0}{8\sqrt{\pi}}\left(\beta_M I_0 + \delta_g\right), \tag{IV.34}$$

$$d_1 = \frac{\mu V_F\alpha g_0}{2\sqrt{\pi}}, \tag{IV.35}$$

$$d_2 = 0, \tag{IV.36}$$

$$d_3 = \frac{\mu^3 V_F\tilde{\alpha}}{2\sqrt{\pi}}\left[\frac{\mu^3 V_F\tilde{\alpha}\hat{C}}{8}\left(\beta_M I_0 + \delta_g\right) - \frac{3}{2}\right]. \tag{IV.37}$$

The base state of the well-fed scenario represents the maximum rate of glycogenolysis owing to the saturation of the hepatic store of glycogen. When this maximum rate is occurring, the base blood glucose and insulin concentrations are at their maximum values, and the base glucagon concentration is at its minimum value. As time proceeds, the base glycogen store which is given by the time like parameter τ decreases from its very large (almost infinite) value L_0. As τ decreases, the rate of glycogenolysis also decreases ($d_1 > 0$) and this directly leads to a slight decrease in the blood glucose concentration ($b_1 < 0$). This analysis indicates the insulin and glucagon level then follow the change in blood glucose concentration as second order effects, since both $a_1 = 0$ and $c_1 = 0$. In response to the slight decrease in the rate of glycogenolysis, insulin decreases from its maximum value ($a_2 < 0$) and glucagon increases from its minimum value ($c_2 > 0$).

IV.2.2 Near-starved State

For this section, consider a system in contrast to the well-fed state. In this scenario, assume that a sufficiently long time period has lapsed without an external source of

Table 10
Base-state points in the near-starved state for corresponding values of G_n.

G_n	B_0	I_0	g_0
0.20	55.859	0.0873	294.772
0.30	73.541	0.9194	214.365
0.40	79.417	2.0032	180.301
0.50	82.723	3.0981	160.855

glucose (i.e., $\dot{F}(t) = 0$) such that the system approaches a near-starved state. Over an extended period of time in a real-world setting, death to the organism is likely without additional sources of glucose. A reintroduction of gluconeogenesis to the system is required to make the analysis plausible and worthy of note. Thus, the system with gluconeogenesis previously discussed in section III.3.5 is upgraded, and the result is given by

$$\frac{dB}{dt} = -\dot{M}_0 - \beta_M BI + G_n\tilde{\alpha}g - \frac{1}{V_F}\frac{dL}{dt}, \tag{IV.38}$$

$$\frac{dI}{dt} = -\delta_I I + \dot{Q}_I\left\{\frac{1}{2} + \frac{1}{2}\tanh\left(\frac{B - B_I}{r_I}\right)\right\}, \tag{IV.39}$$

$$\frac{dg}{dt} = -\delta_g g + \dot{Q}_g\left\{\frac{1}{2} + \frac{1}{2}\tanh\left(\frac{B_g - B}{r_g}\right)\right\}, \tag{IV.40}$$

$$\frac{dL}{dt} = V_F\left(\tilde{\beta}_L BI\,\mathrm{erfc}(\gamma_I L) - (1 - G_n)\,\tilde{\alpha}g\,\mathrm{erf}(\gamma_g L)\right), \tag{IV.41}$$

where

$$\tilde{\beta}_L \equiv \frac{\beta_L}{\mathrm{erfc}(\gamma_I L_I^*)} \quad \text{and} \quad \tilde{\alpha} \equiv \frac{\alpha}{\mathrm{erf}(\gamma_g L_g^*)}.$$

The parameter G_n nominally represents the percentage of total glucose production owing to gluconeogenesis in the basal state. Previous analysis indicated that liver glycogen slowly depletes during an extended fast and that the energy produced by gluconeogenesis goes, in part, to protecting the store of glycogen in the liver. Now, assume that the relatively low level of glycogen in the near-starved state has been quickly depleted, possibly by administration of a drug that blocks the conversion of glucose into glycogen in the liver. After removal of the drug, the conversion of glucose into glycogen in the liver would proceed at the maximum rate. Assuming that the concentrations of blood glucose, insulin and glucagon have quickly adjusted to this new state, it is feasible to study the initial value problem under the approximation that the initial glycogen level is $L_0 = 0$ and that the leading order approximations $\mathrm{erfc}(\gamma_I L) \approx 1$ and $\mathrm{erf}(\gamma_g L) \approx 0$ are reasonable. The latter relation implies that the

body is totally reliant on gluconeogenesis to provide fuel for the system and fuel for the glycogen replacement. The former relation implies that the body is attempting to replenish the store of hepatic glycogen at the maximum rate. Under this scenario, the glycogen replenishes at the maximum possible rate, $\frac{dL}{dt} = V_F\tilde{\beta}_L B_0 I_0$, while the system maintains a homeostatic state such that B, I, and g remain near the constant values B_0, I_0, and g_0. These values satisfy the three-by-three relationship:

$$0 = -\dot{M}_0 - \beta_M B_0 I_0 + G_n\tilde{\alpha} g_0 - \tilde{\beta}_L B_0 I_0, \tag{IV.42}$$

$$0 = -\delta_I I_0 + \dot{Q}_I \left\{\frac{1}{2} + \frac{1}{2}\tanh\left(\frac{B_0 - B_I}{r_I}\right)\right\}, \tag{IV.43}$$

$$0 = -\delta_g g_0 + \dot{Q}_g \left\{\frac{1}{2} + \frac{1}{2}\tanh\left(\frac{B_g - B_0}{r_g}\right)\right\}. \tag{IV.44}$$

Determination of the appropriate values of B_0, I_0, and g_0, begins by isolating I_0 and g_0 from equations (IV.43) and (IV.44) and substituting their respective results into equation (IV.42). The result is an equation whose sole variable is B_0. Rewriting the equation to reflect the balance between glucose synthesis and glucose uptake yields

$$\frac{\tilde{\alpha} G_n \dot{Q}_g}{\delta_g}\left\{\frac{1}{2} + \frac{1}{2}\tanh\left(\frac{B_g - B_0}{r_g}\right)\right\} = \dot{M}_0 + \frac{\beta B_0 \dot{Q}_I}{\delta_I}\left\{\frac{1}{2} + \frac{1}{2}\tanh\left(\frac{B_0 - B_I}{r_I}\right)\right\}, \tag{IV.45}$$

where $\beta = \beta_M + \beta_L$. An illustration of the effects of G_n on the base state level of glucose during this near-starved state is seen in Fig. 38 – a graph of the left-hand versus the right-hand sides of equation (IV.45).

In the scenario presented, glucose generated by gluconeogenesis is both converted into hepatic glycogen in an attempt to replenish glycogen stores and added to the pool of circulating blood glucose in order to increase the concentration from the relatively low levels. Thus, an increase in G_n results in a larger value for glucose level. For further analysis of the recovery period, consider the initial value problem over a short time scale by introducing the following perturbation series

$$B(t) = \bar{B}_0 + \bar{B}_2 t^2 + \ldots, \tag{IV.46}$$

$$I(t) = \bar{I}_0 + \bar{I}_3 t^3 + \ldots, \tag{IV.47}$$

$$g(t) = \bar{g}_0 + \bar{g}_3 t^3 + \ldots, \tag{IV.48}$$

$$L(t) = \bar{L}_1 t + \bar{L}_2 t^2 + \ldots, \tag{IV.49}$$

for $t \to 0$. By using the initial values from Table 10 where the derivatives of B, I and g have been initially set to zero, it is consistent to set $\bar{B}_1 = 0$, $\bar{I}_1 = 0$, and

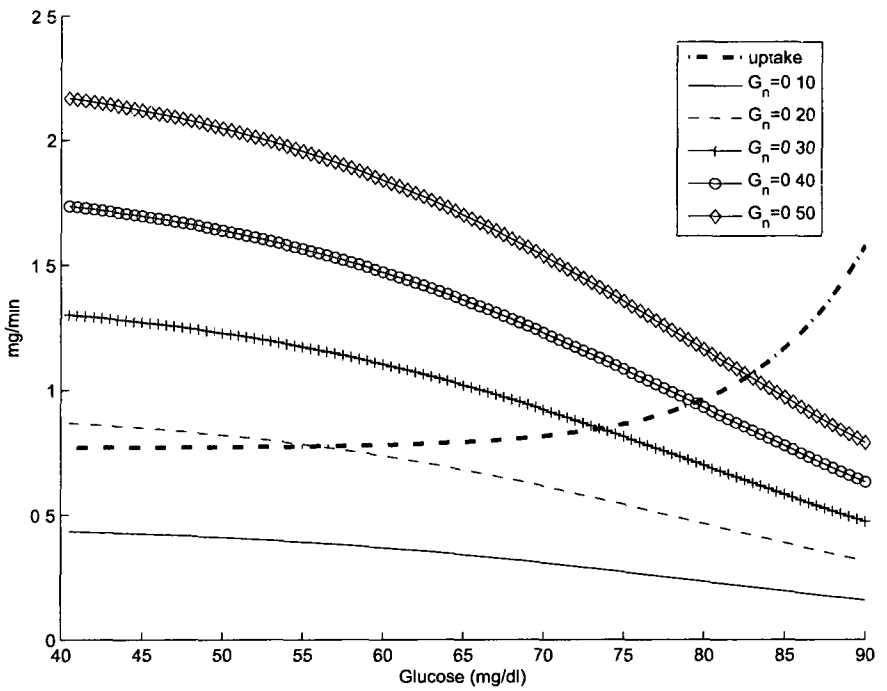

Fig. 38 The base-state glucose point is determined by the intersection of the uptake and synthesis curves.

$\bar{g}_1 = 0$ and to set the value of $\bar{L}_1$ to the maximum glycogen recovery rate. Additional examination of the system determines that $\bar{I}_2 = 0$ and $\bar{g}_2 = 0$. In order to find the leading correction terms (i.e. $\bar{B}_2$, $\bar{I}_3$, $\bar{g}_3$, and $\bar{L}_2$), the perturbation series is substituted into equation (IV.41) giving

$$\begin{aligned}\bar{L}_1 &+ 2\bar{L}_2 t + \dots \\ &= V_F \Big[\tilde{\beta}_L \left(\bar{B}_0 + \bar{B}_2 t^2 + \dots\right)\left(\bar{I}_0 + \bar{I}_3 t^3 + \dots\right) \operatorname{erfc}\left(\gamma_I \left(\bar{L}_1 t + \bar{L}_2 t^2 + \dots\right)\right) \\ &\qquad - (1 - G_n)\,\tilde{\alpha}\left(\bar{g}_0 + \bar{g}_3 t^3 + \dots\right) \operatorname{erf}\left(\gamma_g \left(\bar{L}_1 t + \bar{L}_2 t^2 + \dots\right)\right)\Big]. \qquad \text{(IV.50)}\end{aligned}$$

By using the asymptotic expansion of the error function, the above equation is expanded as

$$\begin{aligned}\bar{L}_1 &+ 2\bar{L}_2 t + \ldots \\ &= V_F \left[\left(\tilde{\beta}_L \bar{B}_0 \bar{I}_0 + \ldots \right) \left(1 - \frac{2\gamma_I}{\sqrt{\pi}} \bar{L}_1 t + \ldots \right) \right. \\ &\quad \left. -(1 - G_n)\tilde{\alpha} \left(\bar{g}_0 + \ldots \right) \left(\frac{2\gamma_g}{\sqrt{\pi}} \bar{L}_1 t + \ldots \right) \right].\end{aligned} \tag{IV.51}$$

Matching like powers of t from the left-hand and right-hand sides yields

$$\bar{L}_1 = V_F \tilde{\beta}_L \bar{B}_0 \bar{I}_0, \tag{IV.52}$$

$$\bar{L}_2 = -\frac{V_F}{\sqrt{\pi}} \left[\tilde{\beta}_L \bar{B}_0 \bar{I}_0 \gamma_I + (1 - G_n)\tilde{\alpha} \bar{g}_0 \gamma_g \right] \bar{L}_1. \tag{IV.53}$$

The process is repeated for equation (IV.38) producing the appropriate value of $\bar{B}_2$ in the near-starved state as

$$\bar{B}_2 = \frac{1}{\sqrt{\pi}} \left[\tilde{\beta}_L \bar{B}_0 \bar{I}_0 \gamma_I + (1 - G_n)\tilde{\alpha} \bar{g}_0 \gamma_g \right] \bar{L}_1. \tag{IV.54}$$

Likewise, substituting the perturbation series into equations (IV.39) and (IV.40), expanding appropriately, and matching like powers of t leads to the following expressions for $\bar{I}_3$ and $\bar{g}_3$:

$$\bar{I}_3 = \frac{\dot{Q}_I}{6r_I} \operatorname{sech}^2 \left(\frac{\bar{B}_0 - B_I}{r_I} \right) B_2, \tag{IV.55}$$

$$\bar{g}_3 = -\frac{\dot{Q}_g}{6r_g} \operatorname{sech}^2 \left(\frac{B_I - \bar{B}_0}{r_g} \right) B_2. \tag{IV.56}$$

Substituting the values of $\bar{B}_0$, $\bar{I}_0$, $\bar{g}_0$, and $\bar{L}_0$ found in Table 10 when $G_n = 0.30$ into the definitions of $\bar{B}_2$, $\bar{I}_3$, $\bar{g}_3$, $\bar{L}_1$, and $\bar{L}_2$ results in

$$\begin{aligned}\bar{B}_2 &= 3.0705 \times 10^{-5}, \\ \bar{I}_3 &= 1.7496 \times 10^{-7}, \\ \bar{g}_3 &= -5.1865 \times 10^{-6}, \\ \bar{L}_1 &= 6.2663, \\ \bar{L}_2 &= -0.0040.\end{aligned}$$

The zero-order terms represent the body in the maximum recovery mode, and

the first non-zero terms represent a correction to this mode. Thus, $\bar{L}_2$ being negative means that glycogen is no longer being replenished at the maximum rate. Hence, a little more of the energy produced through gluconeogenesis is available to help the glucose concentration rebound from its initially low value. This results in $\bar{B}_2$ being positive. Although it appears that the value of $\bar{B}_2$ is very small, one must remember that time is measured in minutes, and that after one hour has passed, $t^2 = 3600$. Thus, the model is predicting that the blood glucose remains nearly constant for an extended period (an hour or two) while the glycogen builds in the system at a near maximum rate. The values of $\bar{I}_3$ and $\bar{g}_3$ represent the correction of the insulin and glucagon concentrations to the maximum recovery mode. In maximum recovery, insulin is at its lowest level while glucagon is at its maximum level. Thus, as the recovery progresses, the insulin level is increasing ($\bar{I}_3$ is positive), and the glucagon level is decreasing ($\bar{g}_3$ is negative).

To further investigate, set $G_n = 0.50$ so that the body's internal glucose production is increased relative to when $G_n = 0.30$. The corresponding values of $\bar{B}_2$, $\bar{I}_3$, $\bar{g}_3$, $\bar{L}_1$, and $\bar{L}_2$ are

$$\begin{aligned}
\bar{B}_2 &= 7.2891 \times 10^{-5}, \\
\bar{I}_3 &= 1.3864 \times 10^{-6}, \\
\bar{g}_3 &= -1.2786 \times 10^{-5}, \\
\bar{L}_1 &= 23.7518, \\
\bar{L}_2 &= -0.0095.
\end{aligned}$$

With an increase in the value of G_n, the initial value of B_0 is higher (see Table 10), and the system has more glucose available to be converted into hepatic glycogen. Hence, the increase in the maximum glycogen recovery rate as seen through the increase value of $\bar{L}_1$. Since the glycogen recovery is faster, the correction to the maximum rate is also larger. Thus, the value of $\bar{L}_2$ and $\bar{B}_2$ essentially double as a result of the increased rate of gluconeogenesis.

CHAPTER V

CONCLUSION

V.1 THE MODEL

The primary goal of this thesis is to create and validate a mathematical model for glucose metabolism that is explanatory but can eventually be used for simulation and data fitting. With the interaction of many different compounds and thousands of chemical reactions being of importance, a complete mathematical model is not yet realistic; therefore, an extensible model is proposed detailing the interaction of the major components: glucose, insulin, glucagon, and glycogen.

The model proposed begins at the basic three-by-three dynamical system introduced by Lasseigne and Adams which governs the interdependencies of glucose and the controlling counter-regulatory hormones insulin and glucagon. The model evolves to a four-by-four dynamical system that includes the system's dependency on the next most important component – glycogen. The various parts of the new model are analyzed and evaluated in detail. In contrast to past models presented in the scientific literature, the basal levels of blood glucose, insulin, and glucagon represent derivable quantities and do not appear as explicit parameters. The proposed model explains how these values are maintained in spite of the body's constant energy usage by drawing upon its stores of glycogen. The dependencies of basal values on other parameters (for example, the insulin sensitivity and the glucose threshold for glucagon secretion) provide important clues regarding the health of the individual.

This model is the next step in the evolution of an extensible model. Currently, the model includes a mathematical description of the storage and release of hepatic glycogen but does not provide full details on the storage of glycogen in the muscle, the stores of substrates required for gluconeogenesis, and the stores of fat. Of the four storage compartments mentioned, liver glycogen is the fastest acting, has the greatest effect on the blood glucose concentration during the post-absorptive period, and is the first storage compartment to be depleted of energy. Thus, the first extension of the model accounts for these effects. In particular, the storage of a glucose load in the postprandial period and dispersion of stored glucose during the extended postprandial period is explained in order to understand how long-term glucose homeostasis is achieved in the presence of continual glucose usage, especially the usage by the central nervous system.

Here, the model incorporates the interactions between the counter-regulatory

hormones insulin and glucagon, each dependent on the current blood glucose concentration, alongside the interdependency of these hormones on the regulation of the blood glucose concentration in the system coupled with and within the dynamics of hepatic glycogen control. Parameter values are chosen to model a "healthy" individual. Though not demonstrated, these parameter values can also model an individual in a diabetic state. Initially, only the hepatic glycogen's availability to the system is modeled; however, to mimic the body's ability to produce glucose from other substrates, a constant rate term representing gluconeogenesis is introduced. The addition of this new term allows for glucose to temporarily remain at basal for an extended postprandial time period in spite of declining hepatic stores. The effect of this item is analyzed in section III.3.5.

The model allows for investigating the effects of introducing food energy into the system without directly modeling the digestive process. The effects of varying the glycemic index of food are investigated in section IV.1.1. This model predicts that the return to the basal state is much faster for high glycemic index foods, and thus, the insulin levels also return to basal state much faster for the high glycemic index foods. The effect of the glycemic index on the overall glycogen level is determined to be negligible, but it is noted that the foods with low glycemic indices lead to slightly greater glycogen storage as the blood glucose remains above basal for a longer time period.

If the body is insulin resistant, normal amounts of insulin are inadequate to produce a normal insulin response by the muscle, fat and liver cells; thus, the pancreas produces additional insulin as a result of the continuing high glucose levels. Eventually, the pancreas cannot keep up with the body's requirement for insulin, and excess glucose builds up in the bloodstream resulting in high basal levels. Individuals with insulin resistance simultaneously have both elevated levels of blood glucose and elevated levels of insulin circulating in their blood. Insulin resistance is modeled by decreasing the value of the primary rate constant β within the model. For the analysis presented here, this rate constant is decomposed into two components: one dependent mostly on the muscle's usage of glucose and another dependent on the conversion of the glucose to glycogen in the liver. The model predicts that insulin resistance in liver cells initially reduces the rate of storage of glycogen at a fixed glucose, insulin, and glucagon level. However, insulin resistance leads to elevated levels of blood glucose and elevated levels of insulin circulating in the blood, which then increases the rate of storage of glycogen. Thus, the net effect of insulin resistance on the glycogen level is not obvious due to the nonlinear nature of the response. It is determined that the maximum postprandial glycogen level is *increased* in insulin

resistant individuals.

Current thought is that net hepatic glucose production is significantly increased in people with diabetes, and that this increased production is the driving mechanism for the increased basal blood glucose levels. Analysis in section IV.1.3 indicates elevated prandial blood glucose and insulin levels associated with insulin resistance increase the glycogen-storage levels. Larger glycogen-storage levels subsequently drive an increase in the net postprandial hepatic glucose production which then lead to increased basal blood glucose levels (especially in insulin resistant individuals). Long-term glycogen storage levels are also effected by the overall level of energy input; however, in the absence of insulin resistance, the resulting increase in the net hepatic glucose production only causes a small elevation in the basal blood glucose and insulin levels. For the insulin-resistant individual, the increased energy input exasperates the problem of elevated basal blood glucose and insulin levels and elevated glycogen storage. This simple model suggests that Type II diabetes results from the development of insulin resistance more than from overeating.

Two extreme states related to food consumption are investigated in this thesis: a "well-fed" state, section IV.2.1, and a "near-starved" state, section IV.2.2. Base-state conditions of a well-fed state represent the maximum rate of glycogenolysis owing to the saturation of the hepatic store of glycogen. When the maximum rate is occurring, the base blood glucose and insulin concentrations are at their maximum values, and the base glucagon concentration is at its minimum value. As time proceeds, the abundant base glycogen store decreases, and thus, the rate of glycogenolysis also decreases directly leading to a slight decrease in the blood glucose concentration. This analysis indicates the insulin and glucagon level then follow the change in blood glucose concentration as second-order effects. Responses to the slight decrease in the rate of glycogenolysis include an insulin decrease from its maximum value and a glucagon increase from its minimum value.

In contrast to well-fed state, conditions pertaining to the near-starved state assume that a sufficiently long time period has lapsed without an external source of glucose, and then, the already low level of glycogen of this state is quickly depleted, perhaps by administration of a drug. These assumptions lead to an initial value problem where the initial blood glucose, insulin, and glucagon concentrations are determined by a balance assuming that gluconeogenesis is the only energy source. Gluconeogenesis provides fuel for the system and fuel for the glycogen replacement. The model predicts that the body attempts to replenish the store of hepatic glycogen at the maximum rate while maintaining an adequate blood glucose concentration.

The leading non-zero terms - from a perturbation analysis of the recovery period conducted over a short time scale - represent the body in the maximum recovery mode, and the next non-zero terms represent a correction to this mode. For instance, the first correction in the series for the glycogen level shows that glycogen is no longer being replenished at the maximum rate and a little more of the energy produced through gluconeogenesis is available to help the glucose concentration rebound from its initial value. The solution indicates that the glycogen recovery remains near its maximum level for at least four to five hours.

V.2 FUTURE WORK

This chapter contains ideas for further research. The model presented in chapter III assumes that glucose only comes from two sources, the food input and glycogen. As a fast progresses beyond a few hours, the body begins to produce glucose through other substrates through the process of gluconeogenesis an item briefly introduced and discussed in section III.3.5 and then again used in section IV.2.2. The actions of gluconeogenesis beyond the constant rate presented in this thesis should, at a minimum, include a functional dependence on the current glucose, insulin, and glucagon concentrations. Furthermore, modeling quantifiable changes in the substrates required for gluconeogenesis would better mimic the metabolic response to glucose incorporated by gluconeogenesis. Inclusion of these dependencies is the next logical step in the extension of the current model.

Another topic of interest is what happens when the glycogen stores are at a maximum. Lipolysis, or the storage and usage of fats in the body, plays a significant role in the long-term metabolic process. The role that exercise has on glucose metabolism, both the short-term and long-term effects, can be investigated in the future. Finally, to make the system more closely mirror that of a human's system, one must consider modeling the system with multiple insulin compartments; for example, the insulin concentration differs in the liver, the plasma, the pancreas and the interstitial fluids. The multiple-compartment theory of insulin dynamics usually produces a time-delay between the changes in the concentration values of glucose, insulin, and glucagon.

Obviously, the model proposed represents only the beginning steps in improving the understanding of blood glucose metabolism through mathematical modeling. It is my goal to continue to improve the system one step at a time.

BIBLIOGRAPHY

Bergman, R., Ider, Z., Bowden, C., Cobelli, C., 1979. Quantitative estimation of insulin sensitivity. American Journal of Physiology. 236, E667-677.

Centers for Disease Control and Prevention, 2005. National diabetes fact sheet: general information and national estimates on diabetes in the United States.

Centers for Disease Control and Prevention, 2007. National diabetes fact sheet: general information and national estimates on diabetes in the United States.

Cobelli, C., Mari, A., 1983. Validation of mathematical models of complex endocrine-metabolic systems. A case study on a model of glucose regulation. Medical & Biological Engineering and Computing. 21, 390-399.

Cobelli, C., Federspil, G., Pacinia, G., Salvan, A., Scandellari, C., 1982. An integrated mathematical model of the dynamics of blood glucose and its hormonal control. Mathematical Biosciences. 58, 27-60.

Foster-Powell, K., Hold, S., Brand-Miller, J., 2002. International table of glycemic index and glycemic load values: 2002. The American Journal of Clinical Nutrition. 76, 5-56.

Hogan, P., Dall, T., Nikolov, P., 2003. Economic Cost of Diabetes in the U.S. in 2002. Diabetes Care. 26, 917-932.

Jenkins, D., Wolever, T., Taylor, R., Barker, H., Hashmein, F., Baldwin, J., Bowling, A., Newman, H., Jenkins, A., Goff, D., 1981. Glycemic index of foods: a physiological basis for carbonhydrate exchange. The American Journal of Clinical Nutrition. 34, 362-366.

Lasseigne, D., Adams, C., 2011. An Extensible Mathematical Model of Glucose Metabolism. Part I: The Basic Glucose-Insulin-Glucagon Model. To Be Submitted.

Saunders, P., Koeslag, J., Wessels, J., 1998. Integral Rein Control in Physiology. Journal of Theoretical Biology. 194, 163-173.

Smith, C., Marks, A., Lieberman, M., 2005. Marks' Basic Medical Biochemistry: A Clinical Approach, 2nd Edition.

VITA

Caleb L. Adams
Department of Computational and Applied Mathematics
Old Dominion University
Norfolk, VA 23529

Education

Ph.D. Computational and Applied Mathematics, May 2011, Old Dominion University, Norfolk, VA.

M.S. Computational and Applied Mathematics, May 2004, Old Dominion University, Norfolk, VA.

B.S. Mathematics, May 1997, North Carolina State University, Raleigh, NC.

B.S. Mathematics Education, May 1997, North Carolina State University, Raleigh, NC.

Presentations and Publications

Lasseigne, D., **Adams, C.** "An Extensible Mathematical Model of Glucose Metabolism. Part I: The Basic Glucose-Insulin-Glucagon Model." Preprint, 2011.

An Extensible Mathematical Model of Glucose Metabolism, Old Dominion University, SIAM Chapter Conference, April 2008.

Honors and Awards

Recipient, Distinguished Teaching Award, Old Dominion University, 2010

Recipient, Shining Start Award, Old Dominion University, 2009

Recipient, Dissertation Fellowship, Old Dominion University, 2007

Recipient, Dominion Scholar, Old Dominion University, 2002

Professional Experience

Adjunct Faculty Member, Old Dominion University, 2008-present

Graduate Teaching Assistant, Old Dominion University, 2004-08

Secondary School Mathematics Teacher, Guilford Public Schools, 2000-01

Secondary School Mathematics Teacher, Wake County Public Schools, 1997-2000

Typeset using LaTeX.